Mechanical Rockcutting
with and without High Pressure Water Jets

By

Levent Tutluoglu

B.Sc. (Middle East Technical University, Ankara, Turkey) 1978
M.S. (University of California) 1982

DISSERTATION

Submitted in partial satisfaction of the requirements for the degree of

DOCTOR OF PHILOSOPHY

in

Engineering

in the

GRADUATE DIVISION

OF THE

UNIVERSITY OF CALIFORNIA, BERKELEY

Approved: Michael Hood 10/19/84
Chairman Date
Neville G.W. Cook 11/8/84
Michael S. King 11/12/84

ABSTRACT

A hybrid rock cutting method using water jets to assist the mechanical tools was investigated. Benefits of using a water jet assist system included: (i) substantial reduction in the bit forces; (ii) reduced rates of bit wear; (iii) reduced dust production; and (iv) reduction in frictional heating.

A series of dry and water jet assisted cutting experiments were conducted with a drag bit in Indiana Limestone. The relative influence of jet parameters in reducing the bit forces was investigated. The optimum performance of the water jet assist system was with a single jet parallel to and about 1 mm ahead of the leading face of the bit. Jet power was the most significant factor in reducing the bit forces. A threshold jet power level had to be exceeded to achieve optimum force reductions. If the jet power was increased beyond this threshold value

no further reduction in bit forces was observed. The influence of bit velocity on bit force reductions was not very significant. An increase in the bit velocity by a factor of four resulted in a six percent decrease, from 50 to 44 percent, in the force reduction achieved with water jets. Potential benefits of the water jet assist approach to oil well drilling were demonstrated by preliminary experiments combining water jets with PDC bits.

Indentation tests were conducted to study the crack growth and chip formation underneath the bit. A sieve analysis was carried out on rock fragments produced during dry and water jet assisted cutting. The surface area of fragments from these cuts was determined. Energetics of the fragmentation process producing these surfaces was studied by using a fracture mechanics approach. It was found that only 10 percent of the applied mechanical energy was used in producing the resulting surface.

Based on a comparative review of results and possible mechanisms, an explanation of the mechanics of water jet assisted cutting was developed. The dominant mechanism was continuous removal of the broken rock that formed ahead of the advancing bit. Finally, a theoretical model was introduced for a better understanding of this mechanism.

MECHANICAL ROCKCUTTING WITH AND WITHOUT HIGH PRESSURE WATER JETS

Levent Tutluoglu

Ph. D. Mineral Engineering

Michael Hood

Chaiman of Committee

ABSTRACT

A hybrid rock cutting method using water jets to assist the mechanical tools was investigated. Benefits of using a water jet assist system included: (i) substantial reduction in the bit forces; (ii) reduced rates of bit wear; (iii) reduced dust production; and (iv) reduction in frictional heating.

A series of dry and water jet assisted cutting experiments were conducted with a drag bit in Indiana Limestone. The relative influence of jet parameters in reducing the bit forces was investigated. The optimum performance of the water jet assist system was with a single jet parallel to and about 1 mm ahead of the leading face of the bit. Jet power was the most significant factor in reducing the bit forces. A threshold jet power level had to be exceeded to achieve optimum force reductions. If the jet power was increased beyond this threshold value

no further reduction in bit forces was observed. The influence of bit velocity on bit force reductions was not very significant. An increase in the bit velocity by a factor of four resulted in a six percent decrease, from 50 to 44 percent, in the force reduction achieved with water jets. Potential benefits of the water jet assist approach to oil well drilling were demonstrated by preliminary experiments combining water jets with PDC bits.

Indentation tests were conducted to study the crack growth and chip formation underneath the bit. A sieve analysis was carried out on rock fragments produced during dry and water jet assisted cutting. The surface area of fragments from these cuts was determined. Energetics of the fragmentation process producing these surfaces was studied by using a fracture mechanics approach. It was found that only 10 percent of the applied mechanical energy was used in producing the resulting surface.

Based on a comparative review of results and possible mechanisms, an explanation of the mechanics of water jet assisted cutting was developed. The dominant mechanism was continuous removal of the broken rock that formed ahead of the advancing bit. Finally, a theoretical model was introduced for a better understanding of this mechanism.

dedicated to

Defne Tutluoglu

Nilufer Tutluoglu

Mehmet Tutluoglu

Huseyin Ogutcen

for their encouragement and support

ACNOWLEDGEMENT

I would like to express my gratitude to Prof. Michael Hood for his supervision, encouragement, and support during the entire Ph.D work. It was his positive attitude and patience in general that made my smooth progress towards this degree possible.

I wish to express my sincere thanks to Prof. Neville G. W. Cook for his invaluable contributions to my research and my entire graduate career and for his review of this thesis.

I would like to thank Prof. M. S. King for his contributions to the indentation experiments and for his profound review of this thesis. I wish to thank Dr. C. Hosten and Prof. K. V. S. Sastry for their assistance in the size analysis.

This work was supported first by the U.S. Department of Energy under Contract DC AC03-768 F00098, and later by the U.S. Bureau of Mines, and the Universitywide Energy Research Group of the University of California under the Energy Science and Technology Program. My personal financial support was provided mainly by NATO Science Scholarship Program through the Scientific and Research Council of Turkey, and partly by the Jane Lewis Fellowship.

TABLE OF CONTENTS

LIST OF FIGURES

LIST OF TABLES

NOMENCLATURE

A	Total Surface Area of Fragments
A_f	Face Area
A_n	Nozzle Cross-sectional Area
C	Normal to Cutting Force Ratio
D_n	Arithmetic Mean of the Opening of Screen (n) and the Opening of Screen (n-1) Above Screen (n)
d	Nozzle Diameter
E	Young's Modulus
G	Fracture Energy
J_e	Jet Energy per Unit Length of Cut
K_{Ic}	Fracture Toughness
F_c	Cutting Force
F_n	Normal Force
N_f, N_B, N_R	Normal Reactions on the Wedge
P	Specific Power
P_c	Constraining Force on the Wedge
P_j	Jet Power
P_w	Uplift Water Force
p	Water Pressure
p_c	Confinement on the Wedge
p_o	Ambient Pressure
Q	Rock Material Handled Per Unit Time
Q_v	Volume Flow Rate
q	Fraction of Mechanical Energy Used for New Surface Area

R	Rate of Advance
r	Radial Distance
S_o	Shear Strength Constant
s_f	Feed Size
s_p	Product Size
T	Temperature
U	Energy Required to Create New Surface Area
U_m	Applied Mechanical Energy
u	Jet Velocity
W_c	Constant Involving Comminution Efficiency and Surface Energy of Fragments
W_r	Rittinger's Energy to Break a Unit Volume of Rock
W_s	Specific Energy
α	Inclination of Rock Surface
α_c	Critical Value of the Inclination
β	Bit Rake Angle
θ_b	Thermal Properties of the Bit
θ_r	Thermal Properties of the Rock
$\Delta\phi$	Mass Fraction
λ	Shape Factor
ν	Poisson's Ratio
ρ	Particle Density
ρ_w	Water Density
μ, μ_f, μ_B, μ_R	Friction Coefficients
σ_n	Normal Stress
τ	Shear Stress Across the Sliding Surface
τ_i	Shear Stress Across the Rock Fragments

MECHANICAL ROCK CUTTING WITH AND WITHOUT HIGH PRESSURE WATER JETS

1. INTRODUCTION

1.1. Importance of Rock Breaking

Breaking rock is an activity that has occupied man from prehistoric times to the modern day. The importance of this activity in our modern technological society often is not appreciated.

Rock breaking consumes as much as 2 percent of total electric power produced in the U.S. (NRC, 1980). A volume of approximately four billion cubic meters of rock material is handled in the world annually. This quantity corresponds to about one cubic meter of rock material per inhabitant of the world per year. In the U.S. this number is four to ten times higher per inhabitant per year. Total rock material handled by the U.S. mineral industry from 1960 to 1981 is shown in Figure 1, (from U.S. Bureau of Mines Minerals Yearbooks, 1960-1982).

Rockbreaking is an essential part of exploration and development activities in the mineral industry. The total length of the holes drilled in the U.S for exploration work reaches 500 km per year. Each year 40 km of new tunnels and drifts are constructed by the U.S. mineral industry (from U.S. Bureau of Mines Minerals Yearbooks).

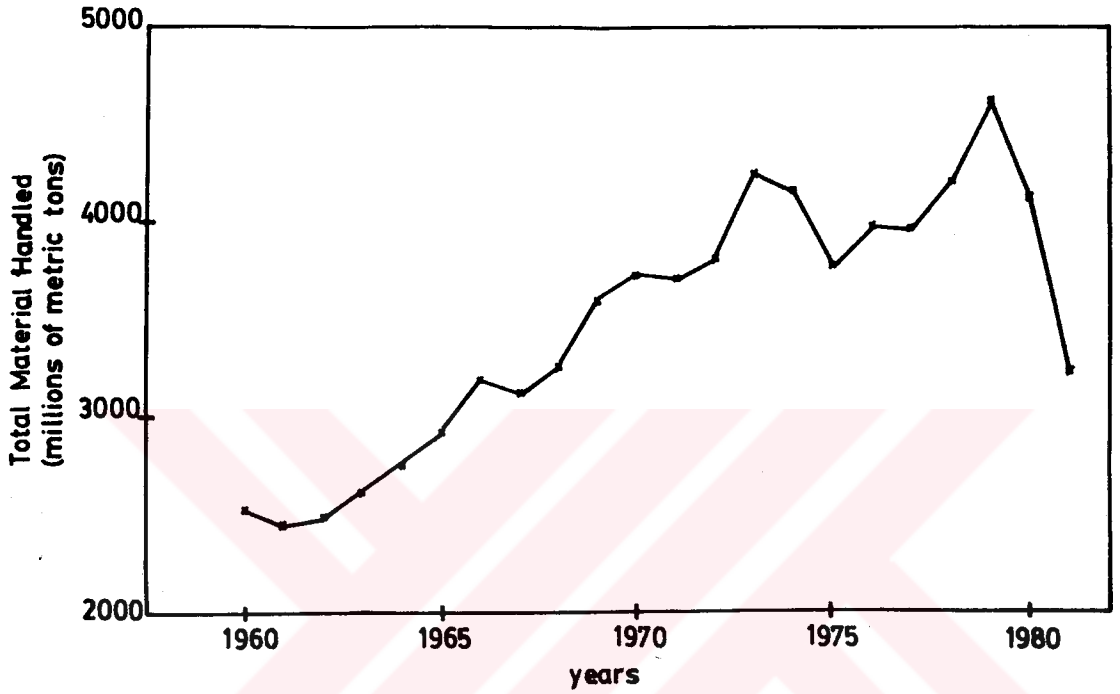

Figure 1. Total rock material handled in the U.S. mineral industry (from U.S. Bureau of Mines Minerals Yearbooks).

1.2. Historical Developments

An important development in the history of rock breaking was the use of black powder for blasting rock in the early 17th century. A later development was the birth of the pneumatic rock drill which was first used for Mont Cenis tunnel through French Alps in 1861. The first hydraulic drill was introduced in Austria in 1878. These developments were the important milestones which provided the technological hardware for today's drill-and-blast technique of rock fragmentation.

The first appearence of rock excavation machines almost coincides with technological advances summarized in the preceeding paragraph for the drilling and blasting methods. The first tunnel boring machine was used for the 4.7 mile long Hoosac Railway tunnel Massachusets in 1856. Raise boring machines appeared in early 1950's. Another development for machine excavation in 1950's was the first use of shearer loaders and continuous miners for coal cutting. Machine excavation, which eliminated the cyclic nature of the drill-and-blast technique proved to be very successsful in this century. From the beginning of the century the productivity for underground mines has increased 350 percent, as opposed to 250 percent for open pit mines in which the drill-and-blast is the common fragmentation technique (Nilsson, 1982).

Machine excavation is still not competitive with drill-and-blast methods in all types of hard rock. Therefore, the most recent research activities in rock breaking have concentrated on developing novel techniques which will be capable of competing with the drill-and-blast

technique in hard rock. These novel techniques, including water jet cutting, flame jet piercing, electron and laser beam cutting, are still in a research stage. However, hybrid rockcutting machines combining two techniques such as water jet erosion and drag bit cutting have already operated successfully in South Africa (Hood, 1976).

1.3. General Principles of Rock Breaking

1.3.1. Important Concepts

Before discussing different rock breaking techniques it is essential to introduce some concepts which are useful in comparing the performance of these techniques.

For all rock breaking techniques, energy has to be spent in order to break the rock. In some applications, such as in tunnelling, drilling, and mining, the objective is to remove rock from the solid. In other applications, the purpose is to achieve further fragmentation, such as in crushing and grinding. This energy consumption per unit volume of rock broken is called specific energy, W_s, and it is used widely in comparing the different rock breaking techniques. Another useful concept is the specific power, P, which is defined as the amount of power that can be delivered to a unit area of the working face.

Specific energy W_s, is expressed in MJ/m^3 or MN/m^2 which has the same dimensional form as the uniaxial compressive strength C_o, of the rock. The specific power, P, is expressed in MW/m^2. The rate of advance, R,

in m/sec for handling Q m^3/sec rock from a face of A_f square meter cross-sectional area is given by

$$R = Q / A_f \tag{1}$$

or

$$R = P / W_s \ . \tag{2}$$

The specific energy is constant for a fixed breaking process and rock type. Therefore, for a given breaking process and rock type, the only way to increase the rate of penetration is to increase the power delivered to the working face. However, there are limitations on increasing the power and these limitations are be discussed later in this chapter.

In addition to the specific energy and specific power, size and uniformity of particles produced after the breaking process play an important role in evaluating the performance of the breaking methods. According to Rittinger (1867), the energy absorbed in comminution increases with the surface area of rock fragments. Since the surface area of rock fragments increases inversely as the size of the fragments, the specific energy is expected to be inversely proportional to the size of the product from any breaking process. Rittinger's postulate can be formulated as

$$W_r = W_c \ (\ 1/s_p - 1/s_f \ ) \tag{3}$$

where W_r is the energy required to break a unit volume of solid rock from feed size s_f to product size s_p, and W_c in J/m^2 is a constant which involves comminution efficiency and relates surface energy of fragments to their size.

1.3.2. A Review of Rock Breaking Principles

General rock breaking principles can be discussed under 5 basic headings, and these principles and their applications in rock breaking are summarized in Table 1.

(i) **Mechanical Attack:** In mechanical attack, breaking forces are applied to the rock surface by a cutting tool. During this process the physical contact between the cutting device and the rock generates stress concentrations in the rock. These stresses cause the rock around the contact area to spall away.

Depending on the geometry of the cutter, the component of force perpendicular to the rock surface or the component parallel to the rock surface is the major force component in the cutting process. The disc type cutter used on tunnel boring machines operating in hard rocks is an example of the cutter with a high normal force component, (Figure 2). This process often is described as indentation. The high normal thrust causes spalling on both sides of the cutter. The major force component when cutting with a sharp drag bit is usually parallel to the surface of the rock. This drag force produces chips immediately ahead of the leading face of the bit. The term cleavage will be used here for this

TABLE.1. CLASSIFICATION OF ROCK BREAKING TECHNIQUES

TECHNIQUES	APPLICATION	PRINCIPLE
MECHANICAL	Percussive drilling Rotary drilling Tunnel boring Raise boring Drag bit cutting Diamond cutting	Cleavage and Indentation
CHEMICAL	Blasting	Cleavage Caused by pressurized gas-rock interaction
	Direct chemical attack	Chemical Reaction
THERMAL	Flame jet-piercing	Spalling
	Laser beams Electron beams	Spalling Fusion Vaporisation
HYDRAULIC	Water jets	Erosion
HYBRID	Drill-and-Blast	Mech.+ Chem.
	Water jet assisted cutting	Mech.+ Hydr.
	Electron or Laser beams and Water jets	Therm.+ Hydr.
	Flame jet and Machine excavation	Therm.+ Mech.

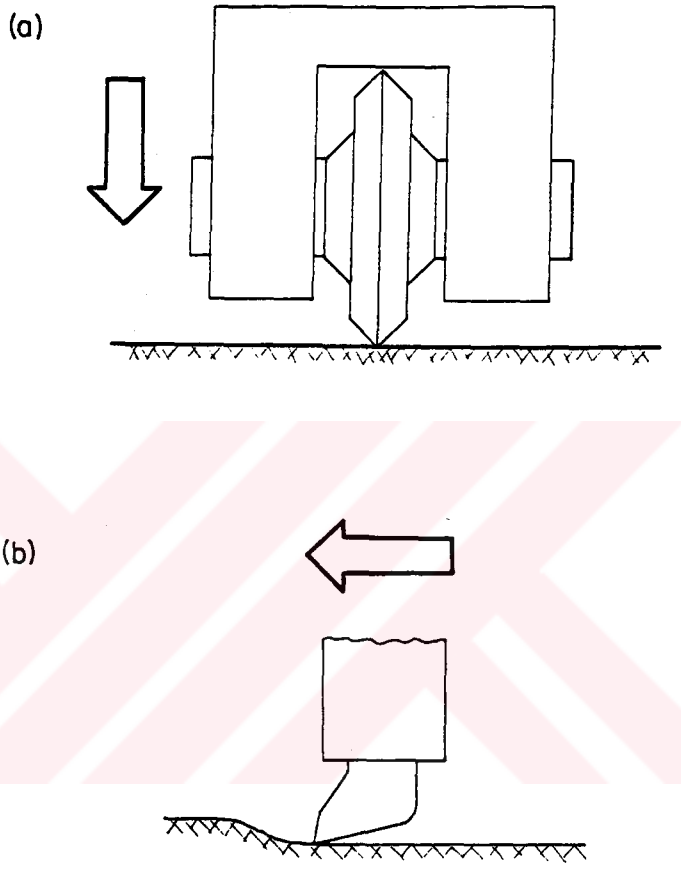

Figure 2. (a) Disc cutter employing a predominantly normal force to induce rock fracture (indentation).

(b) Sharp drag bit employing a predominantly parallel or shear force to induce rock fracture (cleavage).

special case of cutting and chip formation with sharp drag bits. In some cases both force components have the same order of magnitude. An example of such a case is the pencil point pick employed commonly on continuous miners. Normal and horizontal forces on point attack tools during cutting are almost equal or close in magnitude.

(ii) **Chemical Fragmentation:** Chemical fragmentation here refers to the direct or indirect use of chemicals to break the rock. A well known technique which employs chemicals for fragmentation is blasting. In blasting a hole is filled with explosives and the detonation of these explosives starts an exothermic chemical reaction. Immediately following the reaction, gaseous products at pressures of the order of 1,000 MPa and temperatures of the order of 2,000^{o} C apply great radial stresses to the walls of the hole. These high stresses disintegrate the rock, and an annulus of intensely crushed rock is formed around the hole. This crushed zone then exerts a radial stress which forms radial cracks around the hole. These cracks are propagated radially out by the pressurized gases. If there is a free surface nearby, further breaking is achieved by spalling. Spalling occurs as the compressive seismic wave generated by the blast strikes the free surface and a tensile wave is reflected off the free surface.

The direct use of chemical attack principal in rock breaking is not common. In leaching, a mineral is dissolved selectively from its gangue with the use of a leaching solution. Therefore, leaching is an example of the direct chemical attack principle.

(iii) **Thermal Rock Breaking:** Thermal rock breaking can be achieved in two ways:

(a) Thermal stress induced during localized heating of rocks causes spalling

(b) The rock can be fused and the molten material is removed. The fusion temperature is usually higher than the spalling temperature. and melting consumes relatively more energy.

Flame jet-piercing drills apply heat to spall the rock with a flame which is directed by nozzles on to the rock at the bottom of a hole. These drills have been used successfully in rock types that are prone to spalling such as taconite, quartzite, and dolomite. In general rocks containing minerals with high thermal expansion properties spall well. A low thermal conductivity improves the spallability by inducing high thermal gradients right under the heated rock surface.

High energy electron and laser beams produce high temperatures of between 1,000° C and 2,000° C in the rock. The heat is concentrated on a small area of the surface of the rock. The power density of electron beams can be as high as 10^7 MW/m^2. The power density of laser beams is two orders of magnitude greater than the electron beam power density. Laser and electron beams cause the removal of rock by fusion and vaporisation. Spalling is usually a more efficient way of rock removal than the fusion and vaporisation. The energy used for spalling is about 1,500 MJ/m^3 whereas fusion and vaporisation requires 5,000 MJ/m^3 and 10,000 MJ/m^3 respectively, (Cook and Harvey, 1974).

(iv) **Hydraulic Rock Breaking:** Two important applications of hydraulic rock breaking are: (i) rock removal with low pressure water jets; (ii) rock cutting with high pressure water jets.

Hydraulic monitors, with large nozzle diameters in tens of millimeters represent the low pressure ($\sim$1 MPa) application of water jets. The material excavated by the low pressure hydraulic monitors is usually loose surface soils, clays, and soft sandstones. In general the primary action of these monitors is to provide the high rate of water flow required for the removal of the loose material as a slurry.

Nozzle diameters for high pressure applications of water jets are an order of magnitude less than the nozzle diameters for the low pressure monitors. Industrial materials cut by high pressure water jets include paper, wood, and plastics. The water jet erosion process is believed to be a result of the removal of grains by hydraulic forces which are built up by the high pressure water penetrating into the cracks and pores of the material. A discussion of existing theories of water jet erosion will be presented later in detail, since water jets play an important role in most of the hybrid techniques including the one investigated in this program.

(v) **Hybrid Systems:** A hybrid rock breaking system is a combination of two or more different techniques listed in Table 1. The purpose of hybridization is to increase the breaking efficiency by combining individual advantages of these techniques. The drilling and blasting

method is an example of a hybrid system. The method combines drilling under mechanical breaking with blasting included in chemical techniques in Table 1.

Most of the hybrid systems include water jets. Thermal breaking which is efficient in breaking very hard rock can be combined with water jets for effective removal of the weakened material. Water jets, by cutting slots on the surface of the rock, can facilitate the mechanical breaking with a disc or drag cutter. Another hybrid system involving water jets, namely drag bit cutting with the assistance of water jets is the subject of this research program. In summary, water jets are employed commonly in hybridization because they are very effective:

(i) in removing the broken material;

(ii) in eroding porous rock or fractured rock weakened by other means;

(iii) in cutting fine slots in the rock.

1.4. Current Methods of Rock Fragmentation

1.4.1. A Comparison of Efficiency of Rock Breaking Techniques

As stated earlier two of the important factors in analyzing the efficiency of different breaking techniques are the specific energy and the particle size. These are plotted for various rock breaking techniques in Figure 3, (Cook and Joughin, 1970). Results are summarized below:

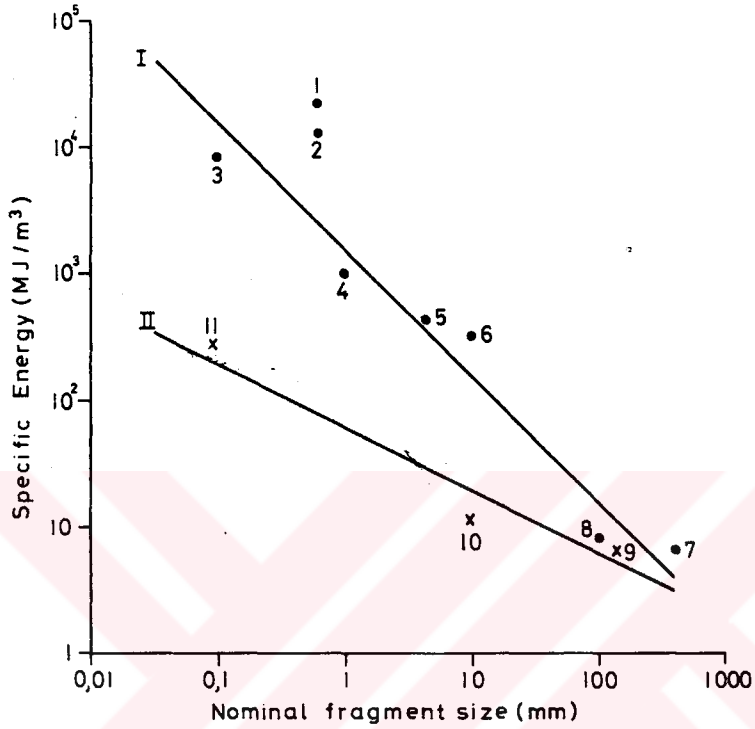

Figure 3. Specific energies as a function of nominal particle size for different methods of breaking hard rock (after Cook and Joughin, 1970).

(1) Flame jet piercing
(2) Water jet erosion
(3) Diamond cutting or drilling
(4) Percussive drilling
(5) Drag bit cutting
(6) Roller bit boring
(7) Impact driven wedge
(8) Explosive blasting
(9) Jaw-crusher
(10) Milling

(i) Points for different excavation techniques in Figure 3 tend to fall on line I which corresponds to Rittinger's inverse relation between energy required for breaking process and particle size. The slope of line II is 1/2, that is, specific energy is inversely proportional to the square root of the particle size for line II. This line corresponds to Bond's (1952) energy relation for comminution, and points for crushing and grinding are located on this line. It is interesting to note that excavation processes which involve removal of small pieces of rock from a large mass of rock under confinement consume a large amount of energy in producing undesirable fine dust. Comminution processes which are on line II are seen to be more efficient means of fragmentation in small size range than are the processes of excavation.

(ii) Explosive blasting is an efficient method in breaking hard rocks. It is the efficiency of the blasting that makes drilling and blasting attractive in hard rock breaking. However, drill-and-blast, while it is an energy efficient method, results in low rates of excavation because of the cyclic nature of the method.

(iii) Novel techniques such as flame jet-piercing and water jet erosion are characterised by high values of specific energy. Mechanical breaking methods -- percussive and rotary drilling, roller bit boring, and drag bit cutting -- are seen to be moderately efficient.

(iv) For drag bit cutting in Figure 3 the value of the specific energy is around 500 MJ/m^3, and the corresponding fragment size is 5 mm. It should be noted that these values apply to a blunt bit operating in a

hard rock with a compressive strength of 200 MPa. The compressive strength of the limestone used for this research program was only one fourth the compressive strength of the rock in Figure 3. But, the average values of the specific energy and the fragment size for the sharp drag pick used in this research were dramatically different than those given for the blunt bit. The specific energy was around 10 MJ/m^3, which is 50 times less than the blunt bit value, and the median fragment size was 30 mm, which is six times more than the fragment size for the blunt bit.

1.4.2. Current Rock Breaking Practice

Rock breaking today is carried out using either the drill-and-blast method or machine excavation. An examination of the explosive consumption in the U.S. over the last two decades reveals some interesting trends in the mineral industry.

Consumption of explosives in the U.S mineral industry increased four times between 1960 and 1980 and exceeded 1.6 million tons in 1980 (Figure 4). Figure 5, which is obtained by normalizing Figure 4 with Figure 1, shows an increasing consumption of explosives per ton of rock material handled annually in the U.S. mineral industry. This indicates that there is a tendency in the mineral industry to use mining methods which employ drill-and-blast as the major rock fragmentation method. One such example of these mining methods is the surface mining. The drilling and blasting method is used widely in surface mining which produces 96 percent of the total material handled annually, (U.S. Bureau of Mines Minerals Yearbooks).

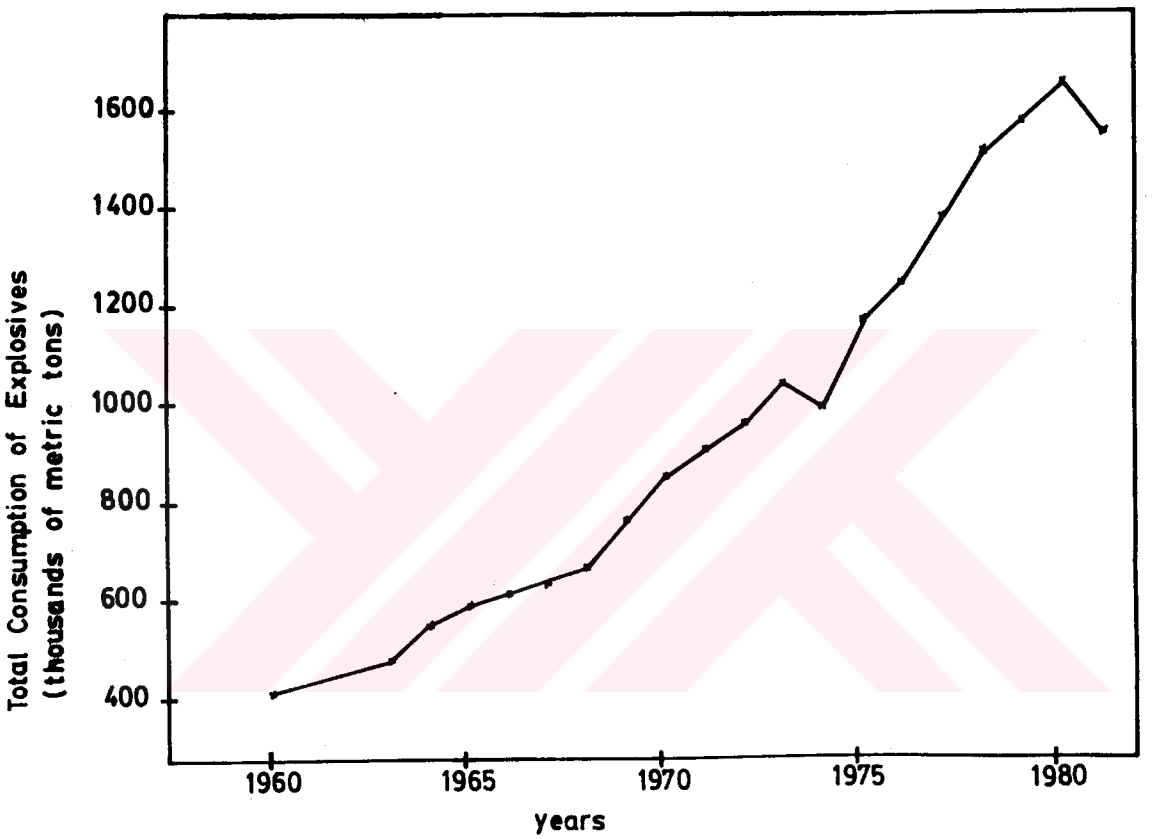

Figure 4. Total annual explosive consumption in the U.S. mineral industry (from U.S.B.M. Minerals Yearbooks).

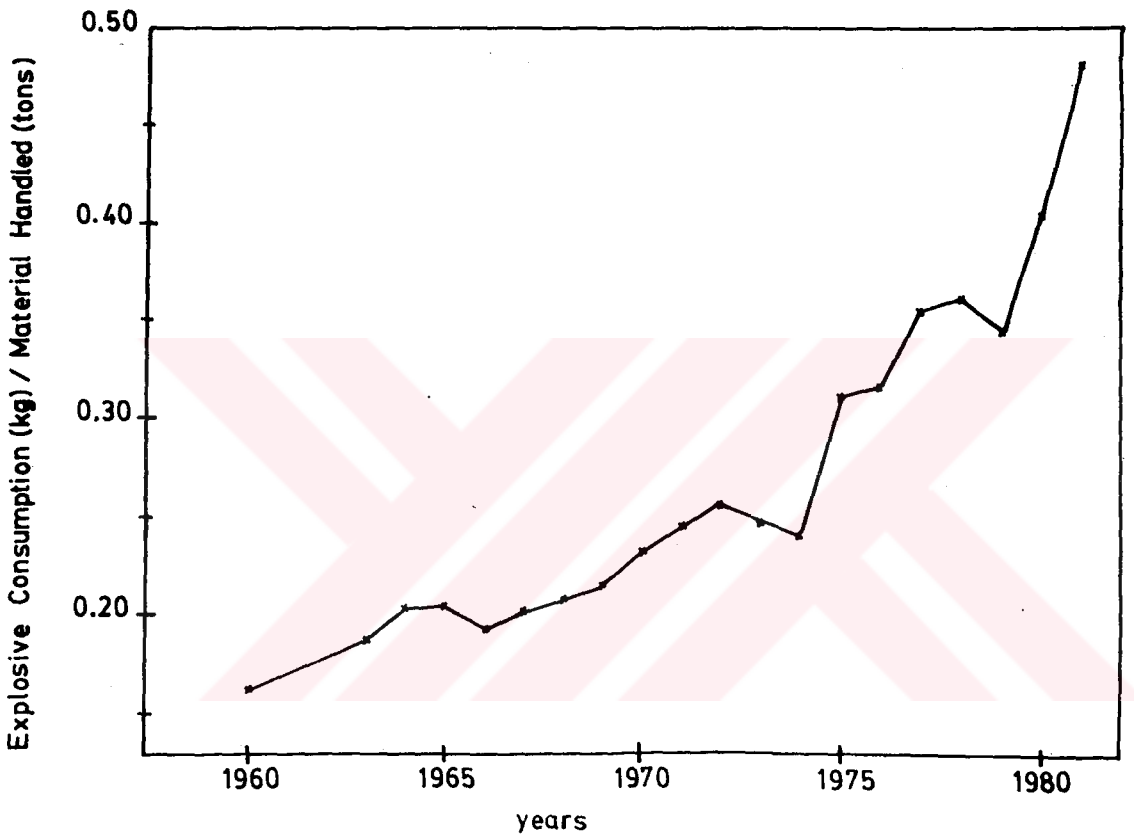

Figure 5. Total explosive consumption normalized by total material handled.

Drill-and-blast is the common choice in hard and abrasive rocks since the operating cost for machine excavation in such rocks becomes too high because of the high rate of cutter wear. However, drill-and-blast methods have the following major disadvantages:

(i) cyclic operation;

(ii) enviromental effects of dust, noise and ground vibrations;

(iii) damage to the adjacent rock in tunnelling and mining operations.

1.5. Fundamental Limitations of Mechanical Cutting Tools

Bit wear is the fundamental limitation on the use of mechanical tools. The bit material subjected to wear is usually tungsten carbide of which the bit inserts are made. There are two factors which lead to the failure of the tungsten carbide inserts:

(i) The hardness of tungsten carbide is reduced considerably at temperatures around 800° C. At a temperature of 1000° C plastic deformation of tungsten carbide begins. These temperatures are not unusual for cutters operating in hard and abrasive rocks. It was shown theoretically that when the power transmitted through the bit exceeds a critical level thermal deterioration of the bit insert quickly leads to bit failure, (Cook, 1984). Figure 6 shows an example of the abrasion of the tungsten carbide insert for a blunt drag bit, (Hood, 1978).

Figure 6. Abrasion of tungsten carbide insert on a blunt drag bit (after Hood, 1978).

(ii) Tungsten carbide is a brittle material. It is extremely strong in compression and relatively weak in tension. Sharp bits are characterized by high drag forces which usually put the tungsten carbide inserts under tension. To avoid the brittle failure of the tungsten carbide a blunt bit design which results in compressive loading of the insert is employed in hard rock. However, this design promotes high temperatures in the bit material.

Drag bits are usually fairly sharp in the beginning of a cut. It was stated earlier in Section 1.4.1 that sharp bits have low specific energy values. However, it is difficult to maintain this sharpness for a long time. As the bit advances, the width of the wearflat increases and the design clearence of the bit begins to disappear, (Figure 7). The force required to break the rock is higher for bits with larger wearflats. This high normal force on the wearflat increases the frictional heating, and the resulting temperature rise accelerates the bit wear.

In discussing Equation (2) it was stated that the rate of excavation can be increased by increasing the power transmitted to the rock. If this power increase is transmitted to the rock directly through the bit, the strength of the bit material sets the upper limit on the power. This is because the strength of the bit material is reduced significantly with increasing bit temperatures as a result of the power increase. To avoid a high rate of bit wear some of the power required to achieve an improved rate of rock excavation can be supplied by means other than through a cutting bit. One way of increasing the power transmitted to the rock is to use water jets which assist the bit during cutting. This

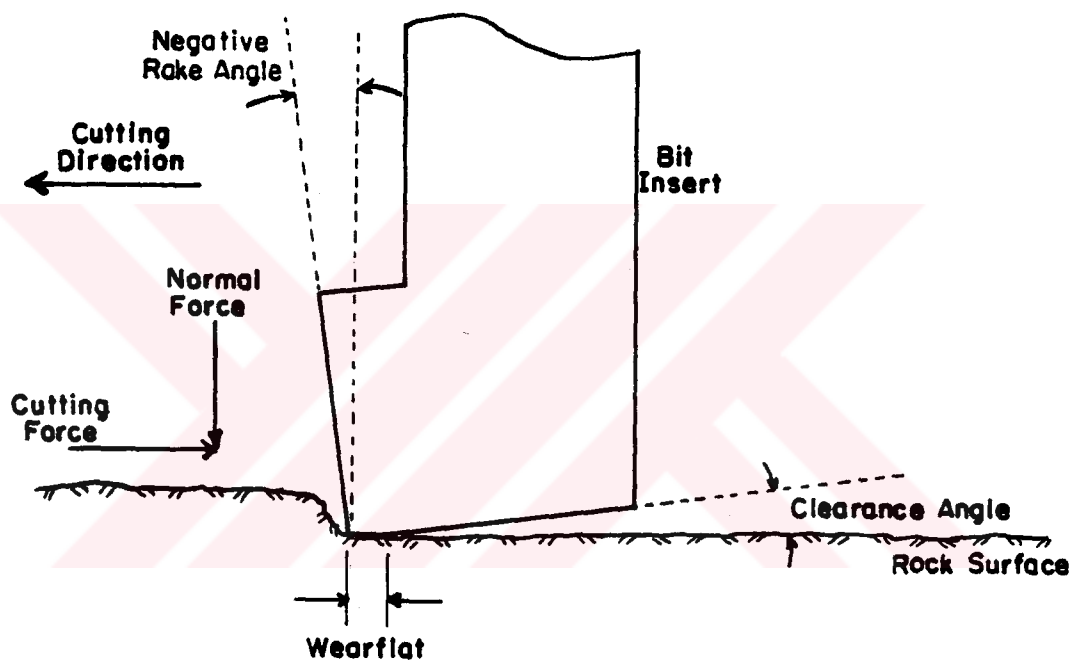

Figure 7. Wearflat and geometry of a drag bit.

way, other benefits of the water jet assist system are added to the cutting operation, as well as the increase in the rate of advance.

1.6. Water Jets In Rock Breaking

First, a review of existing theories will be presented to explain how the pressure is distributed on the surface of a half space when a water jet impinges on the surface, and how a water jet breaks the rock. This will be followed by a summary of developments in water jet assisted cutting. It was stated earlier that the most effective role of water jets in rock breaking is in the hybrid systems. One such system is drag bit cutting with the assistance of water jets. Therefore, the benefits of using water jets to assist drag bits in an underground environment will also be discussed here.

1.6.1. Water Jet Cutting Technology

Nozzle effects on the cutting performance of high pressure water jets were investigated by Leach and Walker (1966). They studied the pressure distribution on a surface at right angles to the jet, using a number of nozzle shapes suggested in the literature. In most of the experiments the jet diameter was 1 mm and pump pressures were below 70 MPa. Leach and Walker found that for rocks there is a critical value of this pump pressure below which no damage is observed on the surface of the rock. Their results also showed that the pump pressure behind the nozzle could be applied effectively to a target 100 nozzle diameters away. For several nozzles the pressure at a stand off distance of 100

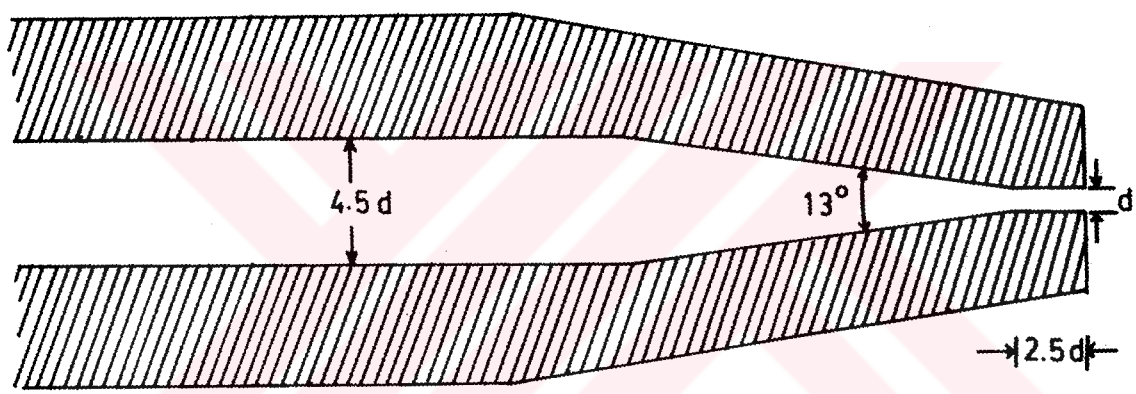

Figure 8. Nozzle geometry recommended by Leach and Walker (1966).

nozzle diameters was over 80 percent of the pump pressure behind the nozzle. The nozzle shape with the best performance was a small angle (13^{o}) cone followed by 2 to 4 nozzle diameters of straight section (Figure 8). Sharp internal corners in the nozzles produced slightly better results than rounded corners.

The additives used by Leach and Walker improved the performance of the jets. The effective stand off distance between the nozzle and the target plate was raised from 100 nozzle diameters to 200 nozzle diameters by using sodium carboxymethyl cellulose, which increases the viscosity of the water. Brook and Summers (1969) used a long chain polymer, polyox as an additive. With polyox, which improves the cutting performance of the water jets by increasing the cohesion of the jet stream, they observed a 20 percent increase in the depth of penetration of a water jet impinging on a sandstone specimen.

The axisymmetric pressure distribution for a water jet impinging on the surface of the half space, as suggested by Leach and Walker, is given by:

$$p(r) = p_o + 1/2\ \rho_w\ u^2\ [1 - 3(r/R)^2 + 2(r/R)^3] \qquad (4)$$

where u is the mean jet velocity, r is the radial distance from the axis of symmetry, p_o is the ambient pressure, ρ_w is the water density, and R is the value of r when $p \sim p_o$. The region where the pressure is significantly greater than the ambient pressure is confined to about 2.6 jet radii.

The pressure distribution in (4) was used by Powell and Simpson (1969) to determine the stress distribution in the half space. They applied a rock failure criterion to this stress distribution to find the critical penetration pressure. Theoretical values of the critical penetration pressure were somewhat higher than those observed in practice. The conclusion was that mechanical fracture resulting from the stress field associated with a water jet impinging on the surface of a half space could not explain cutting action of the water jet.

In a more recent theory developed by Rehbinder (1976) the suggested breaking mechanism for rock under the water jets was the removal of surface grains by the hydraulic forces in the half space; the half space was assumed to be presaturated and permeable. On the boundary of the half space the axisymmetric pressure distribution as a function of the radial distance r was different from (4) and given by:

$$p(r) = p_o \exp\left[-1/2\ (r/r_o)^2\right] \tag{5}$$

where p_o is the stagnation pressure, r_o is the radius of the jet. The half space extends to infinity in the positive z direction, and the pressure $p(r,z)$ satisfies the Laplace's equation in the half space. By using the solution $p(r,z)$ of the boundary value problem, the pressure gradient in z direction, $\partial p/\partial z$ on the surface $z = 0$ was found to change sign and become positive at a distance of 1.81 times the radius of the jet from the jet axis. The force vector on an individual grain was estimated by assuming that the force had the same nature as the drag

force on a sphere given by Stokes' law, and the water in the half space moved according to Darcy's law. The force on a single grain was proportional to the volume of the grain and the pressure gradient, therefore the force changed direction from inwards to outwards at the same location where the pressure gradient, $\partial p/\partial z$, changed sign. It was suggested that outside the zone defined by 1.81 times the radius of the jet, hydraulic forces on the grains worked against the cohesive forces between the grains and erosion took place in this zone since the rocks are weak in tension. A similar analysis showed that for an initially dry rock, the hydraulic forces that separated the grains were much greater in the presaturated rock than the dry rock (Rehbinder, 1977).

1.6.2. Development of Water Jet Assist Systems

Water jets at pressures around 50 MPa have been used in conjunction with drag bits to cut fairly strong and abrasive rocks in South Africa. This was a part of a research program of the Chamber of Mines to replace the conventional drill-and-blast mining operation on the gold mines of the Witwatersrand with a mechanized rock cutting system. It was demonstrated that with water jets assisting the drag bits in a strong quartzite the average depth of cut could be increased up to five times the depth of cut without the jet assistance, (Hood, 1976). In this investigation, the optimum arrangement of the jets with respect to the bit was found to be with two jets, one directed towards each corner of the rectangular bit and impinging on the rock 2 mm ahead of the leading edge of the bit. Force reductions with the water jets assisting the drag bits used for cutting tests on norite are shown in Figure 9. When

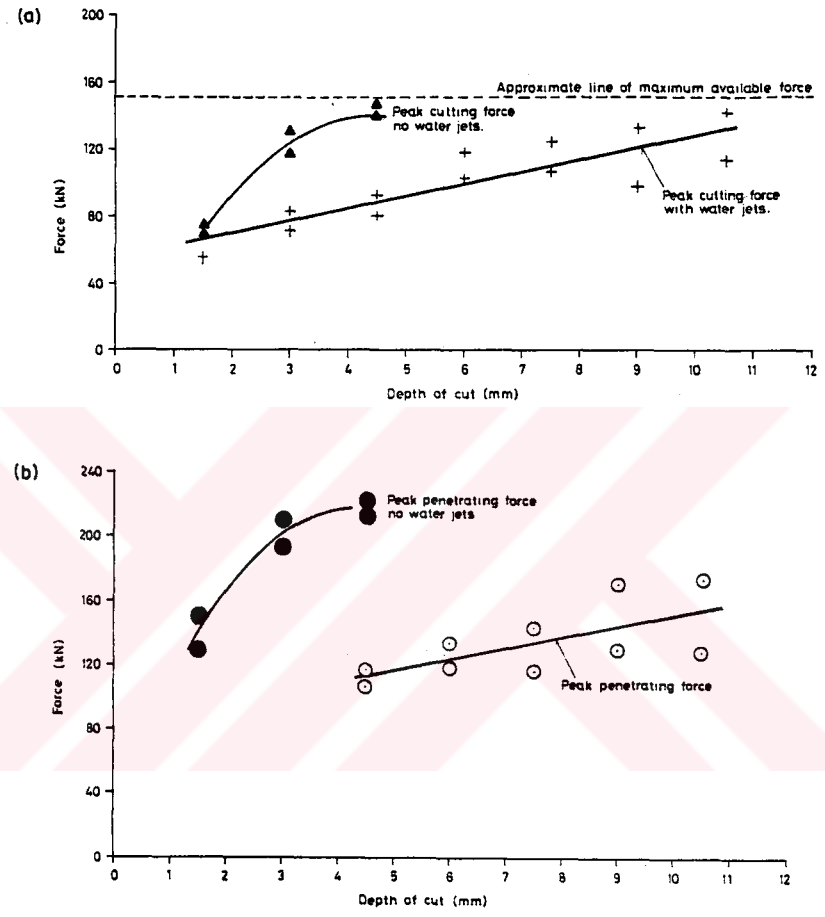

Figure 9. (a) Mean peak cutting force and (b) mean peak normal force for both dry and water jet assisted drag bit cutting in a strong quartzite showing that: (i) maximum depth of cut was increased by a factor of about 3; (ii) the bit normal force was reduced more than the bit cutting force, (after Hood, 1978).

the water jets were activated ahead of the bit during cutting, rates of bit failure were reduced dramatically, (Hood, 1978).

In most of Ropchan's work (1980) conical type drag bits mounted on a linear cutting rig were used in sandstone, shale and limestone. The greatest reduction in the forces on the tool was obtained in the sandstone when a 35 MPa water jet was located behind the bit. Limestone was the least effected rock by the water jet. The results in Figure 10 show a 50 percent reduction in drag forces and 60 to 70 percent reduction in normal forces with the use of a 0.63 mm diameter water jet behind the bit.

Results of field trials with a roadheader fitted with a 70 MPa water jet assist system are plotted in Figure 11, (Tomlin, 1981). Results of dry cutting in the Figure 11 (a) show the tendency for the cutting head to bounce in and out of the cut with resulting boom vibrations. With the use of water jets, fluctuations in the cutting head power and slew ram pressure were restricted to a much narrower band and the machine was cutting evenly, (Figure 11 (b)). Other benefits were reported to be the reduction and elimination of frictional sparking and dust, improved cutting rates and increased pick life.

Dubugnon (1981) used a two nozzle water jet arrangement and reported 60 percent reductions in cutting and normal forces on drag bits in granite and a strong sandstone. Results in Figure 12 are for taking 6 mm deep successive cuts several times in the same groove in the granite.

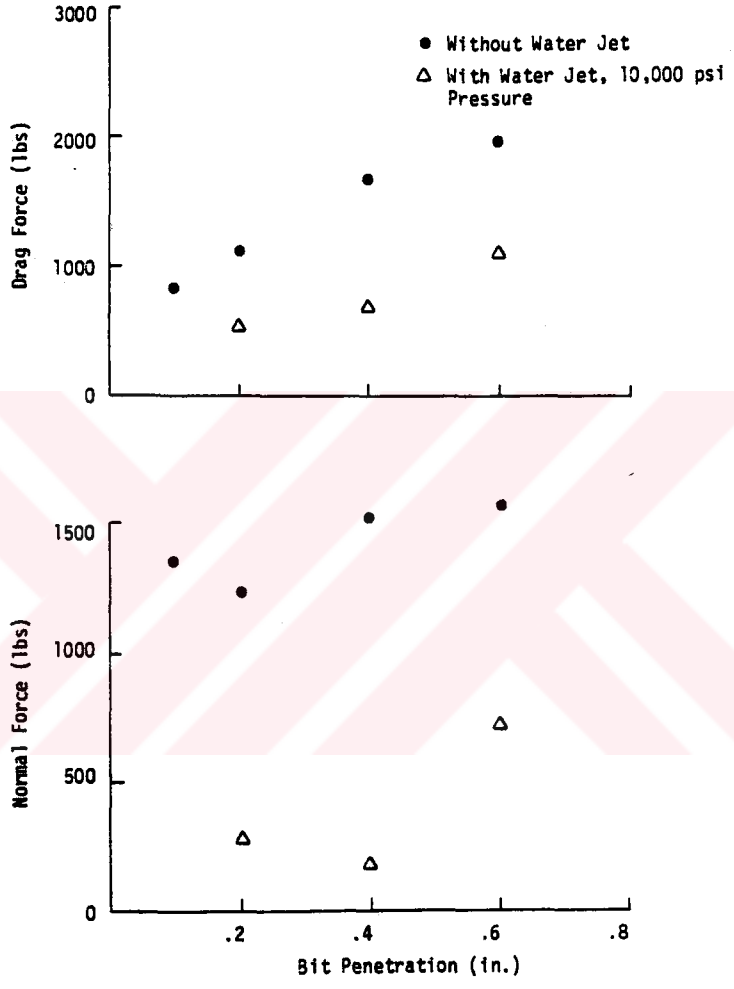

Figure 10. Bit forces with and without water jet assistance, cutting in Dakota Sandstone, (after Ropchan et al., 1980).

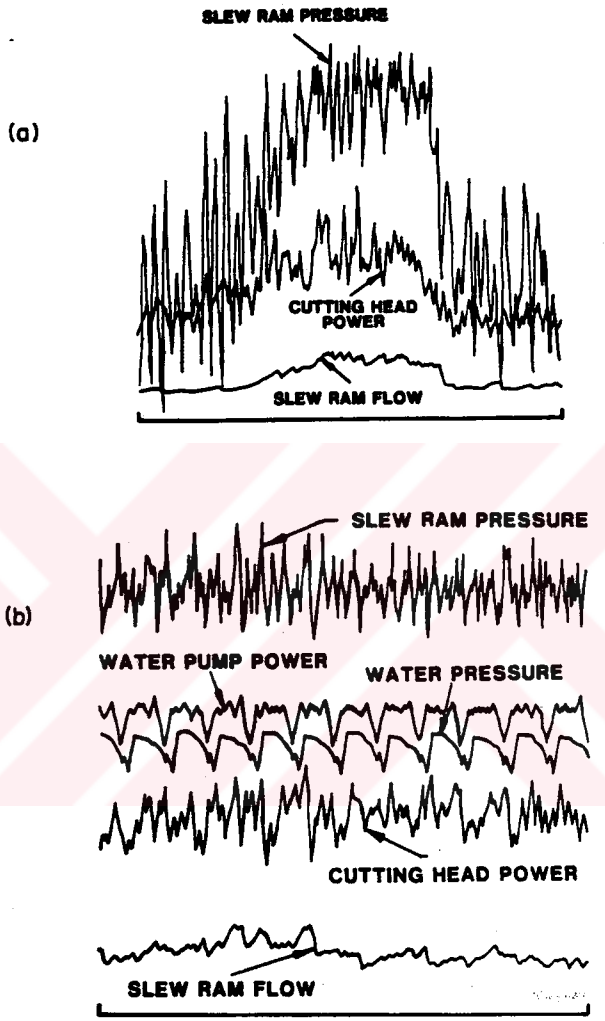

Figure 11. Results of field trials with a roadheader and a 70 MPa water jet assist system in a strong limestone (a) without and (b) with water jets, (after Tomlin, 1982).

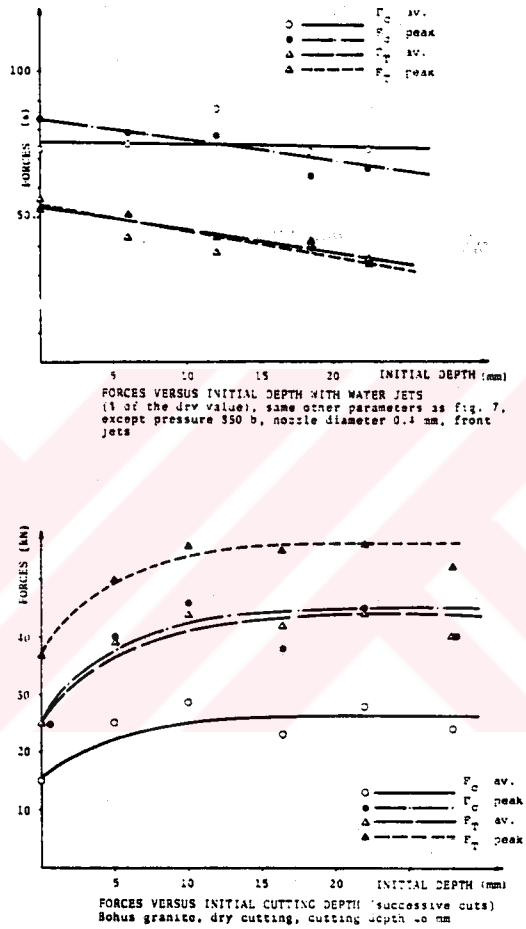

FORCES VERSUS INITIAL DEPTH WITH WATER JETS
(% of the dry value), same other parameters as fig. 7, except pressure 350 b, nozzle diameter 0.4 mm, front jets

FORCES VERSUS INITIAL CUTTING DEPTH (successive cuts)
Bohus granite, dry cutting, cutting depth 20 mm

Figure 12. Bit forces with and without water jet assistance, cutting in Bohus Granite, (after Dubugnon, 1981).

1.6.3. Benefits of Water Jet Assist Systems

(i) **Reduced Dust Make:** Dust in the underground environment is a major hazard in terms of both health (pneumoconiosis) and safety (explosions). A recent MSHA study revealed that nearly all longwall operations are having trouble maintaining compliance with the federal coal mine dust standard, (Anon, 1983). It is known that for coal approximately 36 x 10^6 fine particles, in the respirable size range (less than 5 μm), adhere to the surface of each square centimeter of broken coal, (NRC, 1980). Fortunately, only a small fraction of these particles are released into the air stream and therefore classified as dust.

Dust particles are formed and liberated during the fracture process, thus the cutting machine is a major source of dust underground. If the fragmentation is achieved by a water jet assisted cutting head, the water jets will wet the fine particles as they are produced at the face before they become entrained in the ventilation airstream. Tomlin (1981) observed in his field trials with a water jet assisted cutting machine that water jets cause the dust make at the cutter head to be reduced significantly.

(ii) **Reduced Incidence of Frictional Sparking:** Frictional ignitions represent major explosive safety hazard. It is seen in Figure 13 that the incidence of frictional ignitions has been increasing significantly over the last two decades. Frictional explosions occur when the energy level of the source is sufficient to ignite a 5 - 15 % methane in air

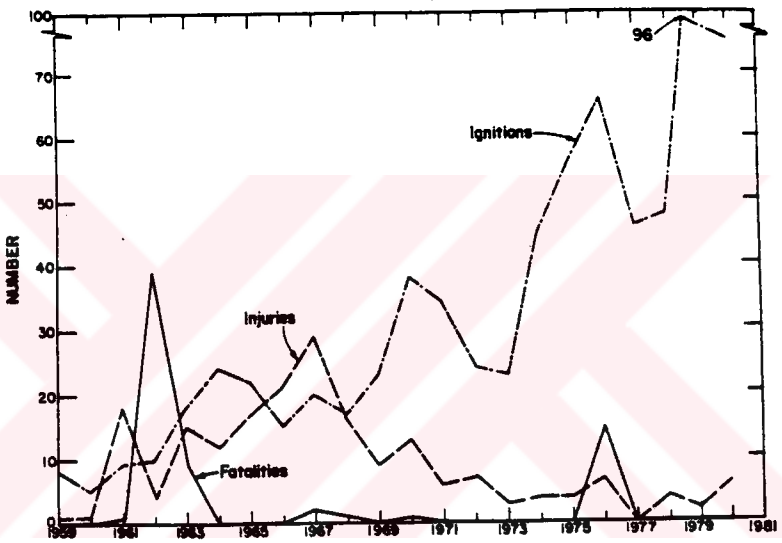

Number of frictional ignitions and associated injuries and fatalities per year, 1959-80.

Figure 13. Number of frictional ignitions and associated injuries and fatalities per year 1959-80, (after Richmond et al., 1983).

mixture. The energy of this source, which often is a spark, depends on both the temperature and the time of exposure of the source in the methane-air environment.

It is illustrated in Figure 14 that the cause of most of these ignitions is the spark generated by contact between the picks and the rock. Recent research has shown that the incidence of ignitions is greatly reduced if a water spray is directed immediately behind the pick during the cutting operation, (Courtney and Agbede, 1982). If water jets are used to assist the picks, the incidence of frictional sparking is expected to be reduced: (i) as a result of reduced heat loads on the pick; (ii) as a result of water cooling the hot rock surface and the hot rock fragments ejected behind the pick.

(iii) Reduced Rate of Bit Wear: Two major causes of bit wear are high temperatures in the bit body and high bit forces. The thermal loading on the bit material results in a significant reduction of the strength of the bit material. Temperatures in the bit material are increased by frictional heating at the bit:rock interface as a result of the high bit forces. High forces on the bit increase the rate of bit wear directly by causing intolerable stresses in the bit inserts. These stresses initiate bit failures when the strength of the bit material is exceeded. Significant reductions in bit temperatures have been reported when water jets assist drag bits cutting in hard rocks (Hood, 1978). Water jets reduce the rate of bit wear in two ways: (i) they act as a coolant for the bit; (ii) they cause a direct reduction in the bit forces.

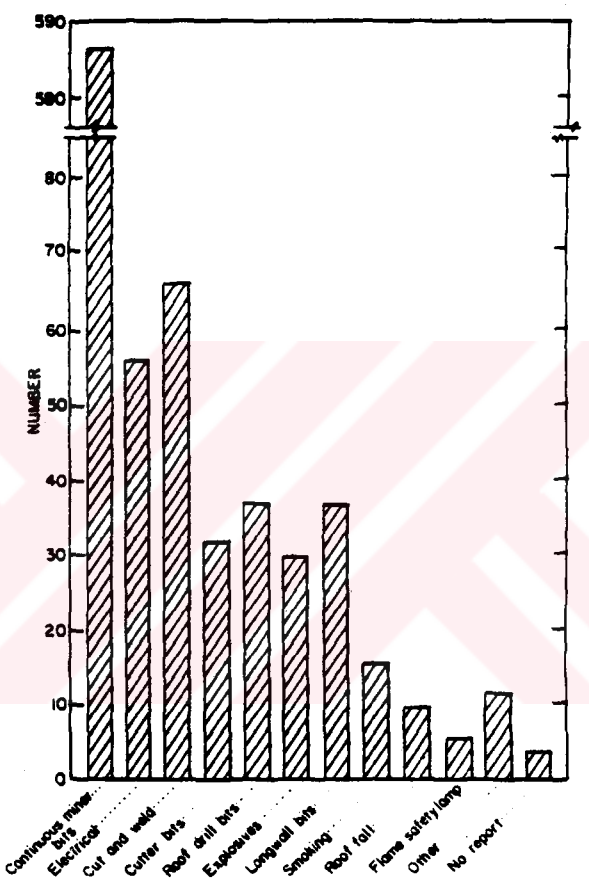

Number of minor ignitions and explosions by cause, 1959-80.

Figure 14. Number of ignitions and explosions by cause 1959-80 (after Richmond et al., 1983).

When a water jet assist system is employed, the reduced rates of bit wear can result in significant improvements in mine productivity. Bit changes cause interruptions in the production time. A recent study revealed that mechanical delays, which are mostly due to the bit changes, are responsible for 75 percent of all shearer delays in underground coal mines, (Pimental et al., 1981). When water jets are used, the production time lost will be reduced because of the improved bit life. Another consequence of the improved bit life will be a decreased cost of bits.

2. STATEMENT OF PROBLEM

Drag bit cutting with the assistance of water jets is a relatively new technique, and very little has been done in understanding the mechanism by which the water jets assist the cutting tool. The purpose of this research is to achieve a better understanding of the mechanism of water jet assisted cutting. Knowing this mechanism, a machine designer can optimize his design by making effective decisions and contributions when special problems are encountered in the field.

The application of water jet assist technology to rock excavation machines is likely to be the next step in rock cutting. This application requires an extensive technological background in addition to a good understanding of the mechanism by which water jets facilitate rock breaking. While trying to develop a mechanism of water jet assistance, this research will also improve the technological background required for designing water jet assisted cutting systems.

3. STRATEGY FOR SOLUTION

An experimental approach was used here. A series of dry and water jet assisted cutting experiments was carried out in a limestone. During the cutting tests, tool forces were recorded. The performance of water jet assist system was evaluated by comparing the forces on the cutting tool for dry cuts with forces for water jet assisted cuts.

The relative influence of the jet parameters in reducing the bit forces was investigated. These parameters included:

(i) jet pressure;
(ii) jet flow rate;
(iii) jet power;
(iv) position of jets with respect to the bit;
(v) number of jets;
(vi) bit speed.

A comprehensive series of tests provided data from which the relative importance of these parameters could be assessed and the mechanisms of water jet assistance could be analysed. Also, an attempt was made to determine the optimum values of these parameters. A tungsten carbide drag pick was the main cutting element for most of the test program. However, a similar investigation to extend the results to other drag bit geometries was conducted by using PDC (polycrystalline diamond compact) drag bits, which are commonly employed in the drilling industry.

In investigating the possible mechanisms of water jet assistance, first a series of dry and water jet assisted cuts was made on the limestone, and rock fragments from these cuts were collected. Then, a sieve analysis was carried out on these fragments. The surface area of fragments for both dry and water jet assisted cuts was determined. Energetics of the fragmentation process which produced these surfaces was studied by using a fracture mechanics approach. The chip formation for dry and water jet assisted cuts was observed qualitatively by using a series of high speed films of the cutting process. Finally, a mechanism of water jet assisted drag bit cutting was developed, based on a comparative review of results and possible mechanisms.

4. GENERAL EXPERIMENTAL PROGRAM

4.1. Equipment

4.1.1. Planing Machine

Experiments to study the effect of water jet assistance on the cutting performance of the drag bits have been conducted in the rock cutting laboratory at the University of California at Berkeley. This laboratory is equipped with a large modified metal planing machine, (Figure 15). The machine bed is hydraulically driven and holds a rectangular rock block 0.6 x 0.6 x 1.2 meters in size. The cutting tool is fixed in a 22 kN (5000 lb) capacity triaxial dynamometer (Figure 16) which is attached to the main frame of the machine, and measures the cutting, normal and lateral forces acting on the tool. The position of the tool-dynamometer unit can be varied vertically to fix the depth of cut, and horizontally to fix the spacing between sequential cuts. A cut is taken by first adjusting the position of the bit with respect to the rock block. This block then is traversed underneath the bit, resulting in a linear cut along the length of the top surface of the block. The total cutting length is 1.2 meters, and the maximum traversing speed available is 0.25 meters/sec.

4.1.2. Instrumentation

Force signals from the dynamometer are amplified and displayed on a digital oscilloscope and an ultraviolet strip chart recorder. Signals

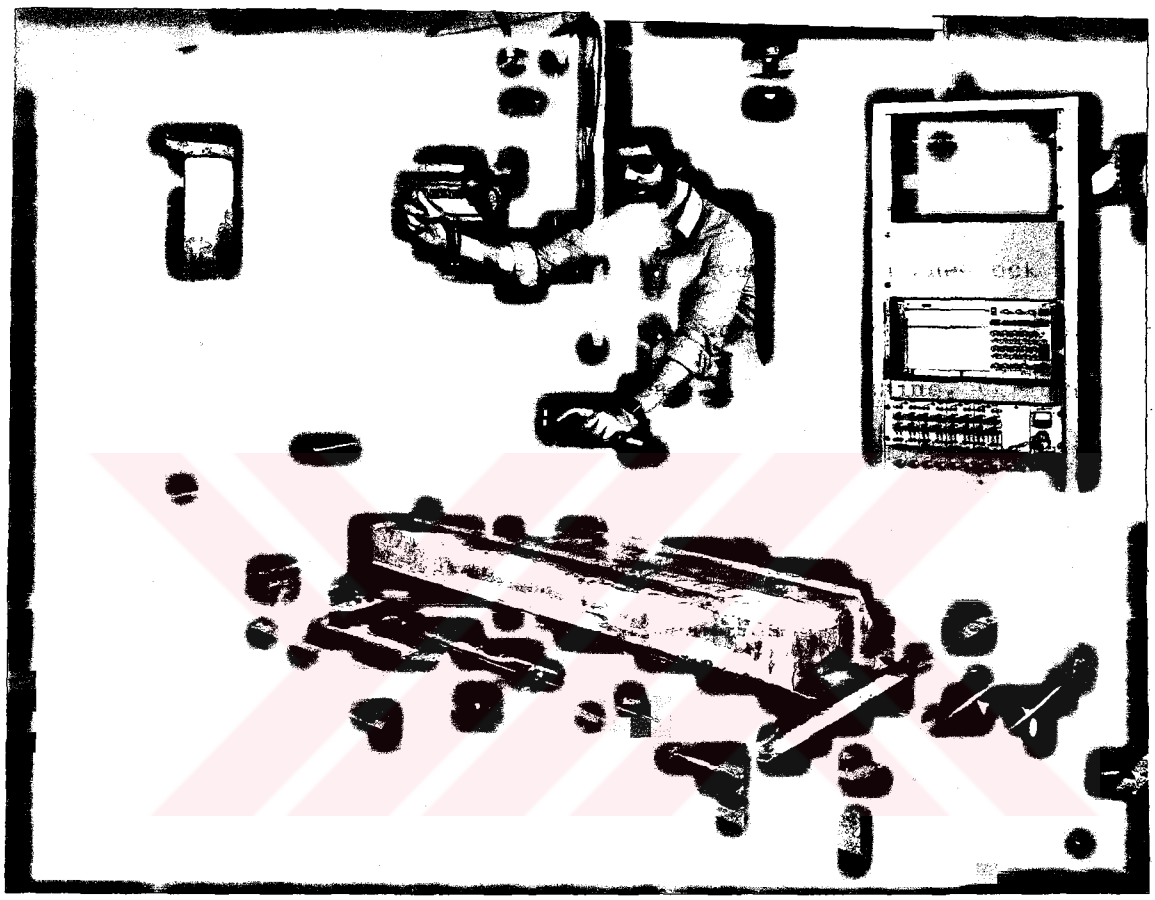

Figure 15. Linear planing machine.

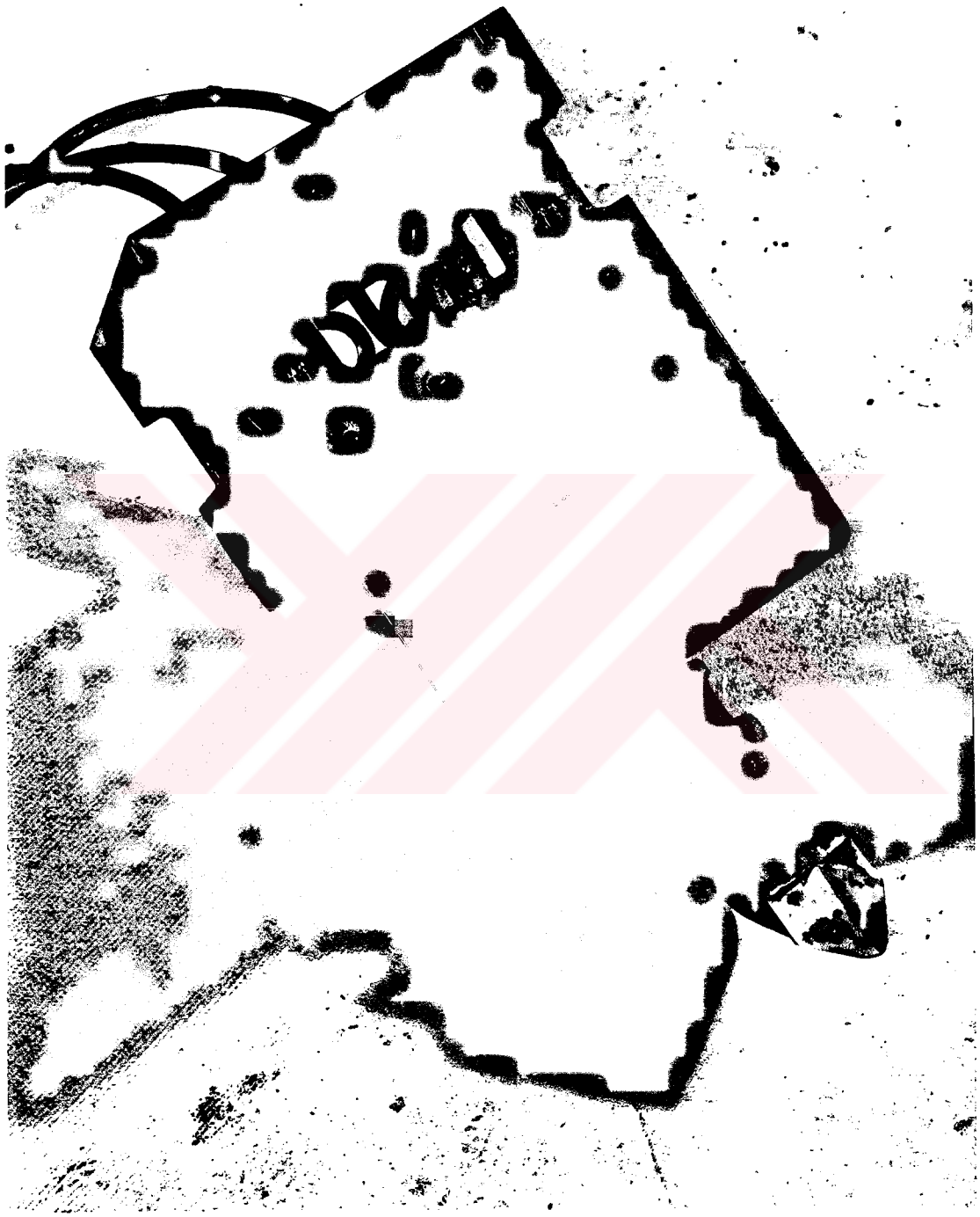

Figure 16. Dynamometer and V-faced pick

are digitized in the oscilloscope and stored on floppy discs for later transfer to a PDP 11/44 computer for analysis and permanent storage. A computer program processes the data and the results of the analysis are given in terms of mean cutting force, mean normal force and mean peak forces.

4.1.3. Rock Type

Indiana Limestone was the only rock used in this test program. The mechanical properties of this rock are given in Table 2. All of these mechanical properties were measured by Krech et al. (1974) with the exception of fracture energy, which was measured by Hoagland et al. (1973).

Indiana Limestone was selected: (a) because its mechanical properties are well known; (b) because it is homogeneous and, therefore, reproducible results can be obtained from cutting experiments; (c) because it is representative of the country rock for many coal and ore deposits; and (d) because limestone is known to be more resistant to water jet assisted cutting than almost any other rock type (Ropchan et al., 1980). Consequently, the findings from this program are regarded as conservative, since the force reductions are likely to be greater when cutting in other rocks.

4.1.4. Geometry of the Cutting Tool

The coal mining industry is the major consumer of drag bits for machine excavation. A number of tool geometries is available for coal cutting.

Table 2. MECHANICAL PROPERTIES OF INDIANA LIMESTONE.

MECHANICAL PROPERTIES OF INDIANA LIMESTONE

Uniaxial Compressive Strength	=	41 MPa (5945 psi)
Uniaxial Tensile Strength	=	5.3 MPa (770 psi)
Elastic Modulus In Compression	=	20 GPa (2.9×10^6 psi)
Elastic Modulus In Tension	=	31 GPa (4.5×10^6 psi)
Poisson's Ratio	=	0.27
Density	=	2340 Kg/m^3 (146lb/ft^3)
Porosity	=	12.5%
Permeability	=	80 x 10^{-6} mm/sec (3.2×10^{-6}in/sec)
Acoustic Velocity	=	4 km/sec (13,100 ft/sec)
Fracture Energy	=	60 J/m^2 (0.34 lb/in)

In general coal picks fall into two broad classes, the so-called point-attack or pencil point picks; and the chisel, sometimes referred to as radial, picks. In spite of years of research work and of practical experience a controversery continues to exist as to which, if either, of these picks is superior. In the U.S., pencil point picks are used almost exclusively, on continuous miners. On shearers, probably because longwall technology has been imported from Europe where chisel picks are favored, this type of pick is employed in most circumstances. In one of the most recent publications in the literature comparing pick types, Roxborough and Pedroncelli (1982) claim that chisel picks give better performances at shallow cutting depths, and that point attack picks are superior at cutting depths greater than 50 mm (2 in).

Two research publications where pick geometry has been examined with water jet assist cutting systems are found in the literature, (Ropchan et al., 1980; Tomlin, 1982). In the latter work the author reported that attempts to conduct cutting operations in hard limestone using a roadheader equipped with point attack picks was impossible because of the high force requirements of these picks. Tomlin reported success for cutting in this limestone using chisel picks only when water jets were used to assist the cutting operation. Ropchan and his co-workers, on the other hand, conducted dry cutting tests with both point attack and chisel picks but reported water jet assisted cutting results only for the point attack picks.

Based on the research findings of these workers, this experimental program has concentrated on the chisel pick. The pick used in these

tests is a Kennametal K-102, a 1 in wide V-face tool shown attached to the dynamometer in Figure 16. This chisel pick had a tungsten carbide insert mounted on the leading face of the bit. Another type of insert tested here was a sintered diamond layer mounted on a so-called PDC (polycrystalline diamond compact) bit. These PDC bits were used here in an attempt to extend the applicability of the results of this test program when different bit geometries are employed.

4.1.5. Hydraulic System

For the water jet assist system, first a 14 kW Kobe triplex pump with a pressure capability of 35 MPa (5,000 psi) and 0.3 ℓ/sec (5 gpm) flow rate was used. Higher pressures and flow rates were needed later in the test program. Therefore, a 70 kW pump of 70 MPa (10,000 psi) pressure capacity at a flow rate of 1.8 ℓ/sec (30 gpm) was added to the system to provide the full range of pressure and flow rate parameters required for the test suite.

A standard nozzle with a 13 degree tapered inlet followed by a short parallel section was used throughout the test suite. The performance of this nozzle was investigated in detail by Leach and Walker (1966), and the geometry of the nozzle is illustrated in Figure 8.

4.2. Experimental Design

A large number of variables exist in cutting tests, and a program to examine all of them would take many years to conduct. The variables

selected for testing in this research program were chosen to contribute to improving the understanding of the mechanisms of rock failure using water jets to assist cutting tools.

4.2.1. Experimental Procedure

A standard smooth rock surface was used for all cuts in the test program. The surface of the rock was cleaned with the compressed air before each new cut to remove the fine debris left from the previous cut. Since the conditioning of the rock surface was a time consuming process, it was decided to use proper spacing patterns which provided a large amount of information with a minimum usage of the conditioned surface.

4.2.2. Depth of Cut

In most of the tests the depth of cut was 15 mm (0.59 in). This depth of cut was chosen because it was deep enough to simulate the depths taken by the drag bits operating in the field and it was shallow enough to assure reproducible mean forces for a number of cuts over the length of the rock block.

4.2.3. Cutting Sequences

The sequence in which cuts are made on a rock block influences the pick forces. This occurs because breakout of the rock into grooves adjacent to those being cut reduces the forces on the cutting tool. Thus, if the

grooves are spaced sufficiently far apart that this interaction does not occur, the forces are a maximum; this condition is termed unrelieved cutting. On the other hand, if the grooves are spaced very close together, the bit forces are low but the quantity of rock removed is greatly reduced. An optimum condition exists wherein the specific energy, that is the energy required to remove unit volume of rock, is minimized. This condition can be expressed in terms of an optimum groove spacing to depth of cut (S/D) ratio. Furthermore, this optimum spacing to depth of cut ratio depends on whether the groove presently being machined is relieved by previous cuts on one side only (single relieved) or on both sides (double relieved). This phenomenon is well known and is described in the literature (Roxborough, 1973). It should be noted that these three cutting conditions all have practical significance. The unrelieved cuts represent conditions experienced by gauge picks. The double and single relieved cuts are representative of conditions experienced by other bits on a cutting head.

First, a series of experiments was conducted to determine these optimum ratios for grooves relieved on both sides and on one side. The results showed that these ratios were 4.0 and 3.3 for double and single relieved cuts respectively. The depth of cut was held constant in most of the tests at 15 mm; thus the spacing between adjacent cuts was 60 mm in the test suite where grooves had previously been cut on both sides of the present cut, and 50 mm where a groove had previously been cut on one side of the present cut.

Two sequences of cutting the rock block were followed in this experimental program. In one sequence, termed test sequence #1, a series of unrelieved cuts was made across the rock surface. These cuts were spaced 120 mm apart and no breakout between grooves was observed at this spacing. A second phase to this test sequence then was to cut between these grooves in a series of double relieved cuts, (Figure 17). The effective spacing between grooves in this second phase therefore was 60 mm. In the other test sequence, termed test sequence #2, a series of single relieved cuts was made by progressively indexing the cutting tool 50 mm from the previous groove, (Figure 18). Test sequence #2 was employed in most of the experiments, since it provided a large number of cuts, and thus more data from a single conditioned rock surface. Results with this test sequence were more consistent, because, in most cases, it was possible to test almost all levels of a single parameter on the same rock layer.

4.3. Preliminary Results

The water jet arrangement and a groove cut in the preliminary experiments on Berea Sandstone is shown in Figure 19. These early experiments on the sandstone was carried out to check and calibrate the system. Figure 20 shows a typical force-time trace for one of these early experiments. Large reductions in forces on the cutting tool are seen in the central portion of Figure 20 where the water jets are used.

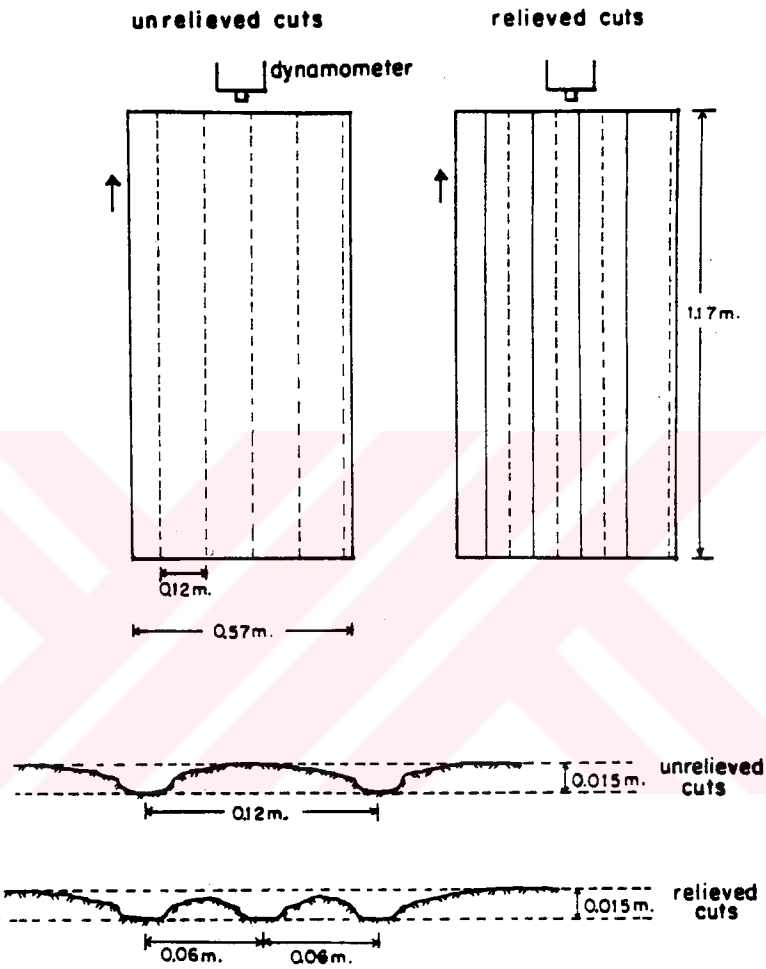

Figure 17. Test sequence #1 showing the unrelieved cut sequence, made first, and the double relieved cut sequence, made afterwards.

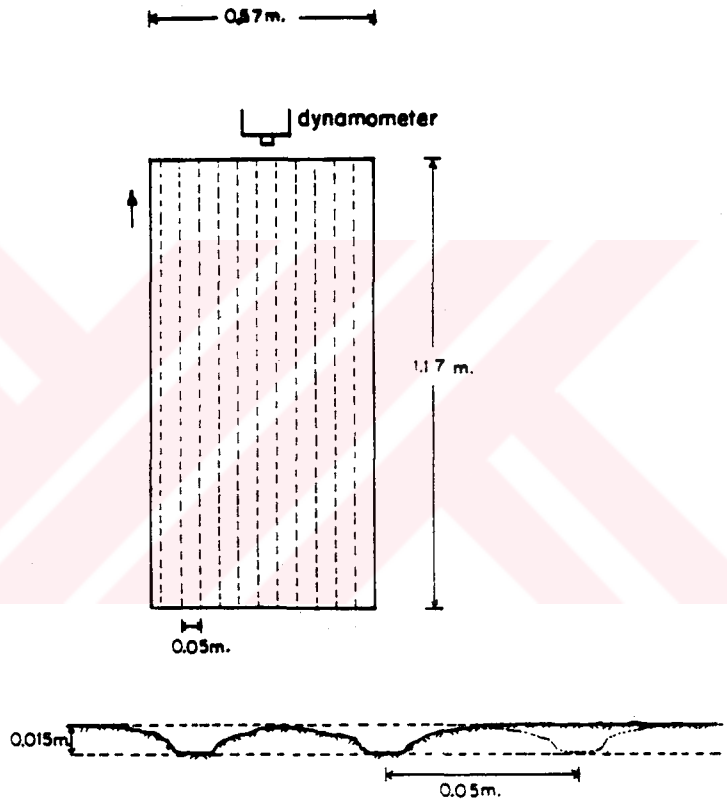

Figure 18. Single relived cuts in test sequence #2: bit was indexed in 50 mm steps from one side of the rock to the other.

Figure 19. Groove cut by a water jet assisted drag pick on Berea Sandstone.

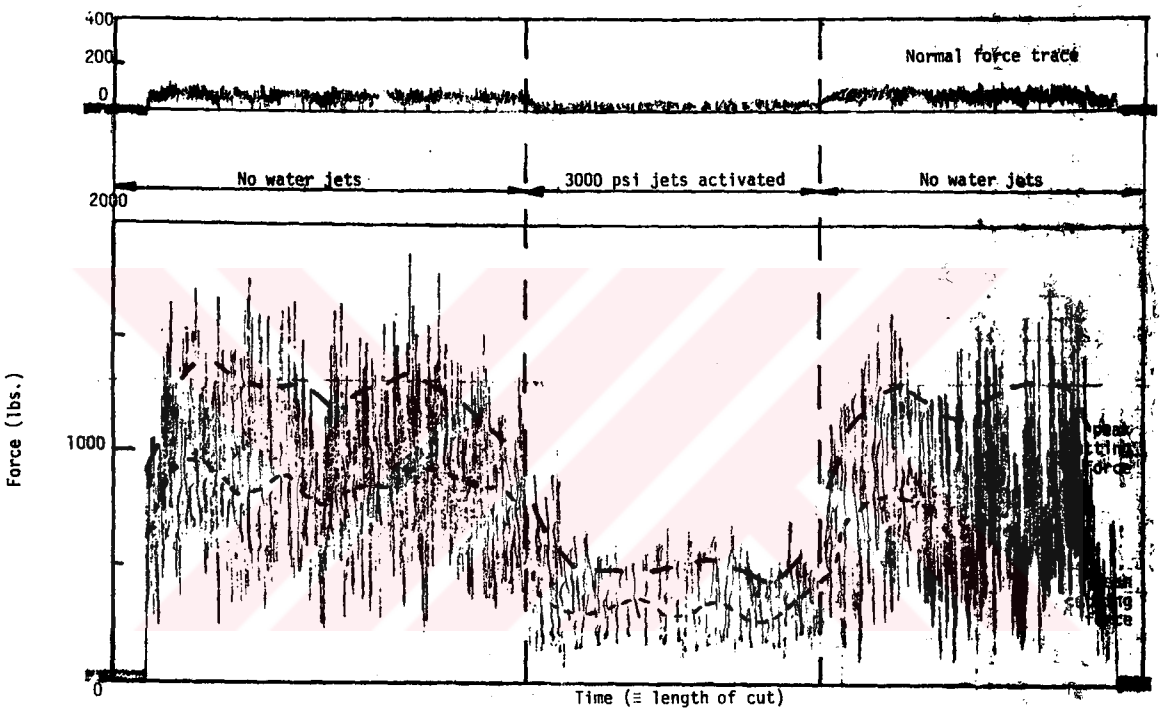

Normal force (upper trace) and cutting force (lower trace) as a function of length of cut showing the marked force reduction when water jets are used.

Figure 20. Typical force-time trace for a cut on Berea Sandstone.

5. EXPERIMENTS AND RESULTS

5.1. Factors Affecting The Performance of Water Jet Assist Systems

This section describes the cutting experiments that were carried out to study the factors influencing the force reductions on the bit with the assistance of water jets. A number of 15 mm deep cuts was taken by positioning a single jet behind the bit and ahead of the bit, and by using a double jet arrangement. The vertical distance, which is defined as stand off distance, between the nozzle and the rock surface was changed in order to investigate the effect of stand off distance on the performance of the water jet assist system. After optimizing the position, a range of jet pressures and nozzle diameters was examined. The results compare the bit cutting force, with and without water jet assist. For different cutting situations reductions in the drag force are expressed as percentages of the dry drag force. The bit normal force was also measured during the experiments, but this component of force was low, typically five to six times less than the cutting force. This high ratio of cutting to normal force is a characteristic of chisel bits when they are sharp. Because these tests were conducted in a non-abrasive rock, the normal force component did not increase perceptibly during the experimental program. Cutting speed was 54 mm/sec except for experiments described under the bit velocity section.

5.1.1. Jet Position

Test sequence # 1 was used for these tests and thus results were obtained for unrelieved cuts and double relieved cuts.

Three jet configurations were examined:

a) two jets parallel to the leading face of the bit, about 1 mm ahead of this face at a stand off distance of 25 mm (Figure 21)
b) a single jet parallel to the leading face of the bit, aligned in the center of the tungsten carbide insert, again about 1 mm ahead of the face (Figure 22)
c) a single jet positioned behind the bit in the central plane along the groove (Figure 23)

5.1.2. Single and Double jets

The first experiments in the test suite compared reductions in the drag force for double jets and a single jet directed immediately ahead of the bit. The nozzle diameter was 1 mm and the jet pressure was 35 MPa (5000 psi) for both jet configurations. Table 3 gives the mean cutting forces measured during these cutting tests.

In Figure 24 normalized force reductions are plotted as a function of jet power and jet flow rate for single and double jet configurations. This plot shows that the forces were reduced between 35 and 40 percent for both the relieved and unrelieved cuts when jets were used. The

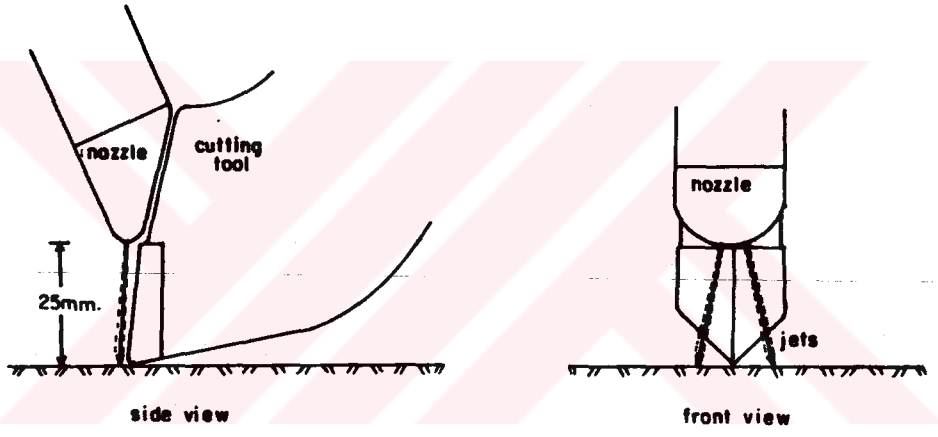

Figure 21. Double jet configuration ahead of the bit.

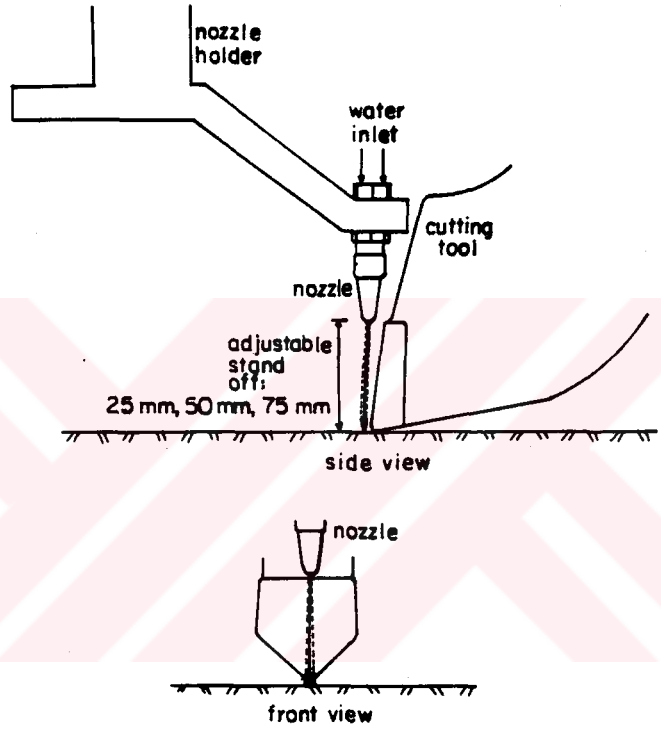

Figure 22. Single jet ahead of the bit.

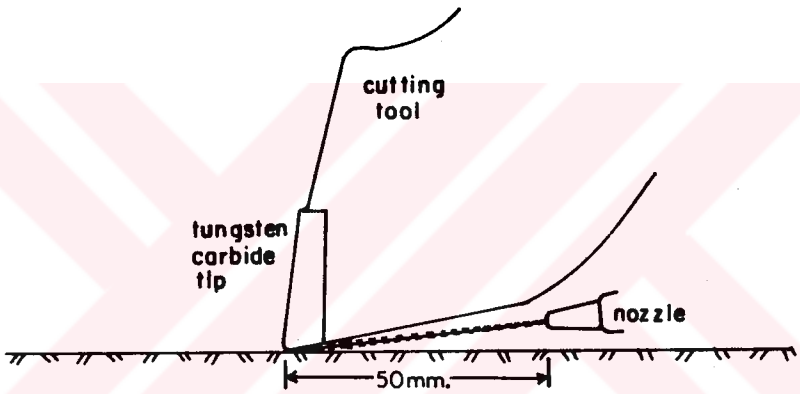

Figure 23. Single jet behind the bit.

TABLE 3. MEAN CUTTING FORCES WITH SINGLE AND DOUBLE JETS

	MEAN CUTTING FORCE F_{mc} (kN)	
	Relieved cuts	Unrelieved cuts
Without jets	3.47	3.97
Single jet	2.12	2.53
Double jets	2.15	2.67

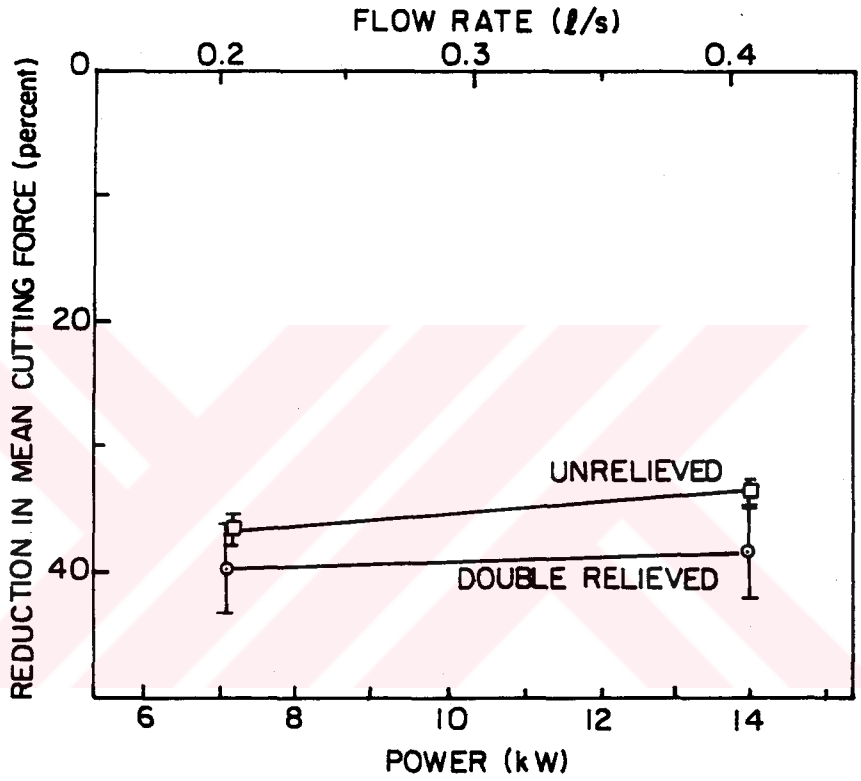

Figure 24. Force reductions with single (7 kW) and double jets (14 kW) ahead of the bit for relieved and unrelieved cuts.

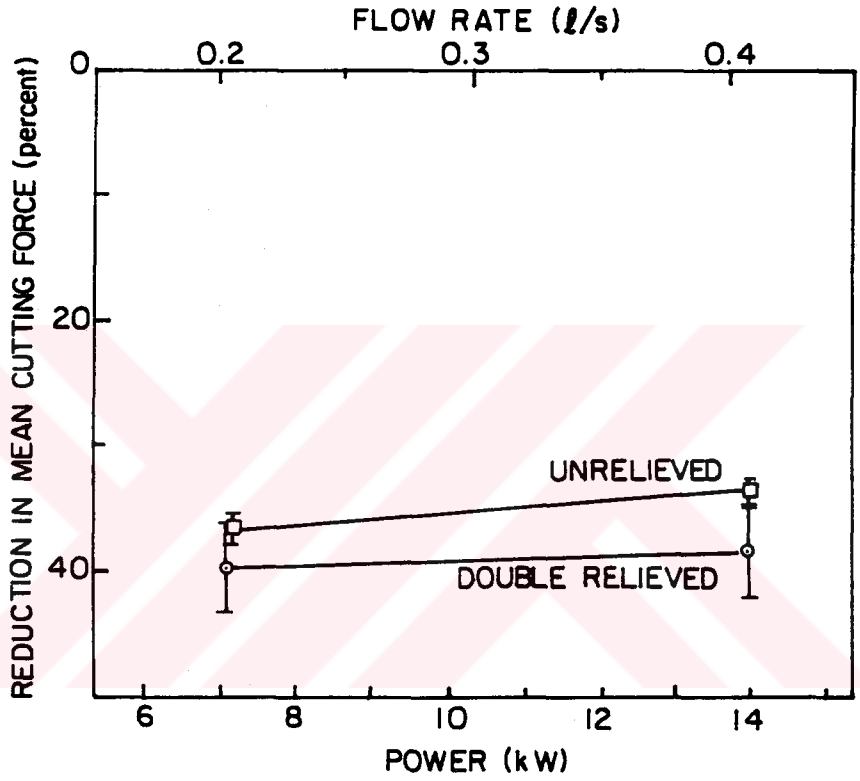

Figure 24. Force reductions with single (7 kW) and double jets (14 kW) ahead of the bit for relieved and unrelieved cuts.

interesting point illustrated by these curves is that no benefit was observed, in terms of increased force reductions, when double jets were employed. On the contrary, the force reductions observed with double jets were about the same as with the single jet, but the cost of achieving this force reduction was doubled, since the total flow rate and therefore total jet power was doubled. Thus it was concluded that with the jets directed ahead of the bit, a single jet system was superior.

5.1.3. A Single Jet Behind the bit

A single jet was positioned behind the bit and the force reductions achieved with this configuration were compared with the force reductions achieved with a single jet ahead of the bit. It was necessary to increase the stand off distance for these tests to 50 mm because of the restricted clearance between the bit body and the rock behind the bit. The nozzle diameter used in these experiments was 0.8 mm. Two jet pressures were examined, 20 MPa and 35 MPa.

Mean cutting forces measured for relieved and unrelieved cuts are given in Table 4. Normalized force reductions are plotted as a function of jet flow rate and jet power in Figure 25. With the jet in front of the bit and with a jet pressure of 20 MPa, the cutting force for the unrelieved cuts was reduced only 20 percent, whereas this force was reduced about 30 percent for the relieved cuts. With the jet in the same position but with the jet pressure increased to 35 MPa, an increased reduction in the bit cutting force, to about 40 percent, was

TABLE 4. MEAN CUTTING FORCES WITH JET BEHIND AND IN FRONT

	MEAN CUTTING FORCE F_{mc} (kN)	
	Relieved Cuts	Unrelieved Cuts
Without Jets	3.47	3.97
Jet In Front With 20 MPa	2.46	3.25
Jet In Front With 35 MPa	2.14	2.44
Jet Behind With 35 MPa	2.61	3.11

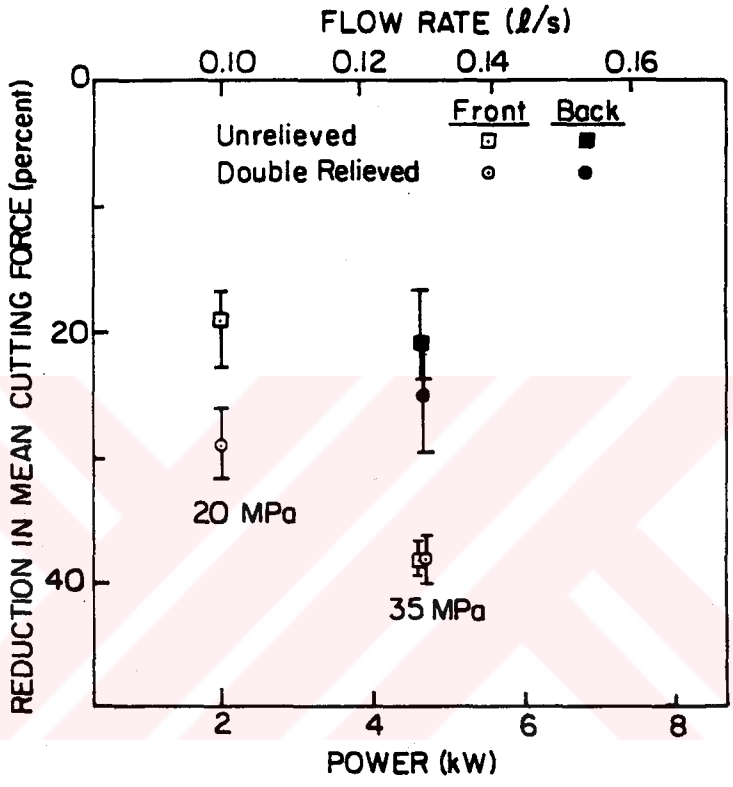

Figure 25. Single jet ahead of the bit and behind the bit at 20 and 35 MPa jet pressures for both relieved and unrelieved cuts.

observed for both the relieved and the unrelieved cuts. However, when the jet was moved to a position behind the bit (Figure 23), and with a jet pressure maintained at 35 MPa, the cutting force for the unrelieved cuts was reduced only about 20 percent, and for the relieved cuts it was reduced only about 25 percent.

This result that the water jet is more effective when positioned ahead of the bit contradicts the findings of Ropchan and his co-workers (1980), who reported greater force reductions with the jet behind the bit. It should be noted that the bit geometry for these two experimental programs was different. Ropchan et al. used a point attack pick for all of their water jet assisted tests and they reported only modest force reductions with the jet directed ahead of the pick. The geometry of the point attack pick may not be ideal to obtain full benefits of a water jet directed ahead of the pick since point attack picks are characterised by a large normal force component and the ratio of cutting to normal force (around one) is about five times less than the same ratio for the chisel bit used here.

5.1.4. Stand Off Distance

A single jet about 1 mm ahead of the bit (Figure 22) was used for these tests. Three standoff distances examined were:

a) 25 mm

b) 50 mm

c) 75 mm

Test sequence # 1 was followed during these tests. Two jet pressures examined were 20 MPa and 35 MPa. The flow rates were 0.075 ℓ/sec, 0.132 ℓ/sec and 0.205 ℓ/sec corresponding to three different nozzle diameters of 0.6 mm, 0.8 mm and 1.0 mm respectively at a constant 35 MPa pressure.

Force reductions at different standoff distances for a jet through a 0.8 mm nozzle at 20 MPa and 35 MPa are given in Figure 26 for double relieved cuts, and in Figure 27 for unrelieved cuts. When the jet pressure was 35 MPa the force reduction achieved was about 40 percent for both relieved and unrelieved cuts. At 20 MPa jet pressure, relieved cuts had a maximum cutting force reduction of 35 percent at a standoff distance of 25 mm. This force reduction decreased to about 24 percent at a standoff of 75 mm. For the unrelieved cuts, force reductions were slightly less than the reductions for the relieved cuts. The force reductions for the unrelieved cuts were 26 percent at a standoff of 25 mm, and 19 percent at a standoff of 75 mm.

Results in Figures 28 and 29 show force reductions at different standoff distances for three different nozzle diameters. Force reductions of about 40 percent were observed for both relieved and unrelieved cuts with 0.8 mm and 1.0 mm nozzles. This 40 percent force reduction was unaffected by the standoff distance. The effect of standoff distance on the force reductions with a 0.6 mm nozzle was strong, especially for the unrelieved cuts. In Figure 29 the maximum force reduction is seen to be 25 percent at a standoff distance of 25 mm, and this reduction decreases to about 5 percent at a standoff of 75 mm.

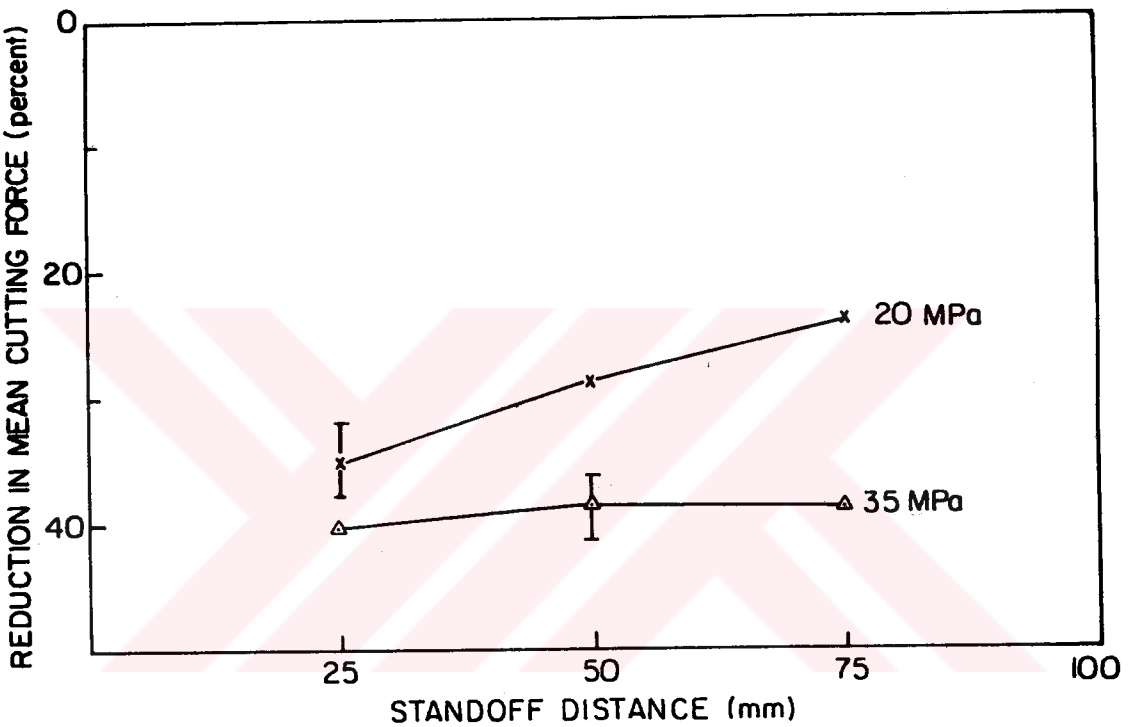

Figure 26. Force reductions as a function of standoff distance with 0.8 mm nozzle at 20 and 35 MPa jet pressures for double relieved cuts.

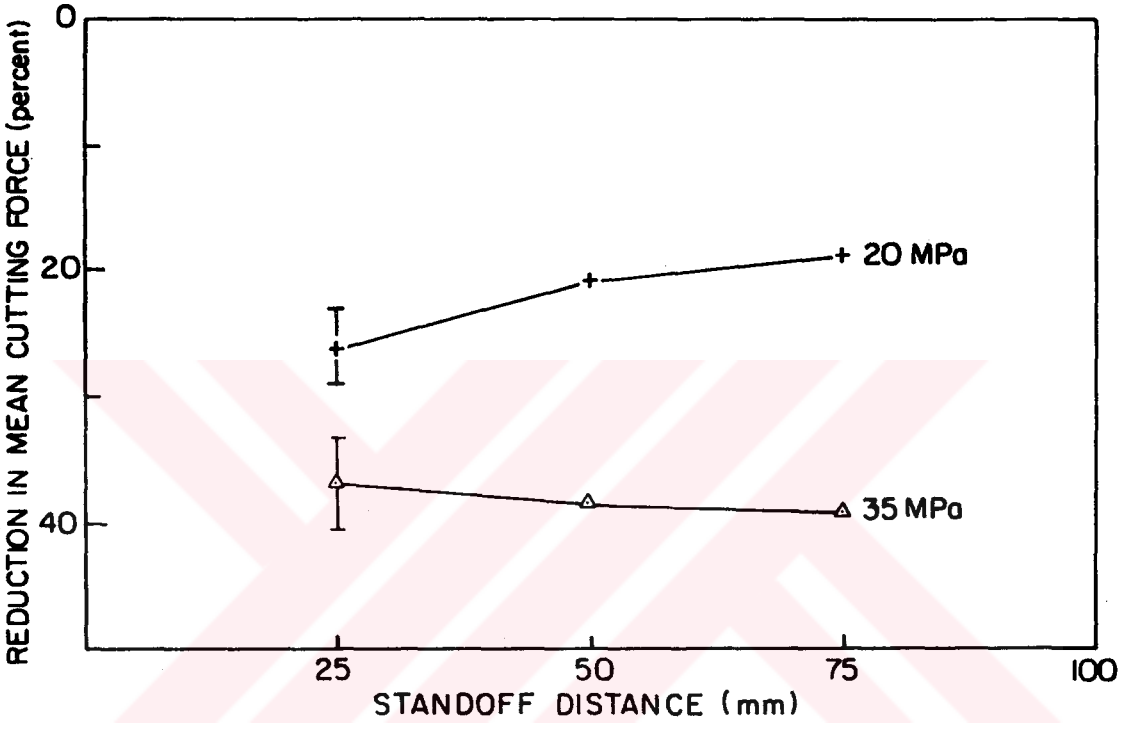

Figure 27. Force reductions as a function of standoff distance with 0.8 mm nozzle at 20 and 35 MPa jet pressures for unrelieved cuts.

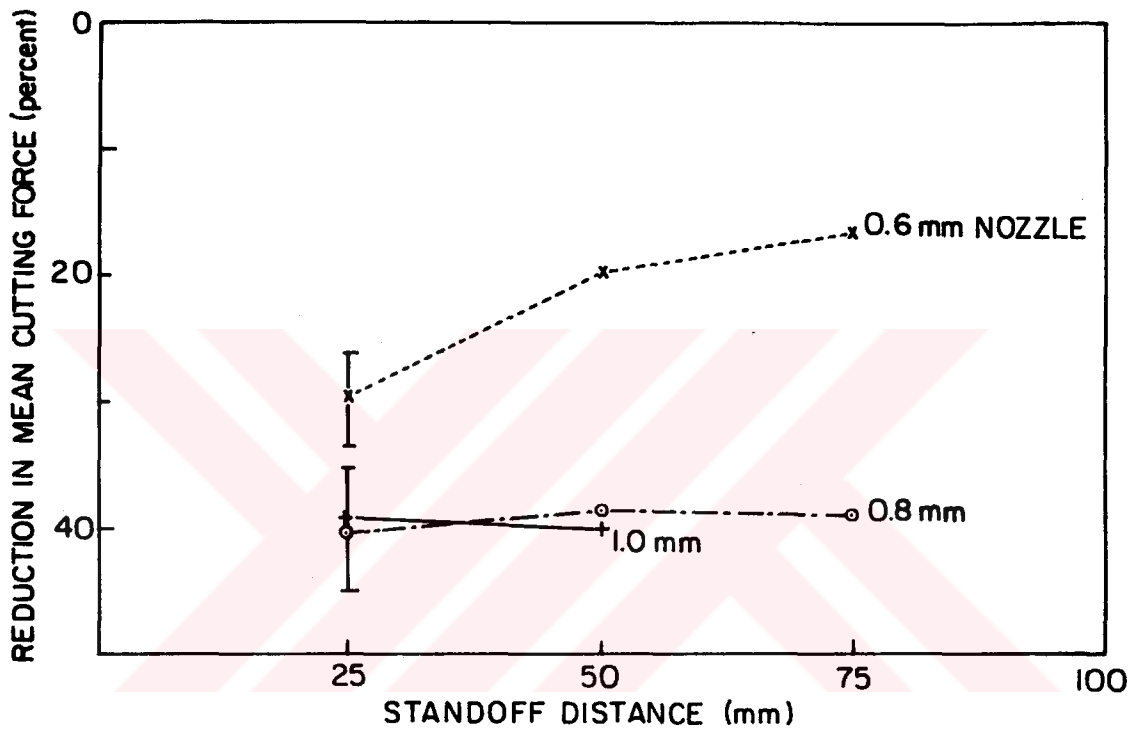

Figure 28. Force reductions as a function of standoff distance with three different nozzles at 35 MPa pressure for double relieved cuts.

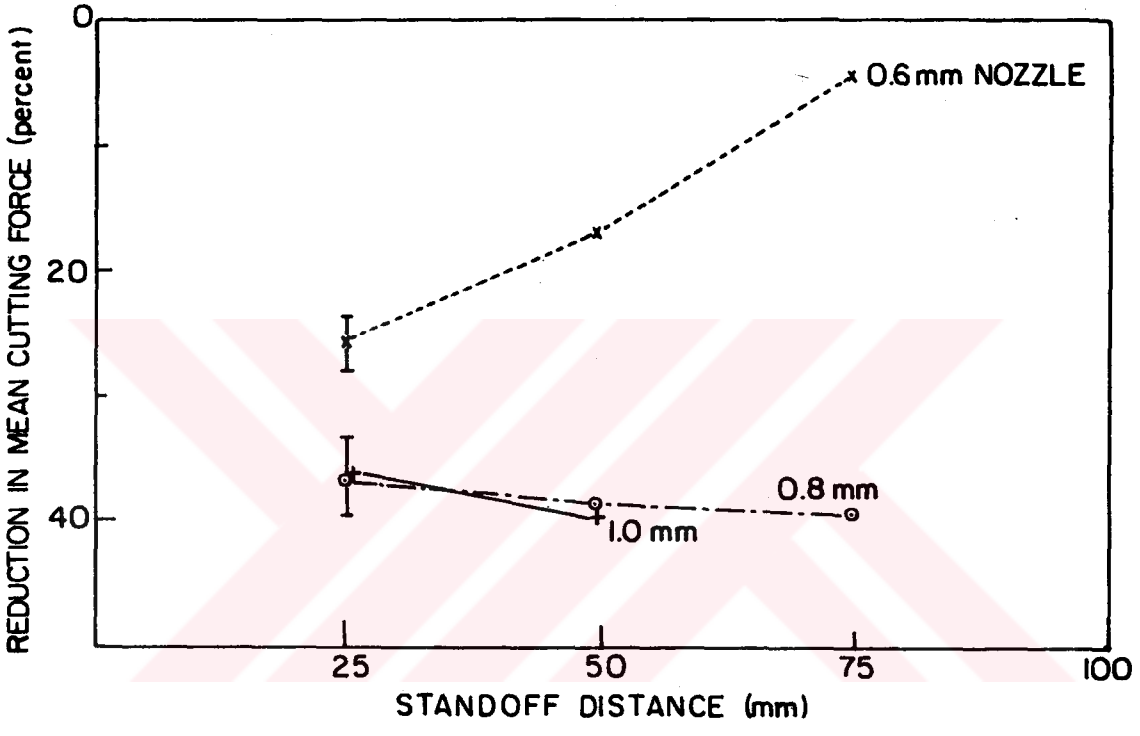

Figure 29. Force reductions as a function of standoff with three different nozzles at 35 MPa jet pressure for unrelieved cuts.

5.1.5. Jet Pressure

Test sequence # 2 was employed for a single jet ahead of the bit at pressures in the range 10-70 MPa. Five levels of jet pressure were 10, 20, 35, 50 and 70 MPa for three different nozzles: 0.6, 0.8, and 1.0 mm diameter. Figure 30 shows the normalized cutting force reductions plotted as a function of jet pressure for these single sided relieved cuts. From this figure it is seen that the maximum observed reduction in the cutting force was 50 percent, and it was achieved at 35 MPa pressure using a 1.0 mm nozzle.

The most interesting feature of the curves given in Figure 30 is the relatively rapid increase in the force reduction as the pressure increases from 10 to 35 MPa. At pressures higher than this, the rate of increase of force reduction falls off. It is interesting to note that at this pressure the jet itself initiates significant damage on the surface of the rock. In the case of the 1.0 mm nozzle, the force reduction appears to decrease after this pressure, indicating that an optimum pressure/flow rate combination might exist. Also, it is interesting to note that these curves are all grouped closely together, implying that at a given pressure little benefit is achieved by increasing the nozzle diameter and thereby the jet flow rate.

5.1.6. Jet Flow Rate

A large amount of water is undesirable in practical applications of water jet assist systems. Therefore, the quantity of water flowing

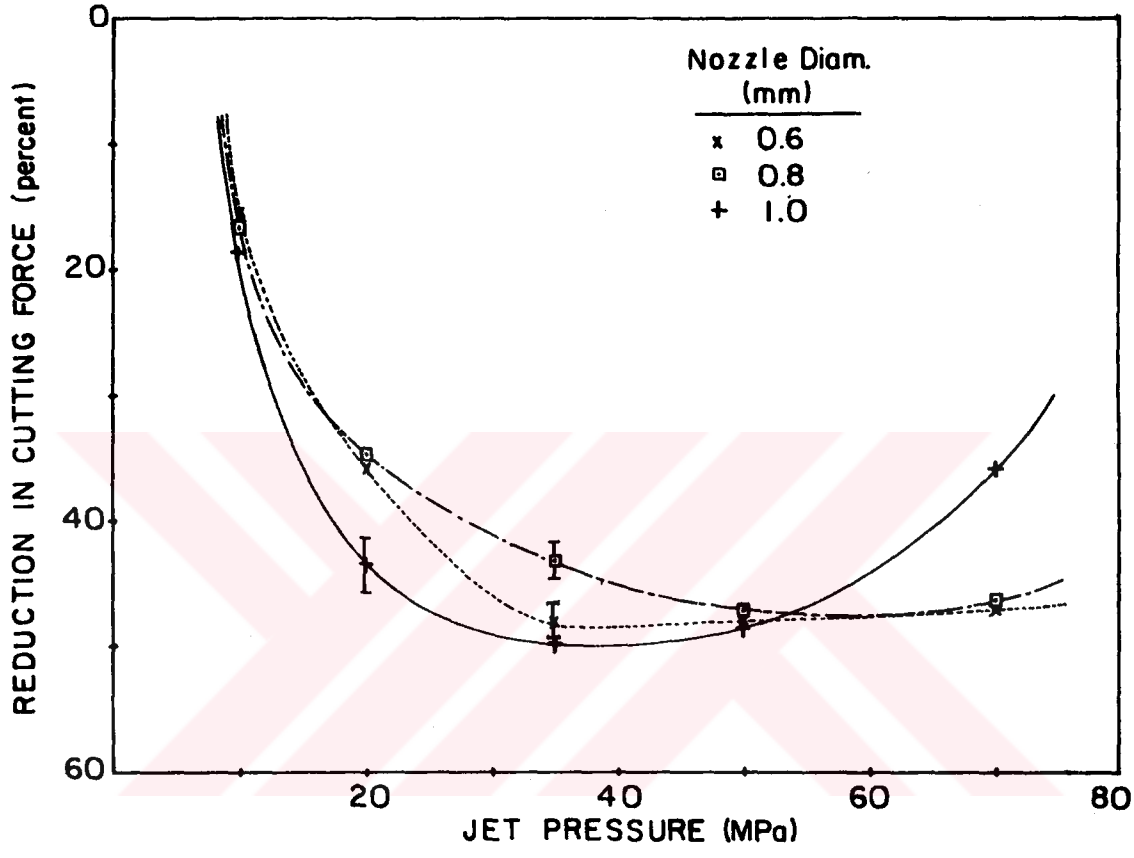

Figure 30. Force reductions for single relieved cuts as a function of jet pressure with three different nozzles.

through the nozzle has to be minimized, while benefits of the water jet assist system are maintained. Results of jet pressure experiments are replotted in terms of jet flow rate in Figure 31. Maximum force reductions are about 50 percent for all three nozzles. This implies that it is not necessary to employ large flow rates in order to achieve substantial force reductions.

The curves in Figure 31 show that force reductions increase rapidly at low flow rates, but again they appear to attain a maximum and beyond this value the benefit either decreases or, at least, does not improve. Obviously force reductions are not related to the flow rates in a simple manner. For example, with a flow rate of 0.08 ℓ/sec and a jet pressure of 35 MPa, the measured force reduction was 49 percent. At almost the same flow rate, 0.07 ℓ/sec, but at a jet pressure of 10 MPa, the force reduction was only about 16 percent. Thus it appears that reductions in bit forces depend more strongly on the pressure than the flow rate.

5.1.7. Jet Power

Results shown in Figures 30 and 31 are plotted again in Figure 32 to study the influence of jet power on the force reductions. This plot illustrates clearly that jet power is the key to understanding the nature of force reductions. Within experimental error the three curves obtained for the nozzles that were tested are almost indistinguishable in Figure 32. The force reduction increases very rapidly at low jet power levels. Beyond a jet power of about 3 kW, no benefit is observed in terms of increased reductions in bit forces. If the jet power level

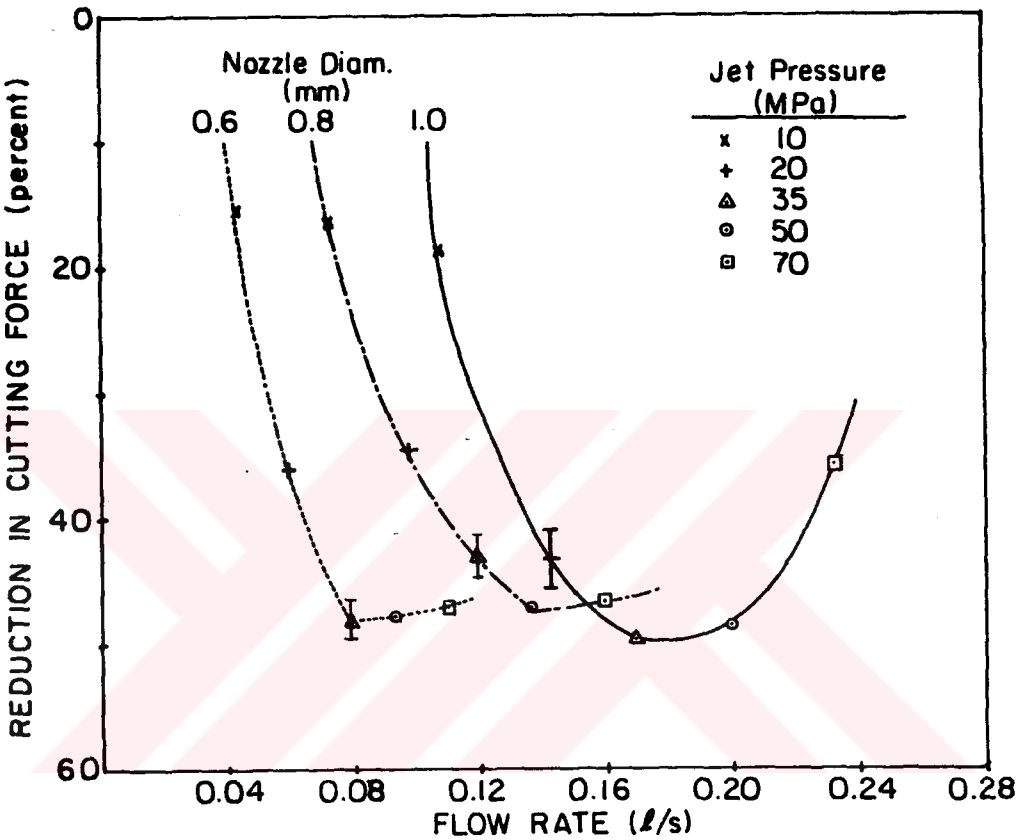

Figure 31. Force reductions for single relieved cuts as a function of flow rate for three different nozzles.

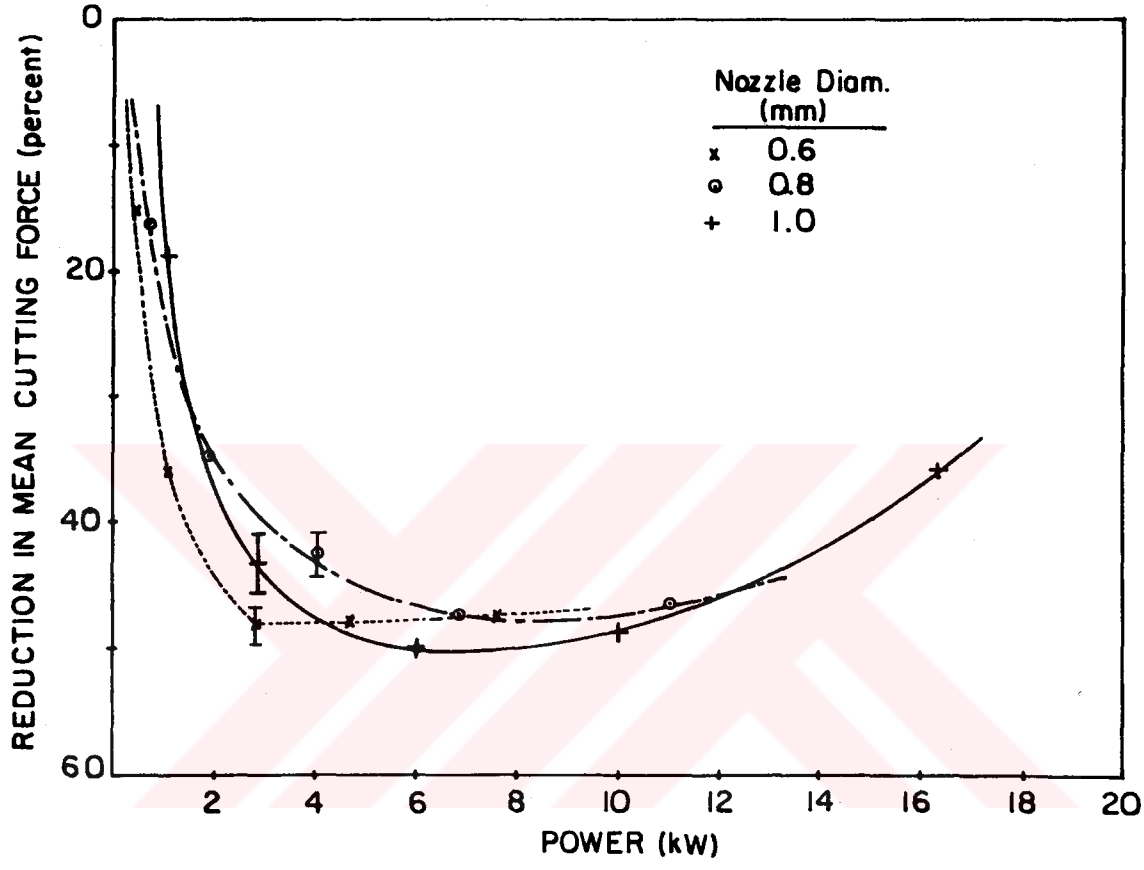

Figure 32. Force reductions as a function of jet power.

exceeds 11 kW, force reductions begin to decrease. The nature of this decrease is not clear. In Section 5.1.5 it was noted that when these powerful jets were used, the jet, after a certain pressure level, would cut the rock ahead of the moving bit. The amount of material cut by the jet alone is not much, and this cutting action might be absorbing the jet energy which could have been used for assisting the bit in more effective ways.

5.1.8. Bit Velocity

Laboratory studies, covering cutting speeds within and well beyond the range commonly associated with mining machines, consistently show that bit speed does not effect bit forces and cutting energies, (Roxborough and Pedroncelli, 1982). However, when water jets are used in conjunction with bits, it is not clear that this result will hold. In other words, it may be that a certain jet energy per unit length of cut is required to achieve the force reductions described in previous sections. Examining this behaviour in detail is necessary for the water jet assisted cutting technology to progress out of the laboratory phase.

The bit velocity was increased four times from 54 mm/sec to 216 mm/sec in this test suite. Test sequence # 2 in Figure 18 with single relieved cuts was again used for these experiments. Results in Figures 33, 34, and 35 illustrate the influence of jet pressure, jet flow rate, and jet power on the force reductions for the high speed tests. These figures are equivalent to Figures 30, 31, and 32, respectively. Curves for the high speed cuts are similar to those discussed previously for the slow

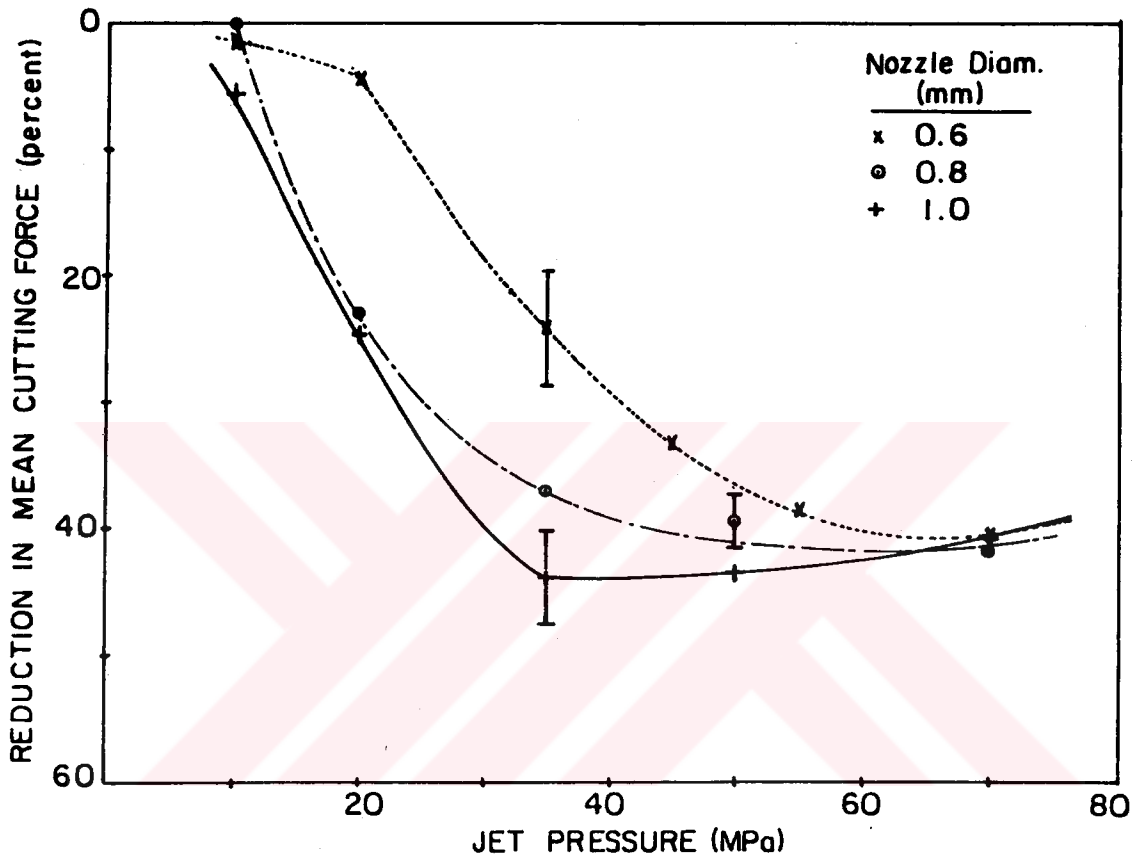

Figure 33. Force reductions as a function of jet pressure at the higher bit velocity.

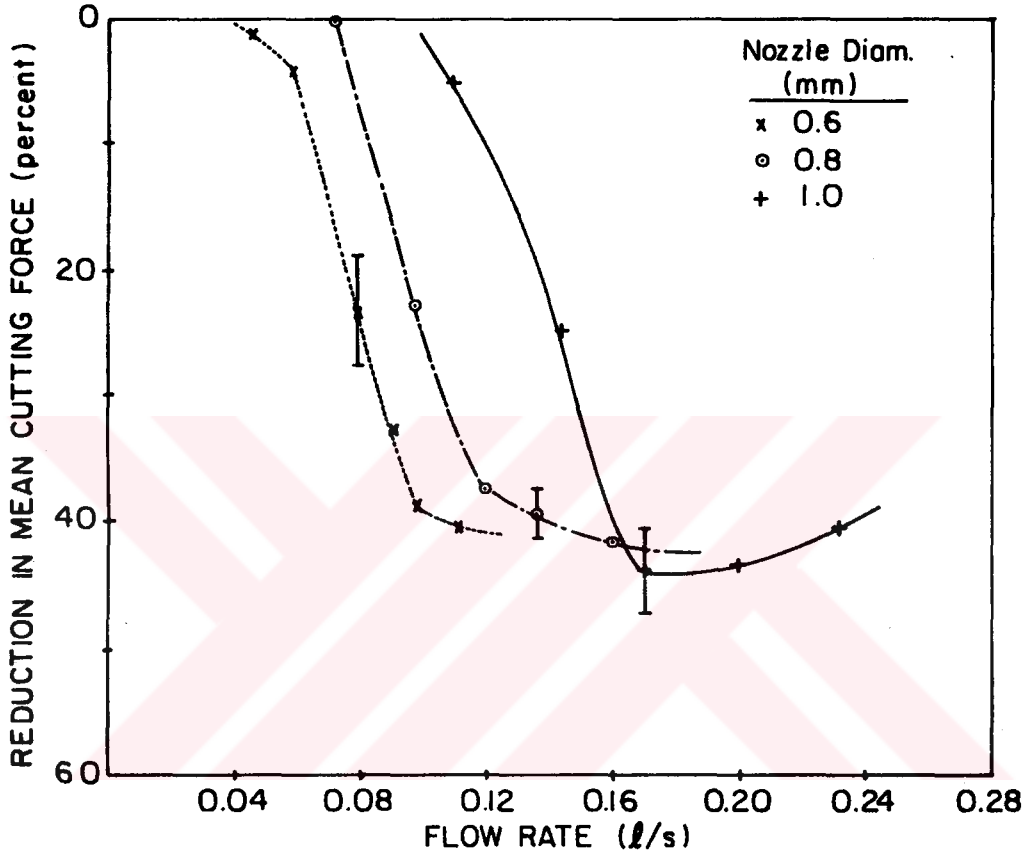

Figure 34. Force reductions as a function of jet flow rate at the higher bit velocity.

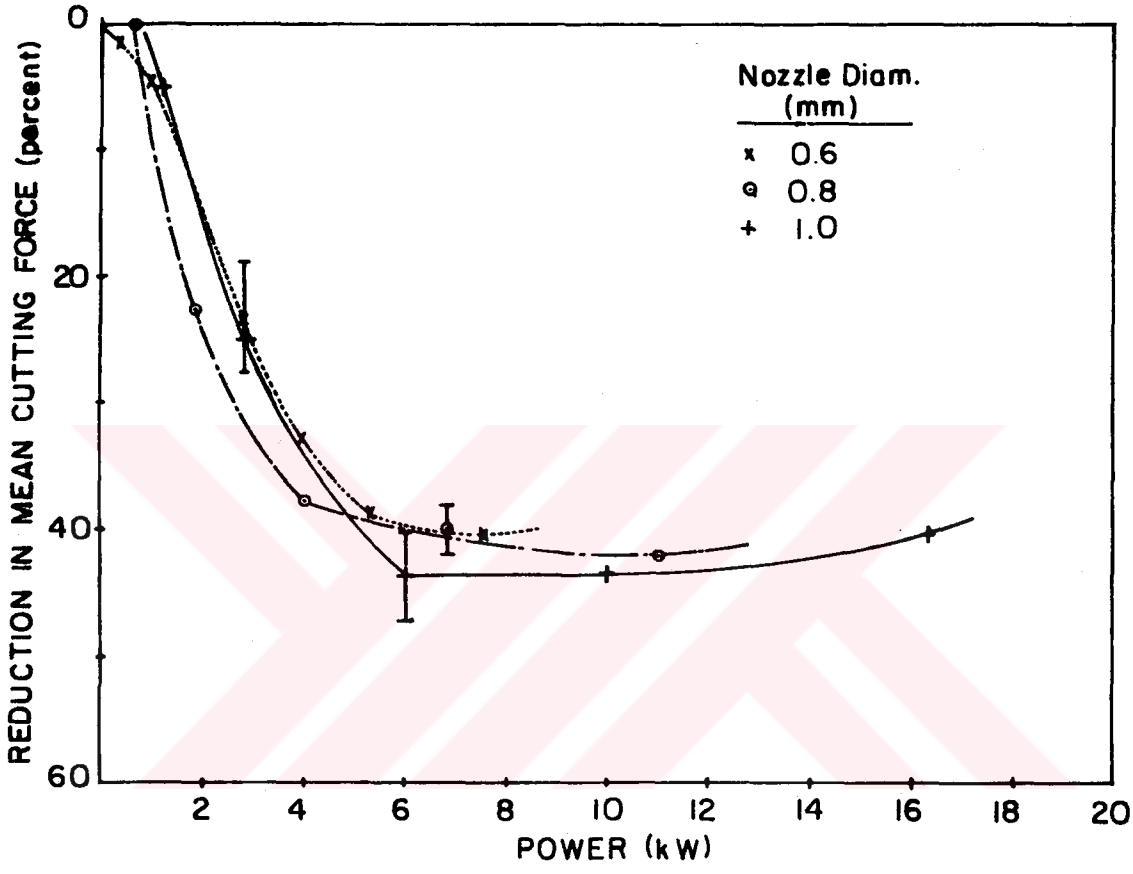

Figure 35. Force reductions as a function of jet power at the higher bit velocity.

speed cuts. However, when the two figure groups are compared, it is observed that there is a slight decrease in benefits for the higher speed. Maximum force reductions are about 40 percent at the high speed, compared with about 50 percent at the slow speed. As was true at the low cutting velocity, the three curves relating the jet power to force reductions can, within experimental error, be treated as one curve at the high cutting speed.

The influence of the jet pressure on the bit force reduction at different bit speeds is illustrated in Figure 36, which was obtained by normalizing the jet pressures in Figures 30 and 33 with the bit velocity. Similarly, force reductions are replotted in Figure 37 by normalizing the flow rates in Figures 31 and 34 with the bit velocity. The graphs obtained were similar for all three nozzles that were employed in this test suite. Consequently only curves that are presented here are for the 1 mm diameter nozzle.

The normalized flow rate curves in Figure 37 are interesting because they show that, when the cutting speed was increased by a factor of four, the quantity of water used per unit length of cut at the point of maximum force reduction was decreased from 3.2 ℓ/m to 0.8 ℓ/m, also a factor of four. The corresponding maximum force reduction changed from about 50 percent at the low cutting speed, to about 44 percent at the high cutting speed. This means that when the cutting speed was increased by 400 percent the bit force reduction was decreased by only 6 percent.

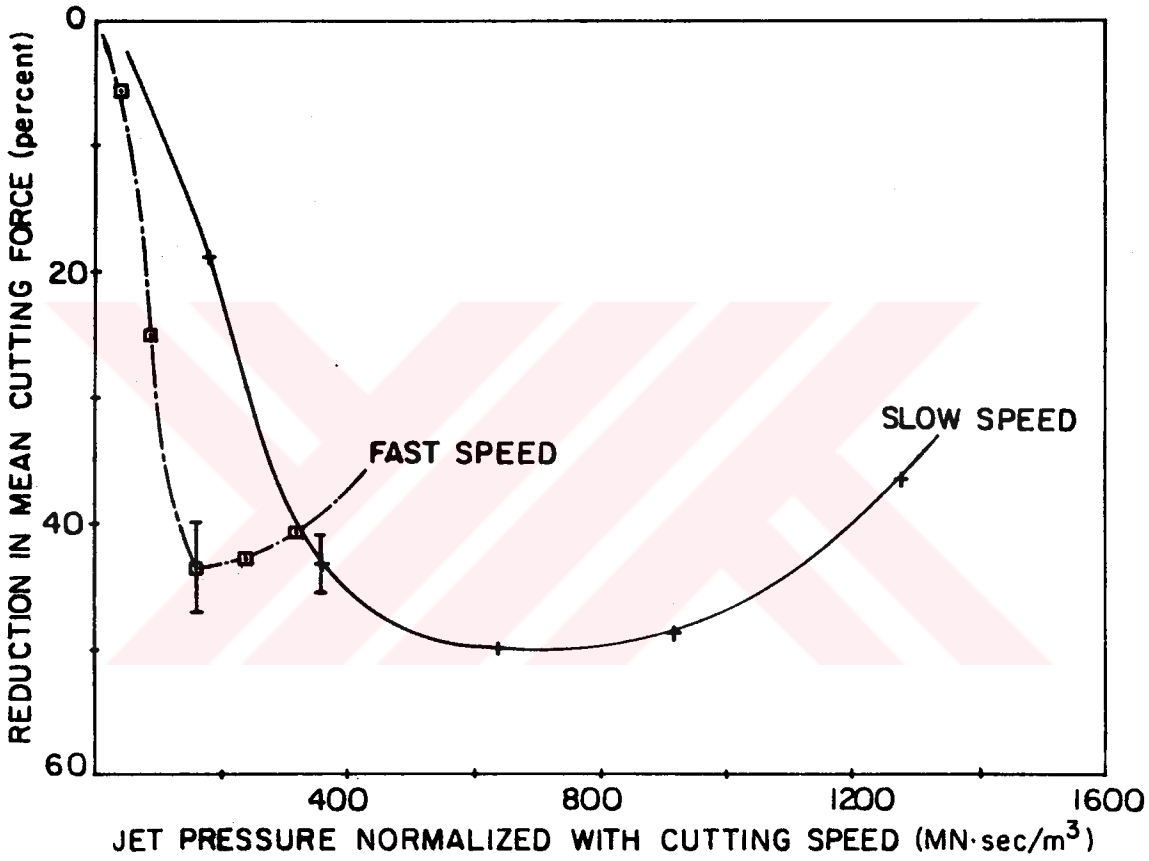

Figure 36. Force reductions as a function of normalized jet pressure at the fast and slow cutting speeds for 1 mm nozzle.

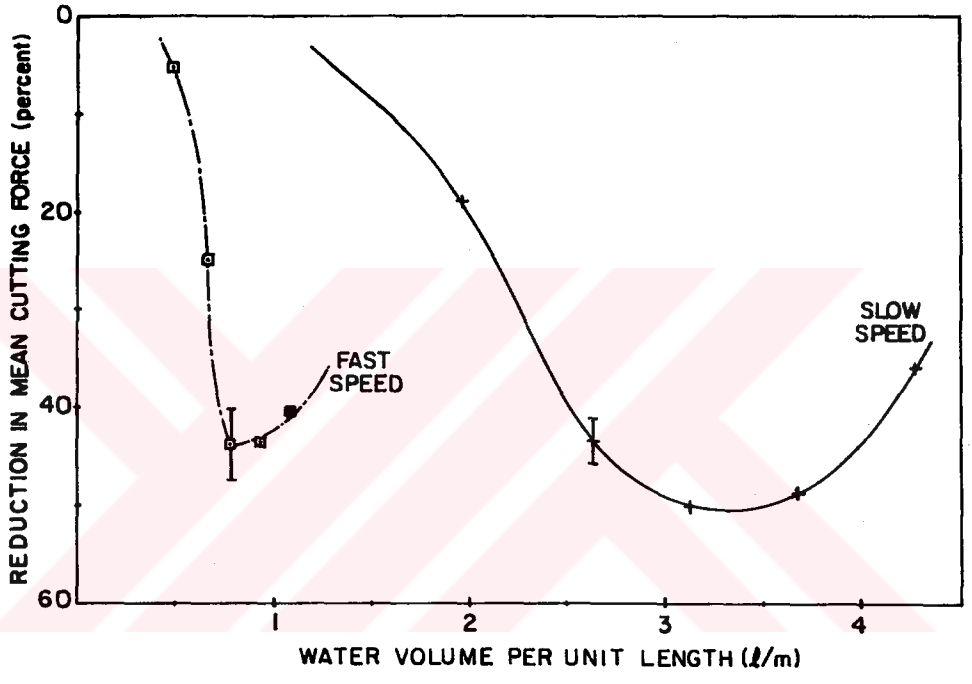

Figure 37. Force reductions as a function of normalized jet flow rate at the fast and slow cutting speeds for 1 mm nozzle.

Normalizing the jet power with the cutting speed gives the required jet energy per unit length for a certain force reduction, and the resulting curves are the most interesting of the set of the normalized curves developed in this section. For this reason, the jet energy per unit length of the cut in kJ/m is given for all three nozzle diameters, and these curves are presented in Figures 38, 39, and 40. The shape of all of these curves is essentially the same. Because the maximum jet pressure was limited to 70 MPa, the curves at the smallest jet diameter, 0.6 mm, are not fully developed at high jet energy levels. The most fully developed curves are the ones given in Figure 38 for the 1 mm diameter jet, since the highest jet energy level is reached for this nozzle diameter at 70 MPa pressure.

As noted previously, a characteristic of the curves in Figures 38, 39, and 40 is that the force reduction increases rapidly at low jet energy, or jet power, levels. There is a transition region where the slope of the curves changes rapidly, and at somewhat higher jet energy levels the force reduction continues to increase, but at a lesser rate. The curves then reach an apparent minimum (Figure 38), and the force reduction begins to decrease rather slowly. Figure 38 is the only plot where the minimum for both the high and the low speed curves is developed, and these minimums are identified by arrows in the figure. The minimum for the low bit speed occurs at a jet energy level of about 140-150 kJ/m. For the high bit speed curve the minimum is located at 30-35 kJ/m. This is a difference of a factor of four. With some imagination, the curves in the other two figures can be extrapolated, and this factor of four for the relative positions of their minimums appears to hold. Again

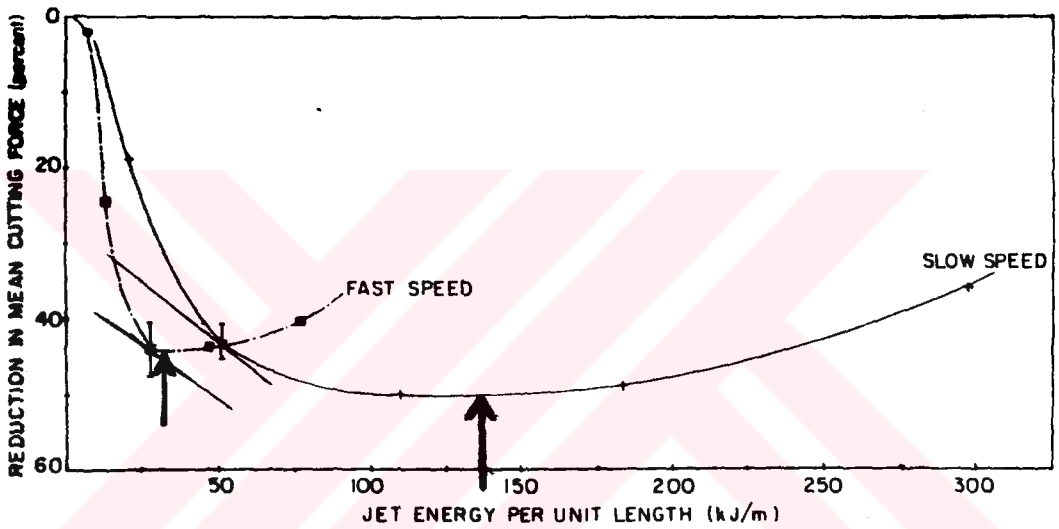

Figure 38. Force reductions as a function of normalized jet power at the fast and slow cutting speeds.

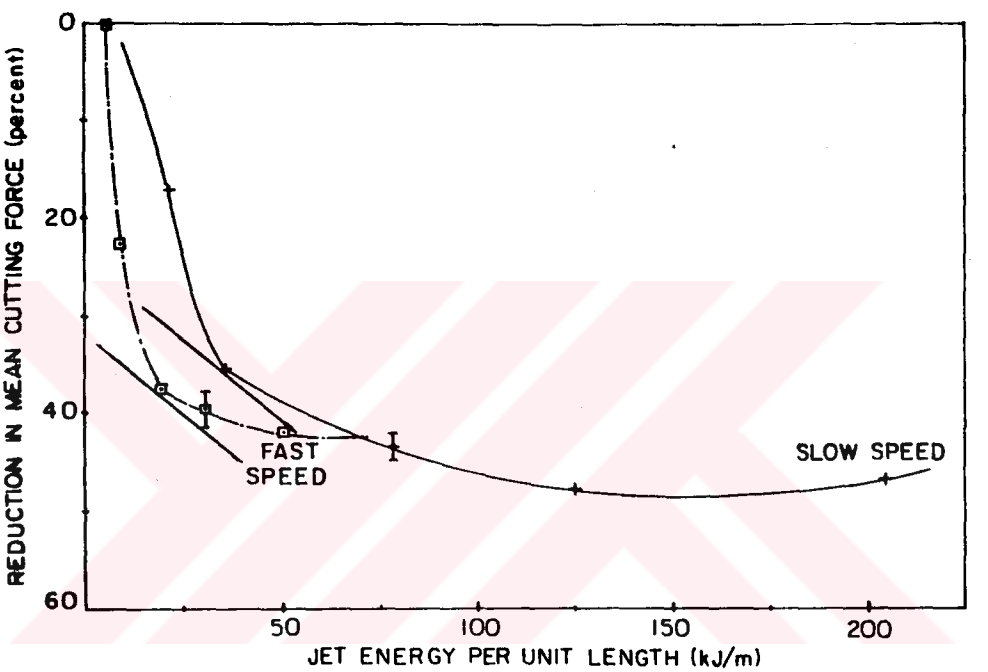

Figure 39. Force reductions as a function of normalized jet power at the fast and slow cutting speeds for 0.8 mm nozzle.

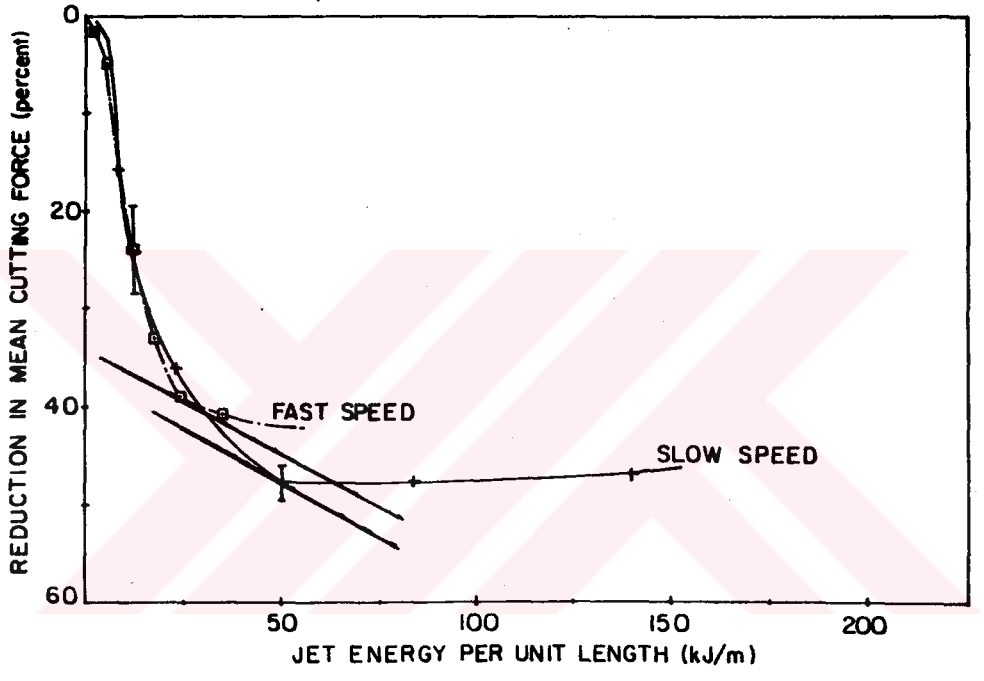

Figure 40. Force reductions as a function of normalized jet power at the fast and slow cutting speeds for 0.6 mm nozzle.

then it appears that there exists a one-to-one correspondence between bit velocity and a jet parameter, in this case jet power. The location of rapid slope change on Figures 38, 39, and 40 are marked with lines tangent to the curves at these slope change points. These points have been identified by visual inspection. These plots reveal that the maximum force reductions are not necessarily the optimum operating points. Because, in most cases, the rate of change of increase in force reductions slows down at these fairly well defined marked points in the curves, and the difference in the force reduction between these points and the minimums is small.

These corner points of the curves may be the most energy efficient points to operate the system. However, for an exact identification of these points in designing a water jet assist system, a benefit analysis must be conducted. The exact slope of the tangent lines in Figures 38, 39, and 40 must be determined as a result of this analysis. Functional relationship between the force reduction, R, and the jet energy per unit length, J_e, in these figures can be written as

$$R = f(J_e) \ . \tag{6}$$

The slope of the tangent lines in the figures is $\partial R / \partial J_e$, and in conducting the analysis this can be expressed as

$$\partial R / \partial J_e = f(\eta) \tag{7}$$

where $f(\eta)$ is some benefit function, and it changes depending upon the relative importance of benefits and disadvantages when water jets are used. The following examples show the way this benefit analysis should be conducted:

(i) In some applications, bit wear might be the most important factor in Equation (7). Cutter cost per unit volume of rock handled might be too high. Therefore, a higher reduction in bit forces, even though this would mean a higher J_e, might be desired. In this case, $f(\eta)$ would be algebraically higher, meaning that the tangent lines marking the efficient operating points would be flatter in Figures 38, 39, and 40. Hard and abrasive rock types, by promoting the bit wear, would also have the same effect on the benefit function $f(\eta)$.

(ii) Cutters may jam too frequently for a low J_e, causing excessive machine vibrations. A higher force reduction,thus a higher J_e might be economically feasible, since these vibrations would increase the maintenance cost for the machine parts. This would again indicate a higher value of $f(\eta)$.

(iii) Beyond some value of the jet pressure, and thus J_e, the operating and capital costs of the high pressure equipment might be too high compared with the benefits of the water jet assist system. This restriction would also have to be included in the function $f(\eta)$, which, in this case, would decrease, and this would result in a steeper slope in the force reduction-jet energy figures.

Finally, assuming that these corner points are the most efficient operating points for the system, an interesting feature of these three plots is that the ratio of the normalized jet power, or the jet energy per unit length at the fast and the slow cutting speeds is 2:1. Thus, a four times increase in the bit velocity requires an apparent two times increase in the jet power. Unfortunately, the limitations of the experimental apparatus did not permit cutting tests to be carried out at higher bit speeds, and thus only two data points are available. Future research work should concentrate on conducting these experiments at higher bit speeds of orders of magnitude of 1 m/sec, because it is power level of each jet on a mining machine where the pick is rotatating with a peripheral velocity of 1-3 m/s, that is of practical concern.

5.2. WATER JET ASSISTED DRILLING BITS

In the previous section significant benefits and interesting results were reported for a tungsten carbide drag bit assisted by water jets. A similar experimental program described in this section aims to investigate the benefits of using a water jet assist system for bits used in the drilling industry. It is also interesting to see if the same results hold for a different bit geometry.

A test series examining polycrystalline diamond compact (PDC) bits of various geometries is described here. These bits have been chosen since they find increasing application for drilling oil and gas wells. Currently PDC drag bits take very shallow (<1 mm), and thus highly inefficient cuts. It is argued that if deeper cuts are taken the overall efficiency of the drilling process will improve. Deeper cuts cause an increase in the bit forces. The approach taken to reduce these forces will be to use the technique of assisting the PDC drag bit with a moderate pressure (<70 MPa) water jet directed immediately ahead of the bit.

5.2.1. Polycrystalline Diamond Compact Bits

The main cutting unit for PDC bits is a sintered diamond surface bonded to a tungsten carbide substrate. This design is an important technological development, since the very hard diamond material promises to offer better resistance to wear than conventional tungsten carbide tools. Although the technology of PDC inserts is still in a developing

stage, already the drilling industry is reporting favorably on its application. (Arceneaux and Fielder, 1983; Offenbacher et al., 1983; Cress, 1983).

The fundamental limitation on the use of PDC bits is bit wear, and the bit wear increases with cutting speed. This increase is presumably a result of the increased temperatures associated with higher speeds. Ortega and Glowka (1984) measured this temperature increase with thermocouples mounted in the bit body, close to the bit:rock interface. Very shallow cuts (0.05 mm and 0.15 mm) were taken on Tennesse marble with 1.12 and 0.44 m/sec cutting speeds. A coolant water jet was directed to impinge on the leading face of the bit, and the bit temperatures were measured again. The jet pressures and nozzle diameters used were not reported. However, the flow rates used were of the same order of magnitude as the ones in this program, and results were given in terms of these flow rates. Temperatures in the bit body were also computed by using finite difference models for two jet flow rates (0.09 ℓ/sec and 0.41 ℓ/sec). A comparison of computed and measured wearflat temperatures is given in Figure 41. The temperature limit for the diamond matrix is around 700° C, and even with the help of a water jet the temperatures in the bit body are shown to reach almost half the limiting temperature of the diamond for these shallow cuts. It is also shown in Figure 41 that the temperatures in the wearflat are reduced with increasing flow rate, and this clearly illustrates one of the ways water jets assist the bit, namely the cooling effect.

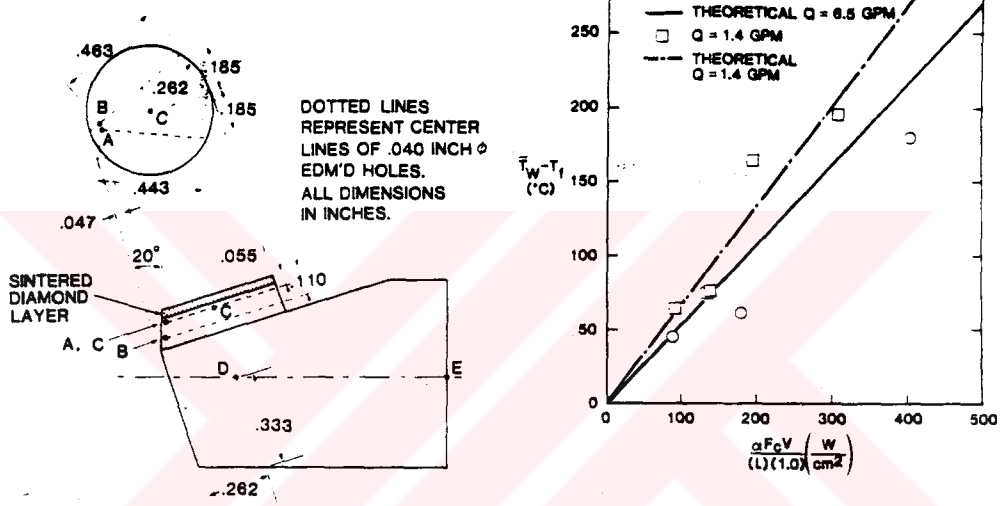

Thermocouple locations in PDC cutter instrumented for temperature measurements.

Comparison of predicted and measured wearflat temperatures.

Figure 41. PDC bit temperatures for shallow cuts on Tennesse Marble, (after Ortega and Glowka, 1984).

5.2.2. Experimental Program For PDC Cutters

(i) Bit Geometry

In addition to investigating the influence of water jets to assist PDC bits, this experimental program was designed to study other factors relating to the performance of these bits, including the effects of bit geometry and depth of cut. Five different bits were used in these cutting tests. These are illustrated in Figure 42. These bits differed only in the shape of the diamond insert, that is the shape of the leading bit face. Bit # 1 had a saucer shaped or concave face; bit # 2 had a convex face; bit # 3 was the conventional flat disc; bit # 4 was a flat disc but was angled sideways; bit # 5 was a flat disc that was cut off along three chords to give sharp corners on the cutting surface. All of these bits were 12.5 mm in diameter.

(ii) Experimental Apparatus

The linear planing machine described earlier was again used for these experiments. The rock type was again Indiana limestone.

The depth of cut taken using the PDC bits is small compared to that taken with say a coal pick. It is important to measure this parameter accurately, since the bit forces are affected significantly by small changes in the depth of cut. Therefore, a new depth gauging instrument had to be added to the equipment described in Section 4.1. This depth instrument consisted of a strain gauged cantilever (Figure 43), that was

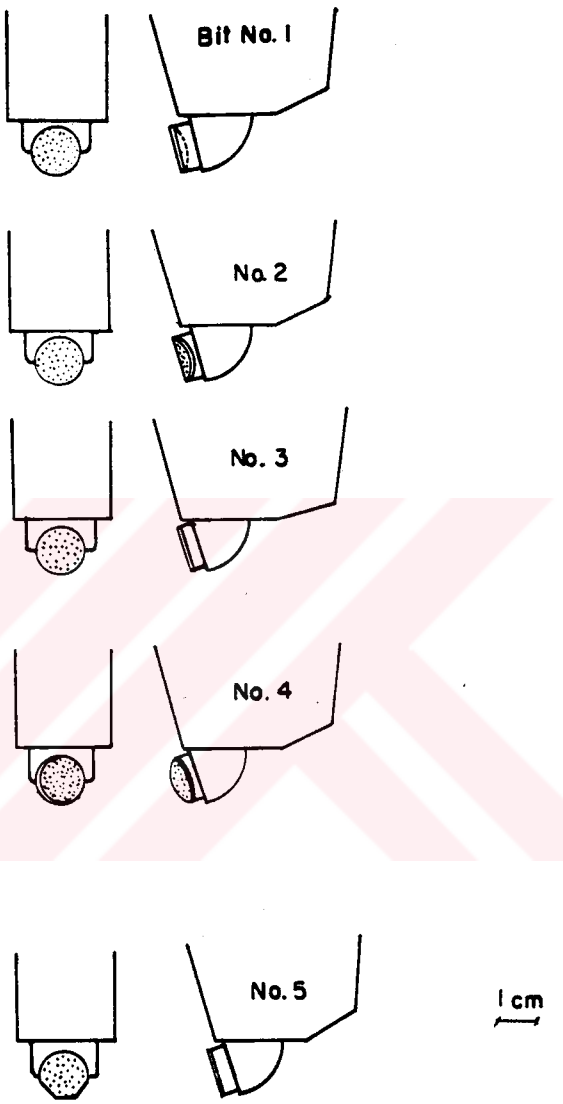

Figure 42. Different bit designs investigated.

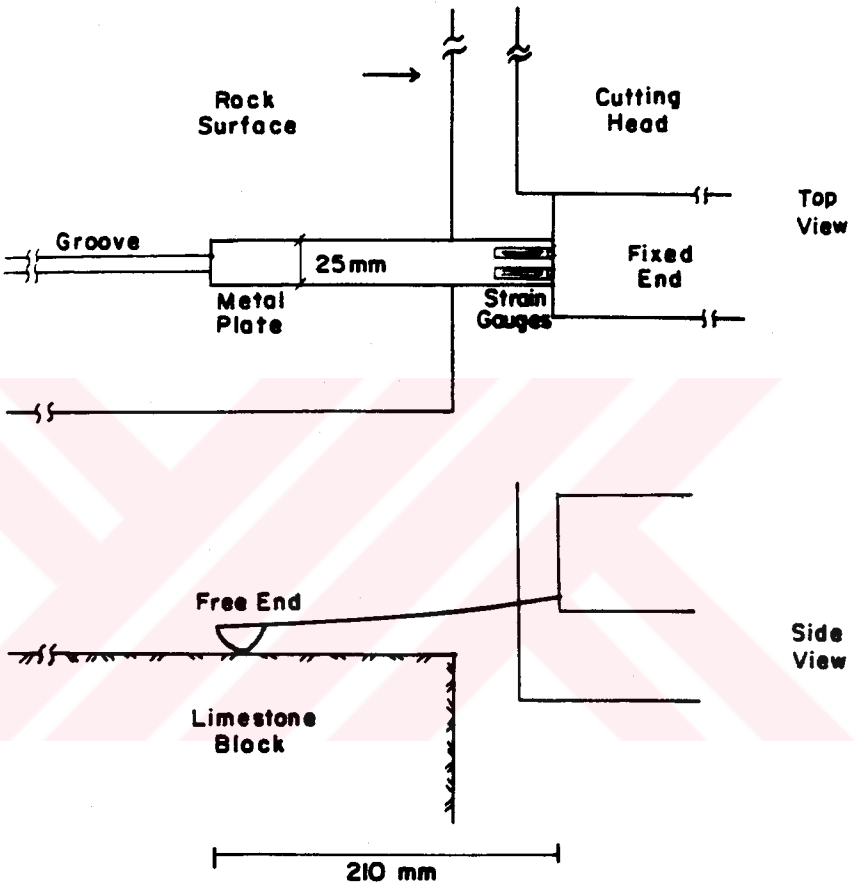

Figure 43. Depth instrument.

rolled across the rock surface before a cut was taken and then again in the groove that had been machined. The depth instrument was calibrated to measure changes in the height of the rock surface to within 0.05 mm.

(iii) Experimental Procedure

The rock surface first was prepared by taking a series of closely spaced cuts. This was done to ensure that changes in the surface roughness were within 0.1 mm. Next an unrecorded relief cut was taken and the depth of cut of this groove was determined. The bit forces on this initial cut would have been higher than on subsequent cuts because there was no adjacent groove for the rock to break into; it was for this reason that these forces were not recorded. The bit was then moved horizontally a distance of 3.2 times the depth of cut and a cut was taken where the forces were recorded. This cycle was repeated for three more cuts at this same depth of cut, (Figure 44).

The specific energy of cutting was determined by carefully collecting all the rock fragments that were produced during a cut and weighing these particles. Knowing the rock density and measuring the mechanical energy supplied to the bit, the energy required to excavate a unit volume of rock then could be found.

The first series of cuts was made without water jet assistance. These cuts were made to examine the influence of bit geometry and depth of cut on the efficiency of the cutting process. The second series of cuts that employed water jet assistance was made using the bit that was

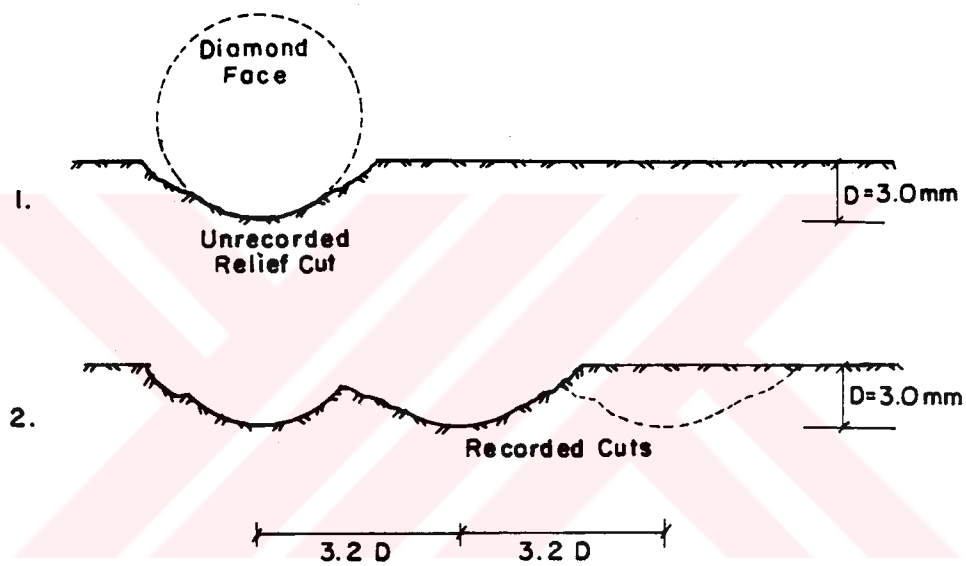

Figure 44. Experimental layout.

selected from the first test series as having the best geometry. For this second test series a 0.8 mm nozzle was directed approximately parallel to and about 1 mm ahead of the leading face of the bit. (Figure 45). The standoff distance between the nozzle exit and the rock:bit interface was 25 mm (1 in).

All of the bits were in a sharp condition at the start of the experiments, and since Indiana limestone is a non-abrasive rock and because the total volume of rock cut by each bit was small, they remained sharp throughout these tests. Consequently, the bit normal force did not increase and the bit cutting force was greater than the other force components during the experimental program, and thus only the cutting force is used in reporting the results.

5.2.3. Results of Cutting Tests With PDC Bits

(i) Dry Cuts

The first series of cutting experiments was to determine the differences between the different bit geometries. These tests all were conducted without using water jets to assist the cutting process. The results are presented in Table 5 and Figure 46. Specific energy is a useful parameter for comparing the efficiency of a cutting process. From Figure 46 it can be seen that for all bit types the specific energy decreases, and therefore the cutting efficiency increases rapidly with increasing depth of cut up to a depth of cut of 3 mm. Beyond this depth of cut the efficiency does not change much. However, it should be noted

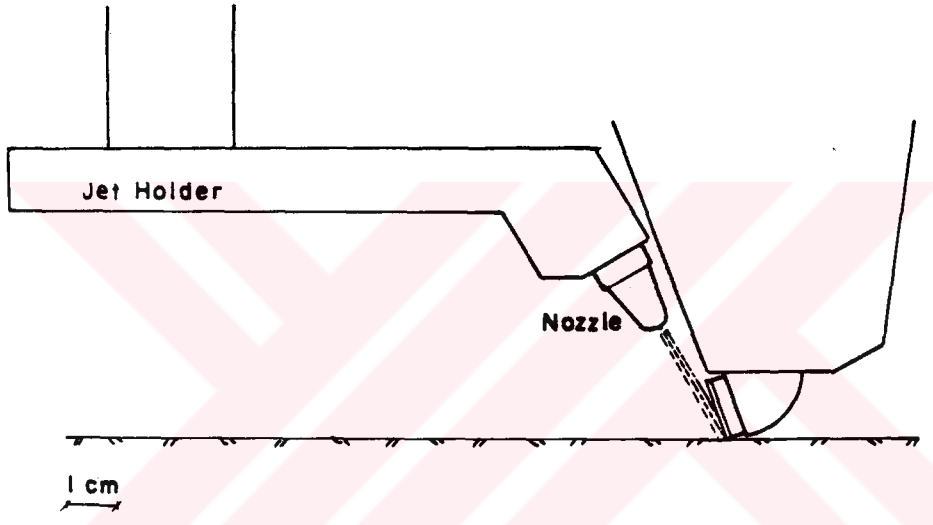

Figure 45. Jet position for PDC bit.

TABLE 5. COMPARISON OF BIT GEOMETRIES

Bit Number #	Depth of Cut (mm)	Mean Cutting Force (kN)	Mean Peak Cutting Force (kN)	Specific Energy (MJ/m^3)
2	0.87	0.211	0.466	145.3
	1.39	0.322	0.661	78.9
	2.33	0.528	1.124	46.3
	3.75	0.950	2.040	33.4
3	1.09	0.211	0.465	93.6
	2.16	0.440	0.947	47.5
	3.06	0.659	1.342	34.9
4	1.00	0.180	0.490	87.9
	1.40	0.259	0.566	ND
	1.72	0.335	0.724	51.9
	2.51	0.507	1.093	ND
	2.72	0.562	1.260	37.5
	3.32	0.747	1.635	32.2
5	2.15	0.446	0.959	47.2
	3.09	0.637	1.393	35.9

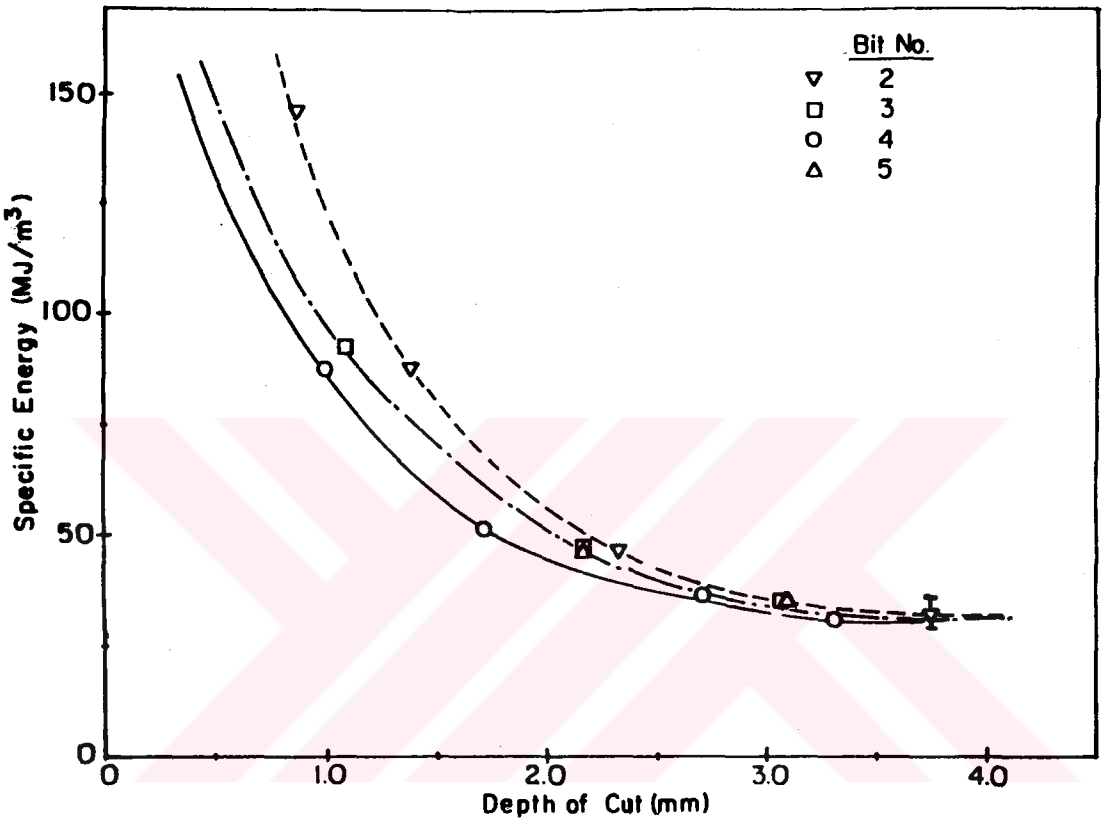

Figure 46. Specific energy vs. depth of cut for various bit designs.

that this is considerably in excess of the depth of cut that these diamond inserts take usually when they are employed on a drill bit. In typical service they take cuts less than 1 mm which, as is evident from this figure, is highly inefficient.

Bit #1 was damaged severely in the first cut which was deeper than 3 mm and it was not used for further experiments. Also it should be noted that at the 3 mm depth of cut, two other bits were damaged. Bit # 5 was chipped. Almost certainly this failure resulted from stress concentrations that were generated at the corners of the bit face. Bit # 3, the standard flat disc, also suffered minor chipping.

It can be concluded from this section that the manner in which PDC inserts are employed on drill bits is highly inefficient at present, because the depth of cut that each insert takes per revolution of the drill bit is extremely small. The consequence of this small cut depth is an increase in the mechanical energy expended in excavating a unit volume of rock. Because bit wear is related to the expenditure of mechanical energy down the hole, this implies that the current design of these inserts tends to promote bit wear. In order to increase the cutting efficiency, the depth of cut, and by implication the spacing between the inserts, needs to be increased. It should be noted that, because fewer inserts will be needed in this configuration, it is not implied that the overall drilling power will need to be increased. Unfortunately, the test results show that in Indiana limestone, a rock that might be classified as medium strength, the depth of cut cannot be increased without causing damage to the bit materials. Two approaches

to achieve the deep cuts with a minimum rate of bit wear are: (a) to improve the strength of the bit materials; (b) to develop a cutting technique that reduces the force levels acting on the bit. The use of fluid jets to reduce bit forces is an example of this latter approach.

(ii) Water Jet Assisted Cuts

Bit # 4 was used for this test suite, since this bit appeared to be the most energy efficient from Figure 46. A series of grooves was made at two depths of cut 2.5 mm and 3.5 mm. The water jet was directed in front of the bit (Figure 45). The jet pressure was changed from 10 MPa to 70 MPa during these tests and the influence of this jet on the bit cutting force was observed.

The results are plotted in Figures 47 and 48. These show that the extent to which the forces are reduced depends on the depth of cut, the deeper the cut the greater the benefit. At 3.5 mm depth of cut both the mean and mean peak forces were reduced by more than 30 percent. This is less than the force reductions reported earlier for water jet assisted drag bit cutting, but probably this is because the depths of cut examined here are relatively shallow. Neverthless, a 30 percent reduction in bit forces could be regarded as substantial because it would permit a drill bit to be designed that would take deep cuts without imposing unacceptably high loads on the individual bit inserts. Alternatively, the drill bits in use today could be used to drill in rock that is 30 percent stronger than they currently are capable of cutting.

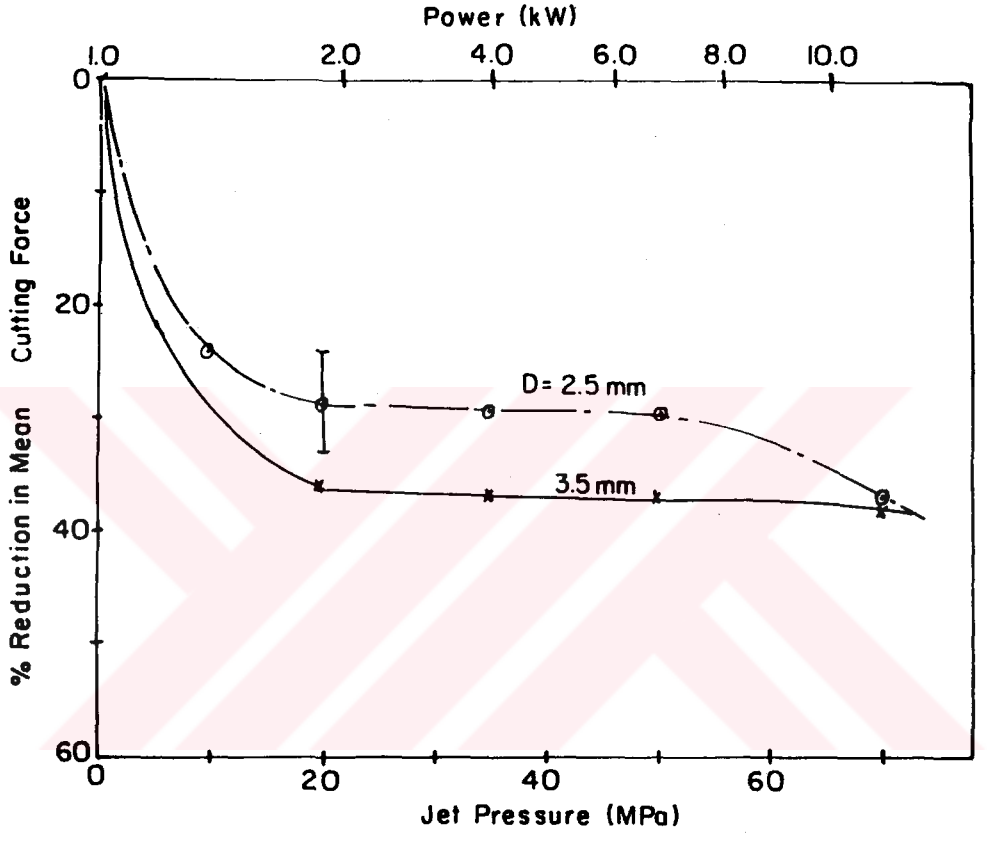

Figure 47. Reduction in mean cutting force with jet pressure for bit # 4.

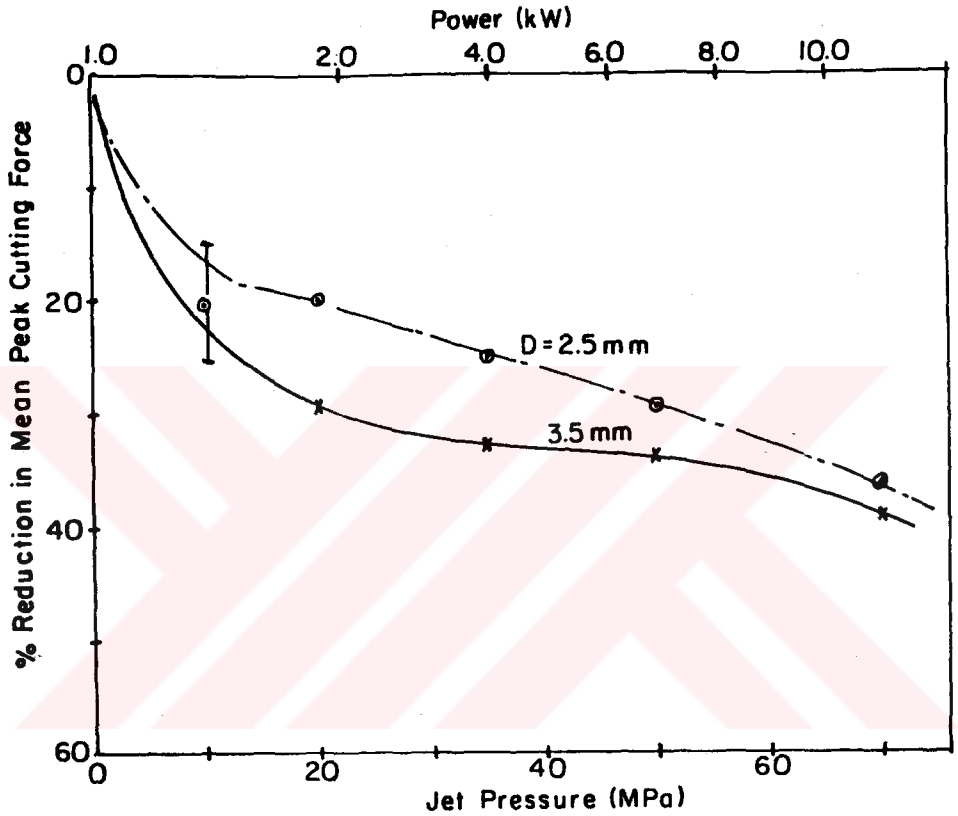

Figure 48. Reduction in mean peak cutting force with jet pressure for bit # 4.

Previous work with the tungsten carbide pick has demonstrated that the jet power, that is the combined effect of the flow rate and the pressure rather than either of these parameters by themselves, controls the reduction in the bit forces. The measured jet power required to achieve a roughly 30 percent bit cutting force reduction at the greater depth of cut was a modest 2 kW per insert.

6. ANALYSIS

6.1. Crack Growth Process In Rock

A general review of crack formation and propagation for different breaking processes in rock is essential for a better understanding of the mechanicm of water jet assisted drag bit cutting. It was illustrated earlier in Figure 3 of Section 1.4.1 that comminution processes are more efficient than the excavation processes. A comparison of fracture mechanisms for comminution processes such as crushing and grinding on line I of Figure 3 and drag bit cutting can provide the lead to explaining higher efficiency of comminution processes in general.

6.1.1. Crack Growth In Comminution

In comminution a concentrated load applied on one end of a discrete particle is opposed by another concentrated load on the other end of the particle, and a crack is forced to form and propagate more or less in a plane containing these two concentrated loads. Crack propagation in this process takes place along the shortest possible path, a straight line, between the two points of application of load. The crack follows this path since it is perpendicular to the direction of the minimum principal stress.

Breakage of a rock particle between the steel balls or rods of a mill or between the jaws of a crusher is similar to the breakage of a

cylindrical rock core between the platens of a Brazilian testing frame. In this test a cylindrical rock specimen is compressed across a diameter between flat surfaces which apply concentrated loads per unit axial length of the cylinder. Failure occurs as a result of the uniform tensile stress normal to the diametral plane and the failure stress is used as a measure of the tensile strength of the rock, (Hobbs, 1964). This process is illustrated in Figure 49.

6.1.2. Crack Growth In Indentation

The indentation process is the basic mechanism of rock breakage for mechanical excavation techniques. Therefore, it is important to understand the indentation process before studying the nature of force reductions when water jets assist the mechanical cutting tools.

In mechanical excavation processes, a portion of a large and confined rock surface is indented by a cutting or drilling tool and this localized disturbance in the form of stress concentration drives a crack in the direction of applied load. As the applied normal load is increased, the crack changes its direction and returns to the surface, thus forming chips around the indenter, (Figure 50). The indentation process for sharp drag bits represents a special case, since the major part of the crack propagation occurs in the direction of the dominant force component, which is the cutting force. Figure 51 illustrates the cleavage fracture which refers to the chip formation ahead of the sharp drag bits. Arrows on fracture planes in Figures 50 and 51 indicate that the chip formation occurs under tension for both cases.

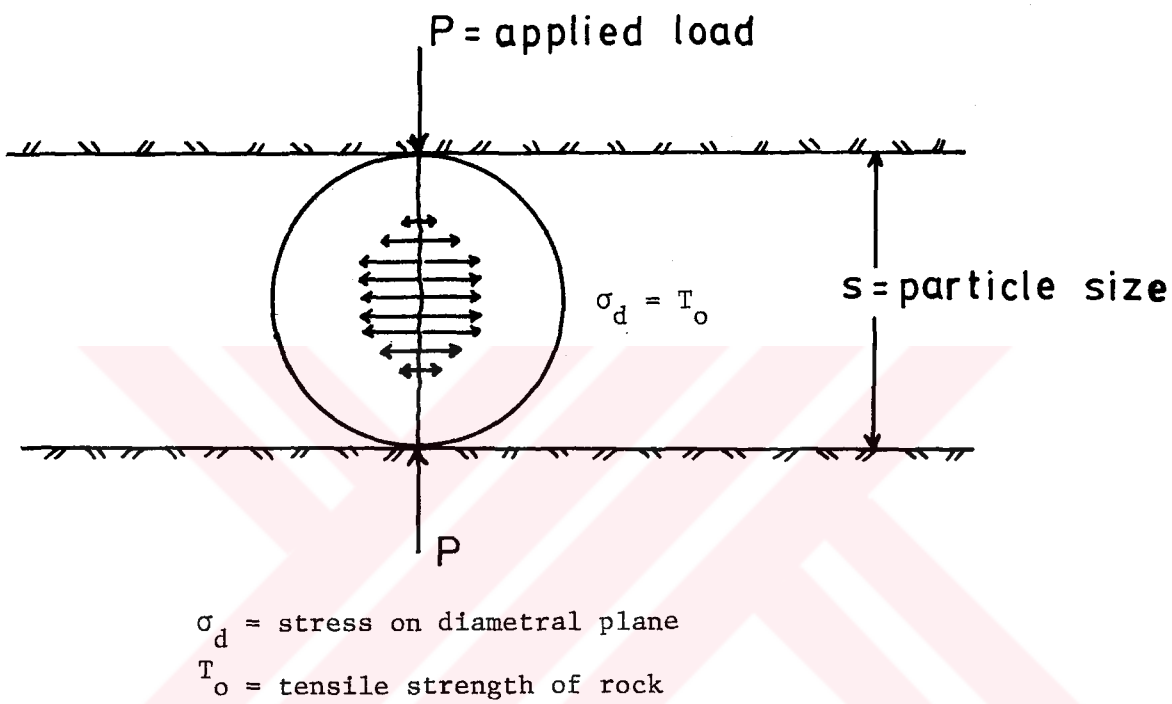

Figure 49. Crack growth process in comminution.

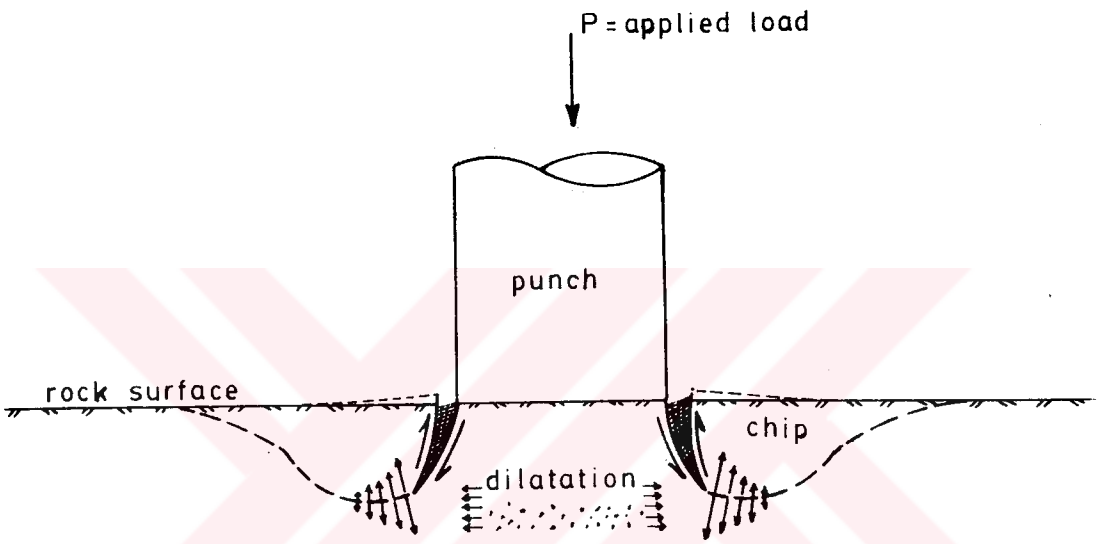

Figure 50. Crack growth in indentation.

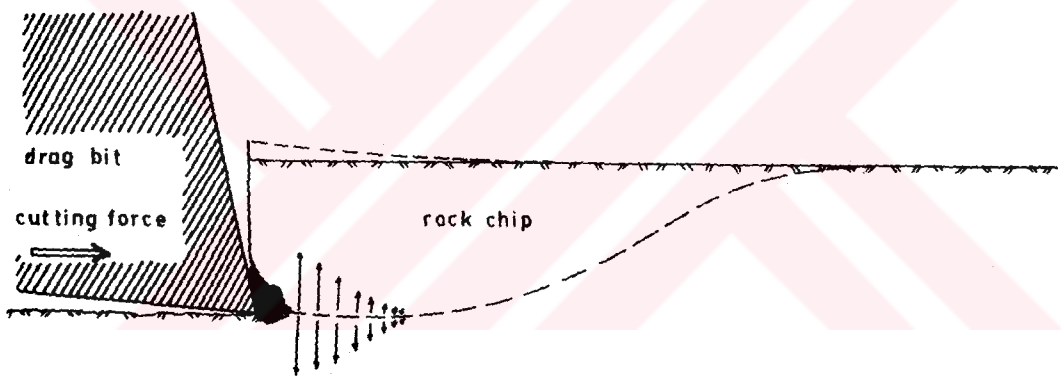

Figure 51. Cleavage fracture ahead of a sharp drag bit.

For a better understanding of the indentation process, experiments with a 10 mm diameter flat circular punch were conducted on Sierra granite, (Figure 52); these experiments were conducted by the author and the results appeared first in Hood and King (1982), and later in Cook et al. (1984). Cylindrical specimens of approximately 90 mm diameter were confined radially by steel jackets. Acoustic emission (AE) tranducers were mounted on the rock surface to monitor the crack initiation and propagation process during the indentation. First, the peak failure load was determined by loading a number of specimens to failure. Then, six loading-unloading cycles were performed in different positions on a single rock sample. In these cycles the applied load was increased successively from 45 percent of the peak failure load that the rock could sustain to 99 percent of this load. When the tests were completed, the rock sample was sectioned and a dye penetrant was sprayed onto the cracked region to observe the crack development at different load levels. Load-displacement curves for these cycles are shown in Figure 53. Figure 54 shows the corresponding sections through the rock illustrating the crack development in these six load cycles.

Both AE counts in Figure 53 (a) and the section in Figure 54 (a) illustrate that first major damage to the rock occurs when the load is about 45 percent of the peak failure load. At this point a conical, Hertzian crack is initiated at the punch corners. This crack, which first propagates into the rock, changes direction and becomes perpendicular to the direction of the applied normal load, (Figure 54 (d)). Then, the crack front moves back to the surface to complete the chip formation adjacent to the indenter. It is interesting to note that

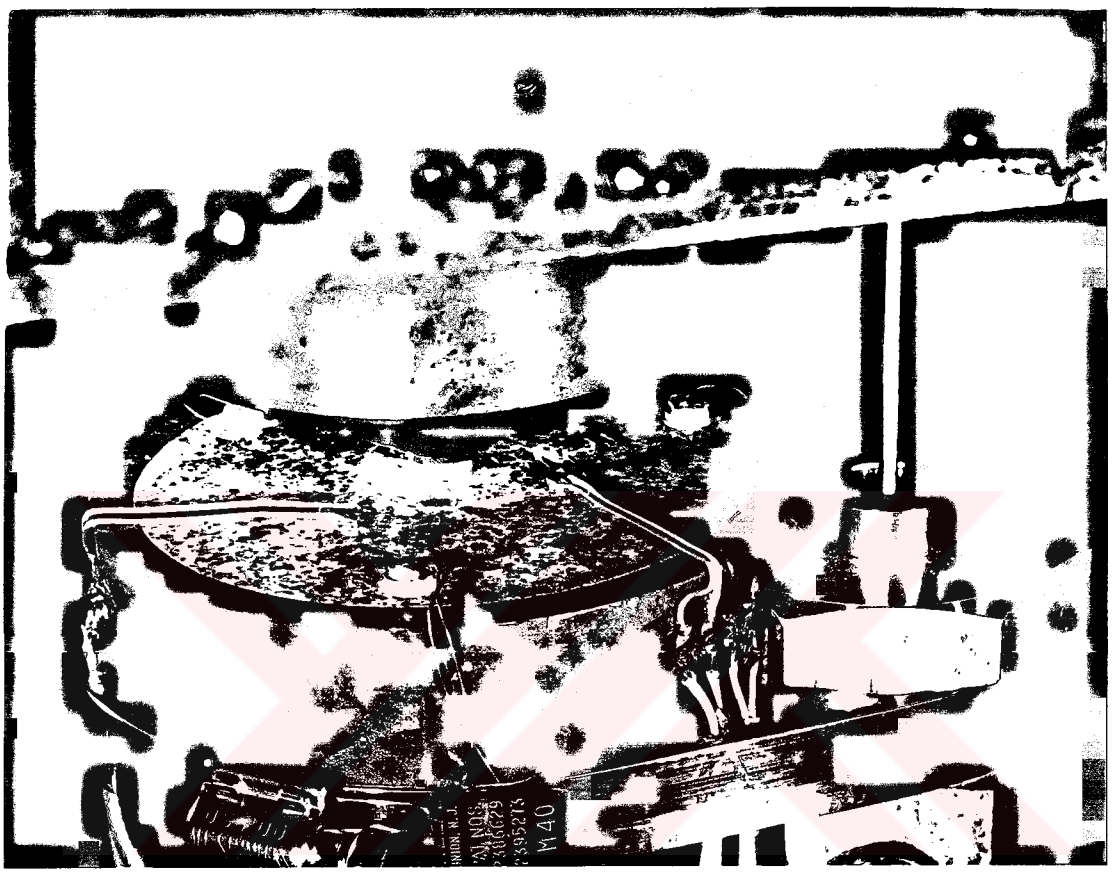

Figure 52. 10 mm diameter circular punch and indentation specimen.

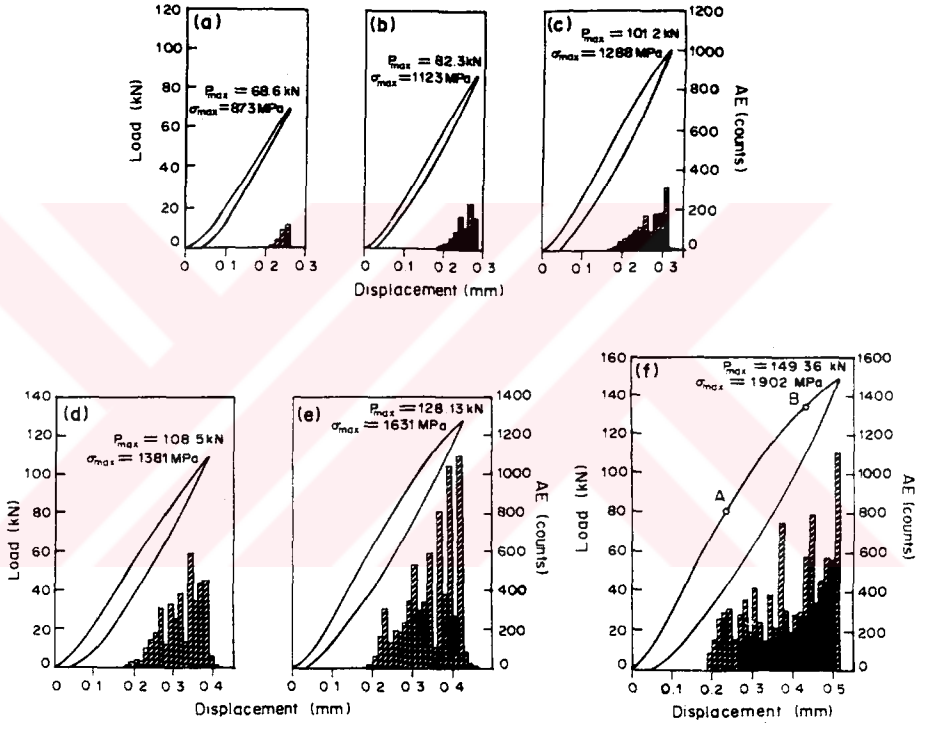

Figure 53. Load-displacement curves and AE event counts for 6 indentation tests. The applied load was increased from (a) 45% of the failure load to (f) 99% of this load.

Figure 54. Cracking and microcracking of granite beneath the circular punch.

the zone immediately beneath the indenter is under an almost hydrostatic compression, and thus remains relatively undamaged. However, this zone is surrounded by a region of intense microcracking. As the load increases, this microcracking causes an increasing expenditure of non-recoverable energy, given by the area between the loading and unloading curves in Figure 53. The microcracked rock exhibits a dilatant behaviour, and a radial compression is applied to the rock as a result of the volumetric expansion in the microcracked region. Wagner and Schumann (1971) suggested that this radial compression following the dilatation is responsible for the described change of the initial crack path and the final chip formation. The energy absorbed in this complicated indentation process with crushing following the final stage of crack development (Figure 54 (f)) is certainly expected to be higher than the simple breakage process in comminution.

In summary, all mechanical breaking techniques generate some kind of tension in rock to take advantage of rocks' weakness in tension. Chip formation for both normal force dominant disc cutters and cutting force dominant drag bits occurs as a result of tensile crack growth. Tensile crack development ahead of sharp drag picks was recognized by Evans and Murrell (1962). More recent research on indentation (Hood, 1977; Hood and King, 1982; Cook et al., 1984) has shown that, although the stress field induced in the rock by an indenter is predominantly compressive, a tensile crack is initiated right around the perimeter of the indenter. The relative inefficiency of the indentation process over the comminution can be explained in terms of the additional energy consumed in microcracking and intensive crushing of the rock beneath the tool.

6.2. Mechanisms of Water Jet Assistance

Three possible mechanisms by which the water jets reduce the bit forces are outlined below:

1. Chemical weakening of the rock by the water, namely stress corrosion cracking.
2. Water entering and thus assisting the propagation of the cracks formed by the bit.
3. Water clearing the previously formed rock fragments that tend to confine any solid rock undergoing fracture and absorb energy ahead of the bit.

6.2.1. Stress Corrosion Cracking

One hypothesis to explain the reduction in bit forces and, by implication, the reduction in the mechanical energy required to excavate the rock, is to invoke a mechanism of chemical attack of the rock by the water. This attack causes a reduction in the rock's fracture strength. This behavior is well known and is termed stress corrosion cracking. Several investigators have reported on this phenomenon in rock fracture investigations, (Rehbinder et al, 1944; Hoagland et al, 1973; Westwood, 1974; Schmidt, 1977). Many of these workers have quantified the reduction in the energy required to drive a crack in a quasistatic manner through a water saturated rock sample. It is not clear how effective this mechanism could be in a dynamic rock cutting situation

where the rock is dry immediately prior to the application of the bit and the water jets. The dynamic situation was investigated in this test suite.

A series of high speed films was taken of the cutting operation at a film speed of 1,000 frames a second. Films were taken both using and not using water jets to assist the cutting process. An interesting observation from these films concerned the speed of crack propagation in the rock. The rock chips typically were about 80 mm in length. These chips were formed within one, or at most two, frames on the film. This implies a crack propagation velocity of about 80 m/s.

Stress corrosion cracking is known to be a rate dependent phenomenon, that is a unique relationship exists between the rate of change of crack length with respect to time and the stress intensity factor at the crack tip, (Barton, 1982). Furthermore, there exists a limiting crack velocity beyond which stress corrosion plays no part in the fracture process. For most brittle materials, including rock, this limiting velocity appears to be of the order of 10^{-4} m/s to 10^{-1} m/s, (Barton, 1982). Thus the measurements made in the present test program show that crack propagation velocities during the rock cutting process are at least two orders of magnitude higher than the velocity at which stress corrosion cracking could be invoked as a mechanism influencing the energy required to drive the cracks. Thus, this hypothesis was rejected.

6.2.2. Crack Propagation by Water

It was discussed earlier in Section 1.4.1 that the specific energy in a rock breakage process is related to the size of the rock fragments by an inverse power law, (Figure 3). Thus, far more energy is required to produce fine particles than course particles. The size distribution of rock particles produced in a drag bit cutting operation is a characteristic of the bit geometry, rock type, and cutting conditions such as the depth of cut and spacing between adjacent cuts, (Roxborough, 1973). Previous work (Hood, 1978), has shown that drag bits, specifically blunted bits, act as sliding indenters and break the rock by initiating cracks from beneath the bit wearflat. It is known (Cook et al, 1984), that a crack is initiated in the rock adjacent to an indenter at low levels of applied load. In order to propagate this crack to form a rock chip, it is necessary to increase the load on the indenter. This causes the rock beneath the indenter to become finely crushed. For sharp drag bits, a similar crushed zone exists in the rock around the corner of the bit. Figure 55, which is based on qualitative observations of the breakage process with a wedge shaped drag bit, shows the traces of this crushed zone adjacent to the bit corner. Another hypothesis then, to explain the reduction in bit forces when water jets are employed, is that the water jets enter the tensile crack that is initiated by and ahead of the bit, and assist the bit in opening up this crack to form a chip. This assistance in driving the crack causes a decrease in the bit force required for chip formation. If this hypothesis is correct then presumably the efficient rock cracking and chip formation process can take place without the inefficient crushing

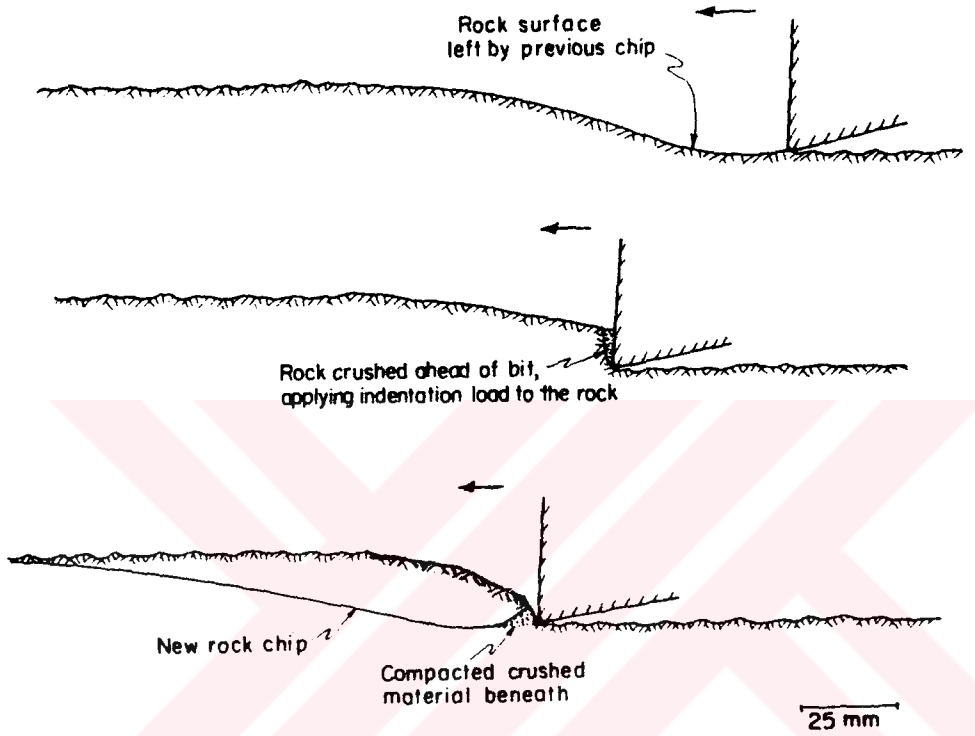

Figure 55. Qualitative observations of chip formation and crushing ahead of a sharp drag bit.

process that occurs beneath the bit.

In investigating this hypothesis a series of cuts was made both with and without the use of water jets assisting the cutting process. Care was taken to collect all of the rock fragments produced in each cut. These fragments were then sieved. Particles in the size range 74 μm (200 mesh) to 590 μm (28 mesh) were wet screened. Particles larger than this were screened dry and particles smaller than this were analyzed using a light scattering technique.

Results from these size analyses are given in Figure 56. In general the steeper the slope of these curves the more efficient the breaking process, since a steeper slope indicates less fines and a more uniform particle size distribution. It can be seen that the curves for both the dry and the water jet assisted cuts have similar shapes and, for the large particle sizes, the curves are coincident. Also, contrary to expectations from the above hypothesis, although the mechanical energy used to excavate the rock is less when jets are employed, the quantities of fine particles are somewhat higher when the jets are used. Possible explanations for the difference between these curves are:

(i) the collection of fine particles was more efficient when jets were employed because fugitive dust was suppressed by the jets;
(ii) erosion of the thin edges of the large rock chips by the jets after the chips were formed, may have increased the quantities of fine particles.

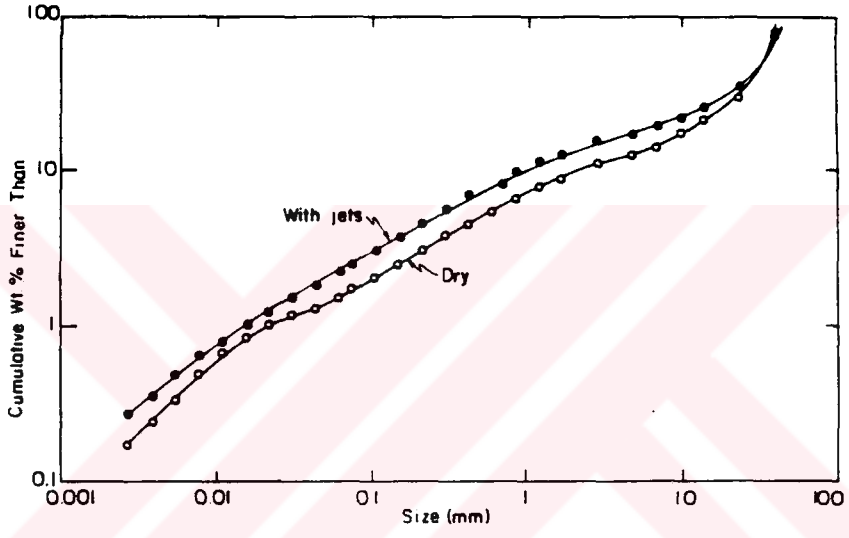

Figure 56. Size analysis of rock fragments.

In any event the differences between these two curves is small, disproving the hypothesis that the water jets permit the formation of large rock chips without the necessity of generating large quantities of fine rock particles.

6.2.3. Clearance of Broken Rock by Jets

A third hypothesis is that the jets act to clear the rock particles, and in particular the finely broken rock particles, as they are formed ahead of the bit. High speed films taken of the cutting operation have shown that the bit pushes a pile of crushed rock fragments as it advances along the cut, (Hood, 1978; Hood and King, 1982). Examination of the cut after the bit has passed, shows that finely crushed material is compacted in the bottom of the grooves, indicating that the bit rides on a cushion of crushed rock as it progresses along the groove. If this cushion was removed, it could permit stresses to be applied to the rock more directly by the bit and enable rock fracture to take place at reduced bit force levels.

An experiment was conducted to examine the influence of ineffective and effective chip clearance from ahead of the bit during the cutting operation. In order to inhibit rock chip removal, a metal plate was mounted parallel to the rock surface ahead of the bit, (Figure 57). This plate was affixed about 35 mm from the rock surface and served to trap the rock fragments as the bit progressed along the cut. Provision was made to mount a nozzle in the metal plate so that water jet assisted cuts could be made with the plate attached, (Figure 57). A suite of

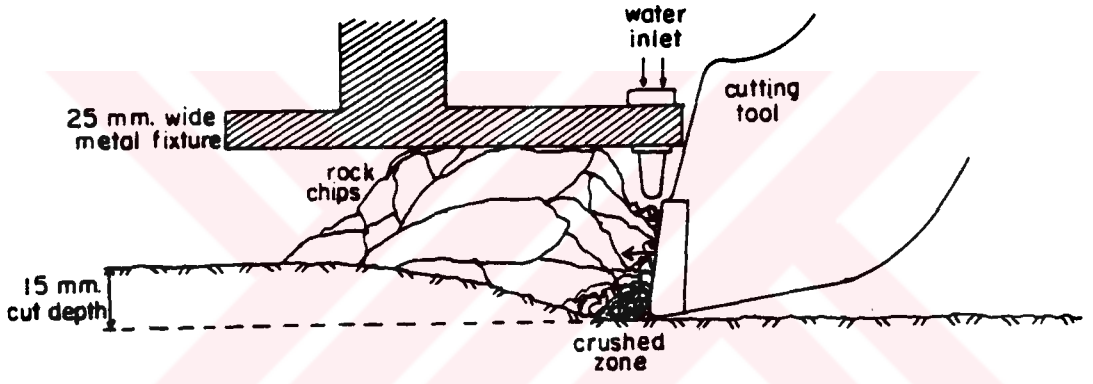

Figure 57. Sketch of metal plate fixture confining the broken rock.

cuts was taken without water jet assistance, and the bit forces were recorded both with and without the metal plate attached. A second suite of cuts was taken with water jet assistance, again both with and without the metal plate attached. A 1 mm diameter nozzle mounted 1 mm ahead of and parallel to the leading face of the bit, at a 25 mm standoff distance was used for these tests. The jet pressure was 35 MPa. The cutting forces measured, both the mean and the mean of the peaks, are given in Table 6.

Representative sections of the cutting force:time trace recordings from all of these test cuts are given in Figures 58 and 59. Figure 58 (a) shows the typical sawtooth trace obtained for a dry cut without the metal plate fixture. The cutting force increases from zero, or some low value, in an oscillatory but linear manner up to a maximum. Beyond this maximum value the force decreases rapidly to a value close to zero and the cycle is repeated. The explanation for this trace signature is that immediately after breakout of a rock chip, the rock immediately in front of the bit is relieved and so the bit cutting force is low. As the bit advances, it encounters a ramp formed by the bottom surface of this previous large rock chip, (Figure 55). Thus the depth of cut that the bit sees increases, in an approximately linear fashion, from a value close to zero to the predetermined depth of cut that is being taken. As the bit penetrates this ramp, it crushes the rock and carries this crushed material ahead of the bit leading face, (Figure 55). This crushing operation causes the force trace to oscillate. The force continues to increase, because the depth of cut relative to the bit is increasing. At some point, the pressure beneath this crushed material

TABLE 6. CONFINEMENT EFFECT OF METAL PLATE FIXTURE

	BIT FORCES WITH AND WITHOUT METAL PLATE (kN)			
	Without Water Jets		With Water Jets	
	Mean	Mean Peak	Mean	Mean Peak
Without Plate	3.94	8.45	2.24	6.82
With Plate	6.63	12.40	2.95	7.99

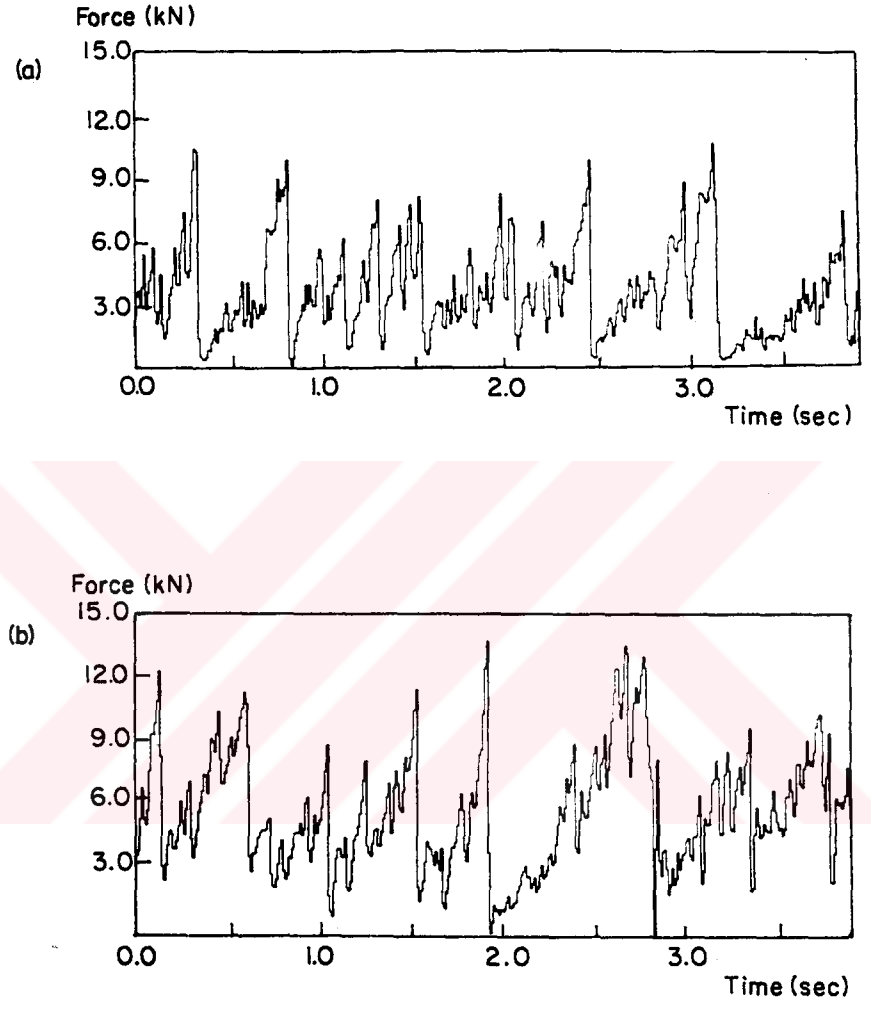

Figure 58. Cutting force-time trace for dry cuts (a) without and (b) with metal plate fixture.

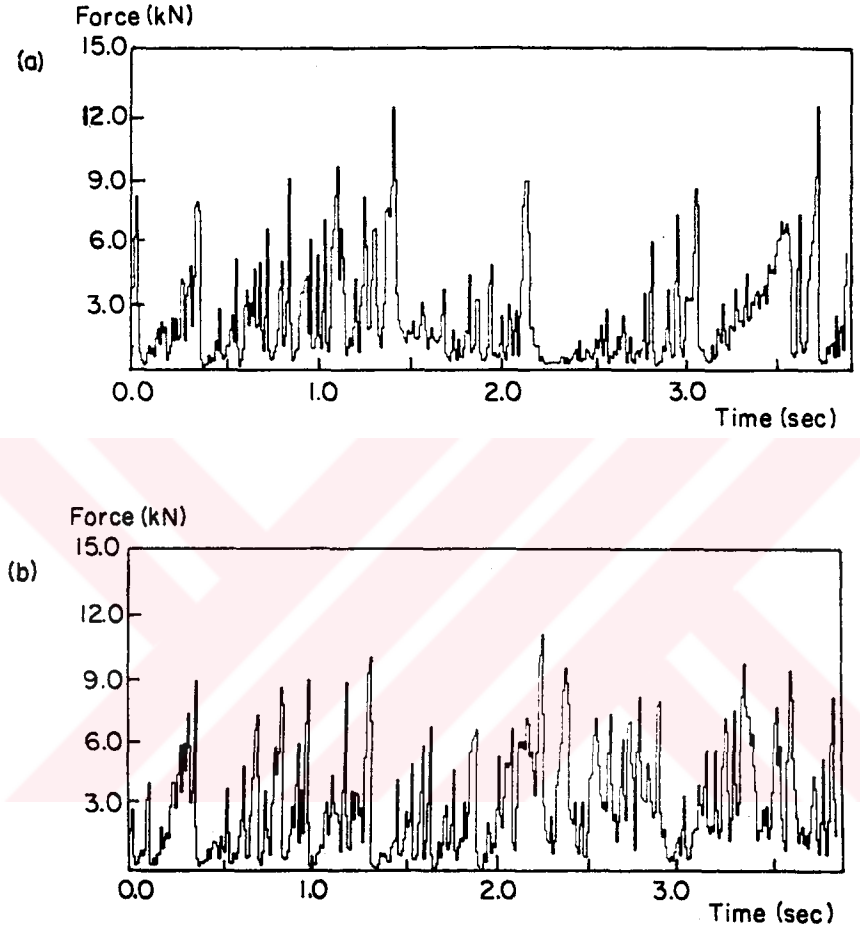

Figure 59. Cutting force-time trace for water jet assisted cuts (a) without and (b) with fixture.

is sufficient to initiate and propagate a tensile crack in the rock, and a new rock chip is formed, (Figures 55).

The equivalent section of the force trace for a dry cut but with the metal plate attached is given in Figure 58 (b). The trace signature is similar. In this case, however, the area beneath each of the individual sawtooth oscillations obviously is much increased. Since the bit velocity was a constant for these experiments, the trace is equivalent to a bit force:bit displacement plot. Thus the area under this curve is a measure of the mechanical energy expended by the bit during the cutting operation. The energy evidently is substantially higher when the metal plate restricts the removal of the rock chips. The values for the mechanical energy measured from the areas under these curves are given in Table 7.

The cutting force traces for cuts made with water jet assistance with and without the metal plate mounted ahead of the bit are given in Figures 59 (a) and 59 (b), respectively. A notable feature of these plots is that although sawtooth oscillations still can be distinguished, in general they are of short duration so that the area under the curves is small and thus the expenditure of mechanical energy also is small, (Table 7). Little difference can be observed visually between the two plots in this figure. This small difference is reflected in the the relatively small difference in the measured cutting forces when the water jets were employed, (Table 6).

TABLE 7. INCREASE IN MECHANICAL CUTTING ENERGY WITH CONFINEMENT EFFECT

	MECHANICAL ENERGY SUPPLIED TO THE BIT (kJ)	
	Without Water Jets	With Water Jets
Without Plate	4.62	2.62
With Plate	7.76	3.46

High speed films were made of the cutting operation when water jets were used to assist the rockbreaking process. These films showed that rock particles were flushed from the region ahead of the bit almost immediately after they were formed. Evidence supporting the effectiveness of this flushing operation was provided by examination of the groove left after the bit had passed. This revealed that no crushed particles were left on either the sides or the bottom of the groove when jets were employed. In contrast, substantial quantities of finely crushed material was found in the bottom of grooves, beneath the path travelled by the bit wearflat, when water jets were not used. Therefore the evidence supports the stated hypothesis, namely that with dry cuts the bit, in addition to pushing a pile of rock fragments ahead of the leading face, actually rides on a cushion of these finely crushed particles. Riding over the cushion of particles and secondary crushing of these particles by the bit uses a lot of energy, therefore it is important to remove these particles efficiently. When water jets are used, these particles apparently are flushed away from the advancing bit and allow the bit to come into direct contact with the still intact rock.

This hypothesis is further supported, indirectly, by the experimental findings reported in Section 5.1.8 earlier. These findings revealed that the reduction in the bit forces was not much affected by a significant increase in bit velocity, even though no change was made in the water jet pressure or flow rate, and thus the specific jet power was much reduced. If the dominant influence of the jets is to remove rock fragments ahead of the advancing bit, the specific jet power is not

necessarily a linear function of either bit velocity or depth of cut. From the results obtained to date this indeed appears to be the case.

Based on these experimental observations and results, a simple theoretical model is developed here to investigate the behaviour of rock fragments in the crushed zone ahead of the bit. The model studies the force equilibrium of a wedge which is pushed ahead by the bit between the leading face of the bit and the inclined rock surface.

Figure 60 shows a general view of the wedge. The surface of the ramp R will be chipped as the bit progresses forward to a new position which is marked as position II in Figure 60. At this position another large rock chip is formed, and a new cycle begins. At the end of a typical cycle, as the bit penetrates deeper into the rock, the rock surface slope angle, which is denoted as α in Figure 60, increases and becomes $\alpha + \Delta\alpha$ at position II. The influence of the increase on bit forces will be investigated in this model. The model will also include the influence of the bit rake angle on the behaviour of the rock fragments in the wedge marked as W at position I in Figure 60.

The main assumption of this model is that the sliding occurs simultaneously on planes B and R, and it occurs without any rotation. For the purpose of this analysis, the zone of broken material ahead of the bit will be divided into two regions:

(i) The well-compacted broken rock in region W behaves as a single rigid wedge. This wedge W can be moved out by sliding on planes

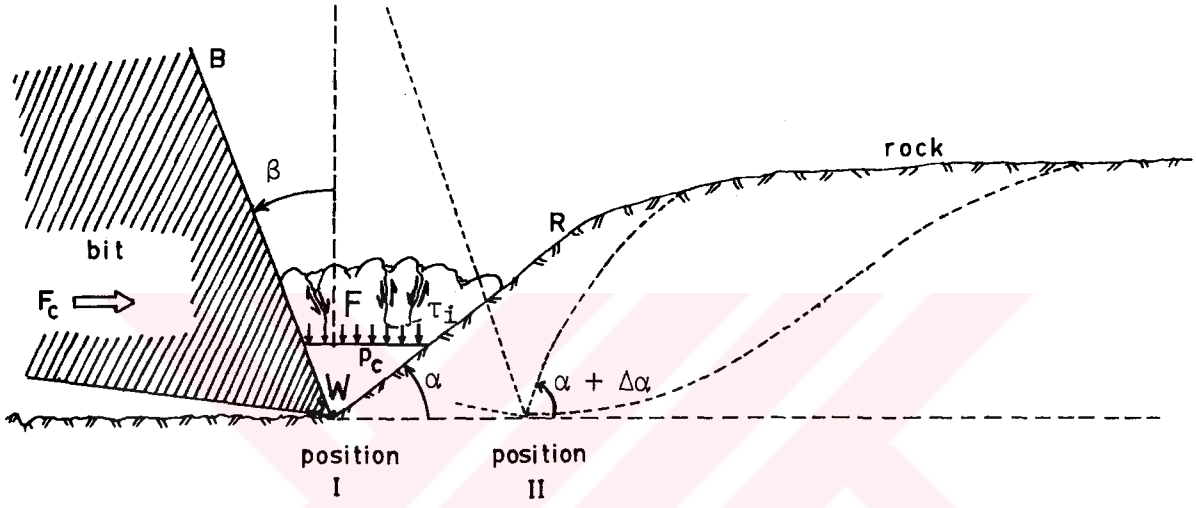

Figure 60. Wedging of broken rock ahead of the drag bit moving from position I to position II.

β = Rake angle

α = Inclination of rock surface

$\Delta\alpha$ = Increment in α as the bit moves from I to II

μ_B = Friction coefficient between bit and rock

μ_R = Friction coefficient between fragments and surface R

p_c = Confinement over rock fragments in the wedge

τ_i = Shear stresses across the rock surfaces in region F

B and R, or it can be crushed by the bit if the sliding cannot occur.

(ii) The broken rock in region F is relatively loose and compressible. The deformation mode during the failure of this material, which is a Coulomb material (Jaeger and Cook, 1979), is the shear along slip surfaces whenever the shear stresses τ_i in Figure 60 satisfy the following failure criterion:

$$\tau = S_o + \sigma_n \tag{8}$$

where σ_n is the normal stress across the sliding surface, τ is the shear stress across this surface to initiate sliding, and S_o and μ are constants.

The chip in the wedge W of Figure 60 is seen to be held in place by an average confining pressure p_c. This pressure p_c on the wedge is assumed to be a result of shear stresses τ_i across the fragments in region F, and stresses between these fragments and planes B and R. When the metal plate was used, fragments in region F were constrained by the plate. The constraint resulted in an increase in the average pressure over the wedge, and this behaviour was illustrated earlier in Figure 58 which showed an exaggerated force-time trace signature with the plate.

Figure 61 shows the free-body diagrams and forces used for studying the sliding of the wedge on planes B and R. In developing the force equilibrium of the wedge, the confinement p_c will be represented by a resultant constraining force P_c over the wedge. In this analysis, the

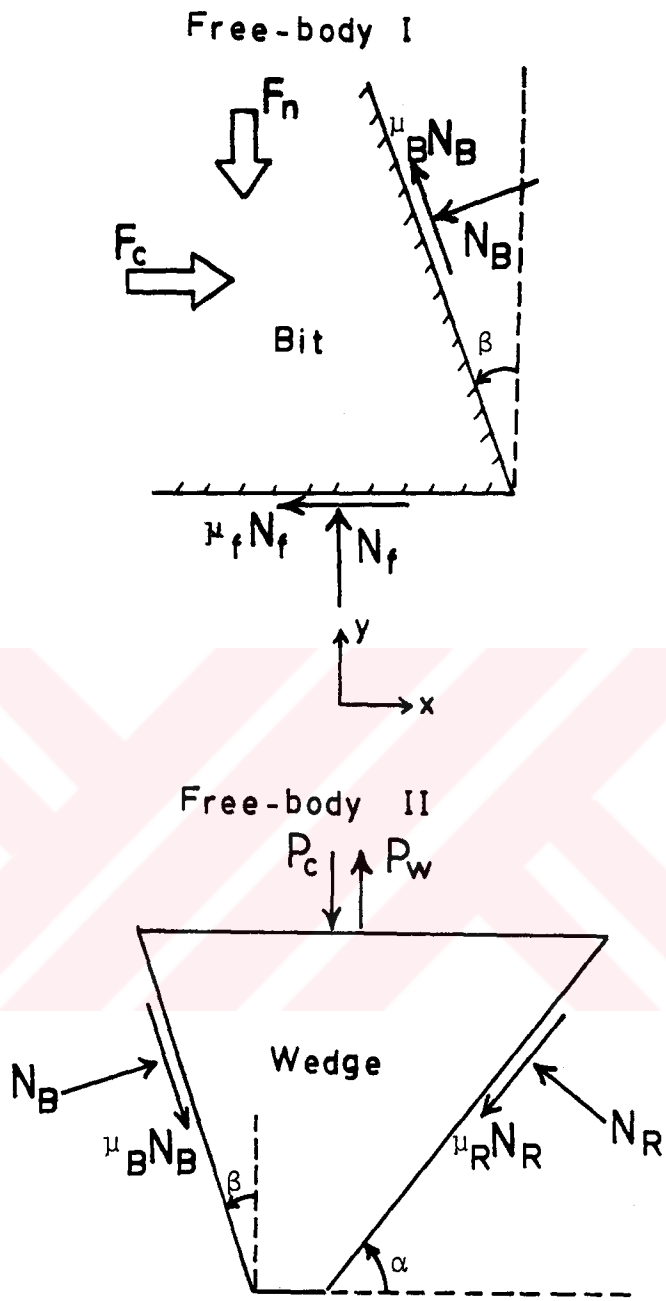

Figure 61. Free-body diagrams and the forces on the wedge.

force P_c might be assumed to include the weight of the material in the wedge. During drag bit cutting on an excavation face, even if the gravity tries to remove the fragments out of this crushed zone, the weight of these fragments will be negligible as compared to the frictional forces in Figure 61. The uplift thrust of the water on the broken rock is represented by P_w, and $P_w = 0$ corresponds to the dry cutting. In the free-body I, the applied cutting and normal forces to the bit are denoted as F_c and F_n respectively. N_f is the normal reaction between the bit wearflat and the rock, and μ_f is the friction coefficient for this contact surface. N_B is the normal reaction between the bit and the wedge, and μ_B denotes the corresponding friction coefficient for this contact. In the free-body II, N_R is the normal force between the rock material in the wedge and the inclined solid rock surface, and the coefficient of friction for this contact surface is denoted as μ_R.

For the free-body I, the summation of forces in the x and y directions yields:

$$F_c - \mu_f N_f - \mu_B N_B \sin\beta - N_B \cos\beta = 0 \qquad (9)$$

$$- F_n + N_f + \mu_B N_B \cos\beta - N_B \sin\beta = 0 \qquad (10)$$

respectively. From Equation (10), N_f is given by

$$N_f = F_n - \mu_B N_B \cos\beta + N_B \sin\beta \ . \qquad (11)$$

Substituting (11) into Equation (9) and solving for N_B gives

$$N_B = \frac{F_c - \mu_f F_n}{[(\mu_f + \mu_B) \sin\beta + (1 - \mu_f\mu_B) \cos\beta]} \quad . \qquad (12)$$

For the free-body II, equilibrium equations in the x and y directions are:

$$N_B \cos\beta + \mu_B N_B \sin\beta - N_R \sin\alpha - \mu_R N_R \cos\alpha = 0 \qquad (13)$$

$$N_B \sin\beta - \mu_B N_B \cos\beta + N_R \cos\alpha - \mu_R N_R \sin\alpha - P_c + P_w = 0 \qquad (14)$$

respectively. Solving Equations (13) and (14) for N_B yields

$$N_B = \frac{(P_c - P_w)(\sin\alpha + \mu_R \cos\alpha)}{[(1 - \mu_B\mu_R) \cos(\alpha - \beta) - (\mu_R + \mu_B) \sin(\alpha - \beta)]} \quad . \qquad (15)$$

Substituting this N_B into Equation (12) gives

$$\frac{F_c}{(P_c - P_w)} = \frac{(\sin\alpha + \mu_R\cos\alpha)[(\mu_f + \mu_B)\sin\beta + (1- \mu_f\mu_B)\cos\beta]}{[1- \mu_f(F_n/F_c)][(1- \mu_B\mu_R)\cos(\alpha-\beta) - (\mu_R+\mu_B)\sin(\alpha-\beta)} \quad .(16)$$

For a constant normal (F_n) to cutting (F_c) ratio, C, Equation (16) can

be expressed in the following form:

$$F_c = \mu^* (P_c - P_w) \tag{17}$$

where μ^* is a function of the friction coefficients and angles involved in the analysis. It should be noted that this form is compatible with the effective stress concept according to which the criterion for slip is expressed by

$$\tau = \mu(\sigma_n - p) \tag{18}$$

where p is the fluid pressure and S_o is neglected.

An examination of the zeros of the denominator in Equation (16) shows that the equation exists only if $\mu_f C \neq 1$ and $\alpha \neq \alpha_c$ where

$$\alpha_c = \beta + \tan^{-1} [(1 - \mu_B\mu_R)/(\mu_R + \mu_B)] \tag{19}$$

If $\mu_B = \mu_f$, Equation (16) becomes

$$\frac{F_c}{(P_c - P_w)} = \frac{(\sin\alpha + \mu_R \cos\alpha)[2\mu_B \sin\beta + (1- \mu_B^2)\cos\beta]}{(1- \mu_B C)[(1- \mu_B\mu_R)\cos(\alpha -\beta) - (\mu_R +\mu_B)\sin(\alpha -\beta)]} \tag{20}$$

The normalized force $F_c/(P_c - P_w)$, which is the force required to push the wedge up against the confinement, is plotted in Figure 62 for various values of surface inclination $\alpha < \alpha_c$ and the rake angle β. This

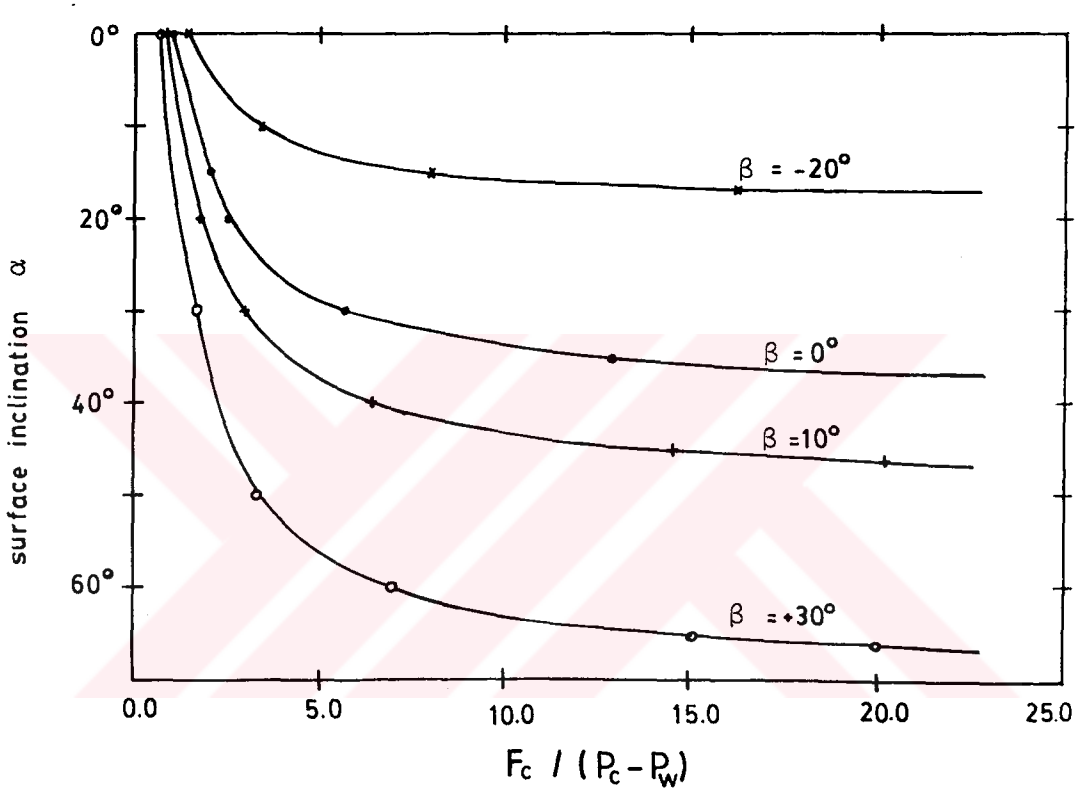

Figure 62. Normalized force required to remove the broken material against confinement as a function of rock surface inclination at different bit rake angles.

plot was generated by taking $C = 0.25$, $\mu_R = 0.75$, and $\mu_B = 0.25$ in Equation (20). The results from Figure 62 are summarized below:

(i) For a fixed rake angle, there is a critical value of the inclination of the surface which is being penetrated by the bit. Beyond this value, increasing the cutting force will not help to remove the broken material between planes B and R, and the bit will jam. This material will be either subjected to a secondary crushing, or will act as a cushion which will spread the stresses applied by the bit to the rock. If the broken material in the wedge shaped zone is not removed then the frictional forces on plane R will resist the opening of a new crack underneath the crushed zone, that is, the portion of the rock to be chipped will be confined by these frictional forces. When a water jet at a certain pressure, that is $P_w \neq 0$, is used the uplift water force P_w will oppose to the constraining force P_c, (Figure 61).

(ii) Higher forces are required to remove the broken material when bits with zero or negative rake angles are used. Cutting experiments by other workers (Roxborough, 1973) have shown that bit forces indeed are increased as the bit rake angle changes from positive through zero to negative. Figure 62 shows that limiting value, α_c, of the inclination α of the sliding surface decreases significantly as the bit rake angle decreases and becomes negative. This implies that, for drag bits with negative rake angles, almost all the cutting force, thus the cutting energy, is used against the frictional resistance of the broken material adjacent to the bit. Therefore,

when the broken rock is removed by water jets, dramatic reductions in the bit forces are expected to occur. Drag bits with negative rake angles are usually employed in hard rock. The previous research work with water jet assisted drag bits operating in hard rock indeed resulted in dramatic reductions in bit forces when water jets were used, (Hood, 1978).

6.3. Energetics of Rock Fragmentation by Cutting

The fracture energy G, which is the energy required to create a unit area of fresh surface, is widely recognized as a material property which can easily be determined by fracture toughness testing. It is instructive to use the data from the size analyses to compute the energy consumed in producing new rock surface area. This energy then can be compared with the mechanical energy applied to the bit, to determine the overall efficiency of the rock breakage process. The energy, U, to create new surface area is given, for plane strain conditions, by:

$$U = K_{Ic}^2 \, (1 - \nu^2) \, A \, / \, E \tag{21}$$

where $U = GA$ (22)

E = Young's Modulus

ν = Poisson's Ratio

K_{Ic} = Rock Fracture Toughness

A = Total new surface area of rock fragments

G = Fracture Energy (= 60 J/m^2 for Indiana Limestone, after Hoagland et al., (1973))

Calculation of U from the above expressions therefore requires a determination of A. This parameter can be obtained directly from the sieve analysis results using (Cummins and Given, 1973):

$$A = \frac{6\lambda}{\rho} \sum_{n=1}^{n_t} \frac{\Delta\Phi}{D_n} \qquad \text{(units = cm}^2\text{/gr)} \tag{23}$$

where $\Delta\Phi$ = mass fraction of the total sample collected on the screen "n", such that $\sum^{n_t} \Delta\phi = 1$

D_n = is the arithmetic mean of the clear opening of the screen (n) on which the sample is collected and the opening of the screen (n-1) immediately above screen n, and n_t is the total number of screens (cm)

λ = Shape factor

ρ = Particle density (gm/cm^3)

The difficulty in using this approach lies in determining the shape factor, λ . For cubes and spheres $\lambda = 1$; for other particle shapes $\lambda > 1$. Examination of the particles produced during the cutting operation showed that the fragments between 10-40 mm were lenticular. The particles became more equidimensional, and therefore $\lambda \sim 1$, as their size decreased below 10 mm. For this reason particular attention was paid to determining the surface area, and thereby the shape factor, of the larger rock fragments. The surface area of these lenticular particles was measured directly using a photographic technique and a Zeiss image analyzer. The specific surface areas were then calculated and these values were substituted into the expression (23) given above to calculate λ. These calculated values are plotted as a function of rock particle size in Figure 63.

Using appropriate shape factors for all of the various size fractions, the cumulative surface areas of rock fragments produced during two

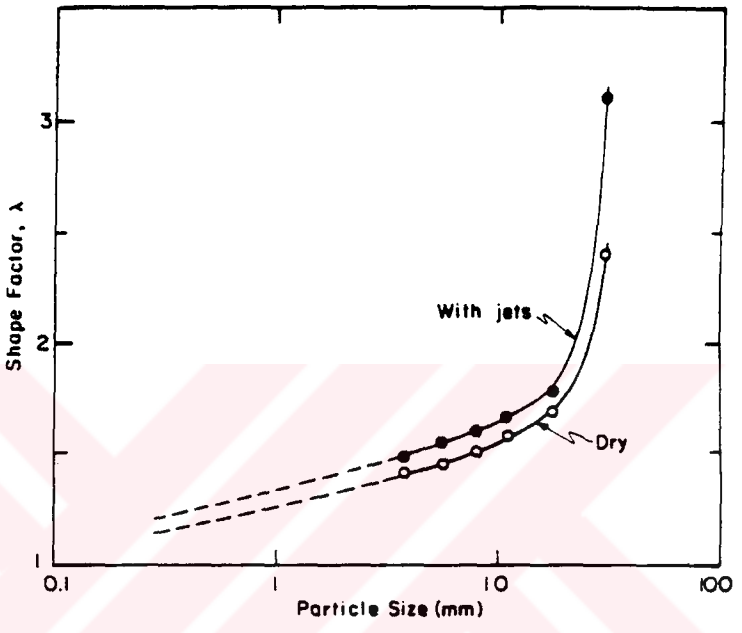

Figure 63. Shape factor as a function of fragment size.

representative cuts are given in Figure 64. This plot shows that the curves for both dry and water jet assisted cuts are approximately the same in this Log:Log space. These experiments were conducted at a constant depth of cut, 15 mm, but two levels of spacing between the cuts were examined, 30 mm and 50 mm. The cumulative surface area for unit mass of rock fragments was found to be independent of the spacing between the cuts and almost independent of the use of water jets, with a value of about 4 m^2/kg. This must be regarded as a minimum value because the laboratory apparatus did not permit analysis of particles less than 2 μm, and from Figure 64 the fine particles provide the major contribution to the cumulative surface area. The mass of the rock fragments was approximately 0.65 kg for both the dry and the water jet assisted cuts when the spacing between the cuts was 30 mm. Thus, from Equation (22):

$$U = 0.16 \text{ kJ}$$

For cuts spaced 50 mm apart

$$U = 0.24 \text{ kJ}$$

The mechanical energy applied to the drag bit during the cutting operation was calculated from the area under the bit cutting force:bit displacement curve. This is plotted as a function of the spacing between the cuts in Figure 65. The ratio of the energy required to create new surface area, U, to the applied mechanical energy, U_m, calculated from this figure and expressed as a percentage is:

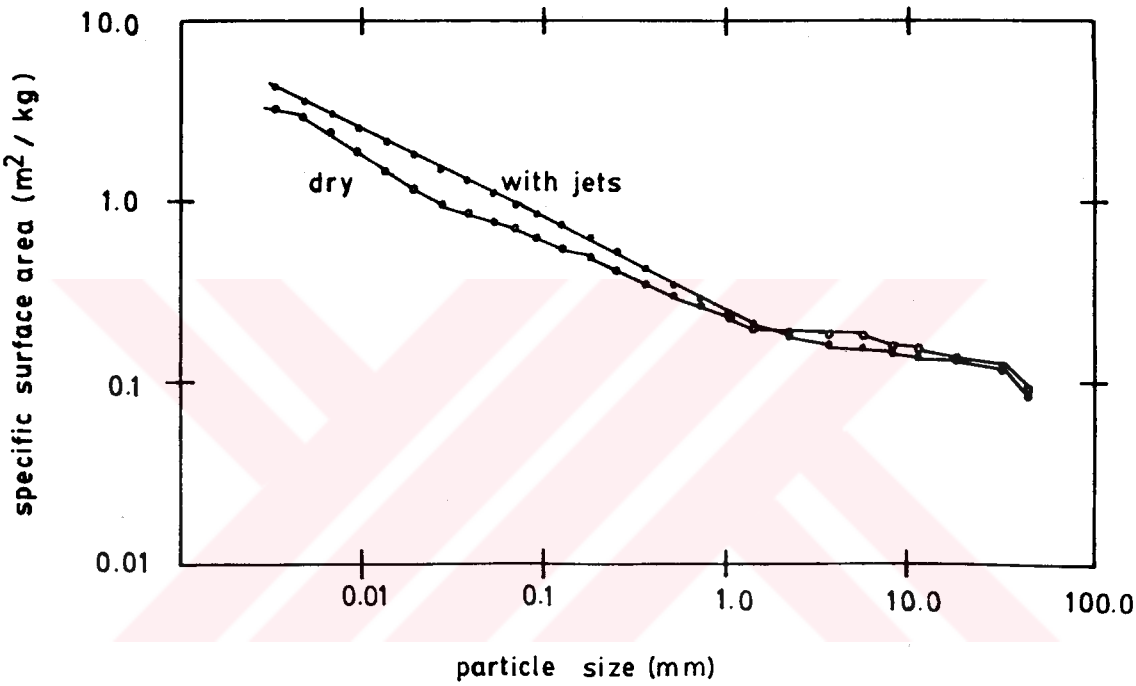

Figure 64. Specific surface area of fragments vs. size.

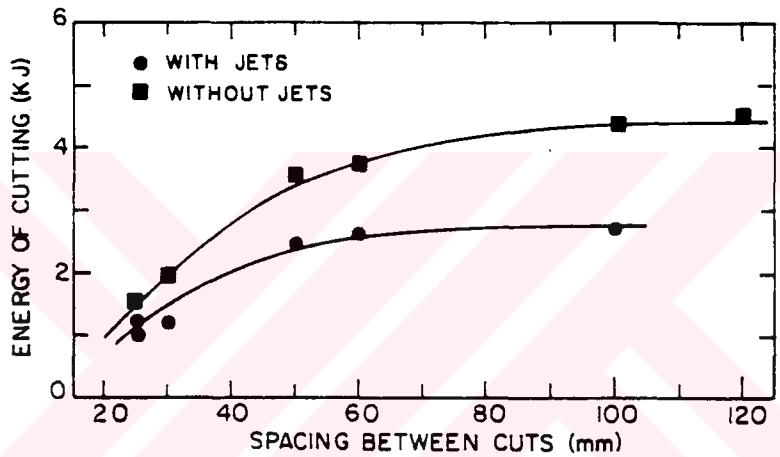

Figure 65. Mechanical energy supplied to the bit as a function of spacing between cuts across the rock surface.

U/U_m = 8% (dry cuts)

U/U_m = 13% (water jet assisted cuts)

for both the 30mm and the 50 mm spacings.

The energy of the water jet has been excluded from these calculations. The laboratory apparatus used for this experimental program had a maximum bit velocity limitation of 0.25 m/s. This is low compared with bit speeds on practical mining machines. A consequence of this limitation is that the water jet energy is a disproportionate fraction, about 50 times, the applied mechanical energy. While it may be argued that the effectiveness of the bit force reductions when jets are used is related directly to their high relative energy input, this is not supported by findings of this thesis and other research work, (Hood, 1976; 1978; Tomlin, 1982). These workers have shown that the same substantial force reductions are achieved when the ratio of the jet energy to the mechanical energy is of the order 1:1. In this situation the ratio U/U_m = 8% for both dry and water jet assisted cuts.

Since only this small fraction of the applied mechanical energy is used for useful work, the remaining 90 plus percent of the energy must be dissipated as heat. Other studies related to the wear of drag bits support this contention. The temperature rise, T, in a drag bit during the cutting operation is:

$$T = f(U_m, (1 - q), \theta_r, \theta_b) \quad \text{(after Cook, 1984)} \qquad (24)$$

where: q = fraction of the applied mechanical energy used to create new surface area

θ_r = thermal properties of the rock

θ_b = thermal properties of the bit

Measurements of T_i (Hood, 1978) have shown that the temperature at the rock:bit interface often exceeds 1,000° Celcius. The hardness of the cemented tungsten carbide bit insert decreases rapidly with increasing temperature. At these high temperatures the hardness of this insert is less than that of many rock constituents such as quartz, (Roxborough, 1973). This leads to high, and often unacceptable, rates of bit wear.

Thus, high bit temperatures are a major impediment to a more widespread use of drag bits for cutting rock. From Equation (24), the bit temperature might be controlled either by a change in the cutting technique resulting in a reduction in U_m or an increase in q, or by the provision of a heat sink. Evidence suggests that these approaches both may be operative when water jets are used to assist the cutting process. Figure 65 shows a substantial reduction in U_m with a concomitant reduction in q when jets are used. Also, it is shown theoretically (Cook, 1984), and demonstrated by measurement (Hood, 1978), that the water acts as a substantial heat sink during the cutting process. These theoretical and laboratory exercises have been validated by field tests where significant improvements in bit life were reported when water jet assisted cutting systems were employed, (Hood, 1978; Tomlin, 1982).

7. DISCUSSION AND CONCLUSION

The dominant mechanism by which the water jets assist the drag bits was found to be the clearance of the rock fragments ahead of the bit. The velocity of the crack propagated ahead of the drag bit was at least two orders of magnitude too high for stress corrosion cracking to be considered as a mechanism for reducing bit forces.

Indentation tests illustrated that right before the final chip formation there was an intensely crushed zone underneath an indenter. This zone absorbed most of the mechanical energy applied to the indenter. It was expected that the consumption of the energy in this crushed zone would be reduced if the pressurized water penetrated into the large cracks and reduced the bit force required to form chips. However, results of the particle size analysis for both dry and water jet assisted cuts showed that crack drivage with water pressure was not the dominant mechanism of water jet assistance. Particle size curves for both dry and water jet assisted cuts were similar in shape, suggesting that particles for both cases were formed by the same mechanism, that is, the drag bit formed the chips and the water jet removed them.

Crack drivage by water pressure might still be effective in a small scale to reduce the bit forces. However, results of the cutting tests by confining the broken material and the simple theoretical wedge model clearly showed that the dominant mechanism of water jet assistance for the drag bit cutting was the chip clearance by jets. It is important to

remove this broken material effectively because:

(i) the broken material acts as a cushion ahead of the bit and mechanical energy is consumed in compacting this cushion. During its compaction, applied mechanical energy through the bit is used for secondary crushing and more importantly for moving the fragments against the friction. It might be argued that the secondary crushing effect would appear in the results of the size analysis. There are two reasons why this effect is not visible in the particle size curves. First, the experimental technique used for particle size analysis, while effectively serving its purpose in the relatively large size range, was not definitive for small particles below 2 μm in size. Second and the most important reason was that the water jets, in addition to having their own secondary crushing effect, had a tendency to suppress the dust.

(ii) the applied stress to the rock through the cushion of broken material is distributed more evenly and over a larger area, thus eliminating the benefits of a sharp drag bit in opening the cracks.

(iii) the frictional forces between this broken material and the inclined intact rock surface ahead of the bit resist the opening of a crack by the corner of the drag bit under the crushed zone. This behaviour is namely the confinement effect of the broken material.

(iv) the removal of the wedge of the broken material, which forms between the bit and the intact rock surface usually following the

compaction, requires high forces especially against the frictional resistance of a steep rock surface ahead of the bit. For bits with negative rake angles, the force required to remove the wedge is so high that the early removal of fragments before they form a wedge can result in dramatic reductions in the bit forces.

This discussion of the suggested mechanism can be extended by examining the relative influence of the water jet velocity and the bit velocity. For a water jet impinging on the intact surface of rock, the velocity of the water after the impact is proportional to the pressure gradient of the water on the impact surface. The pressure distribution in Equation (4) or in Equation (5) indicates that a small distance away from the impact area, the water pressure on the impact surface decreases rapidly. Thus, the velocity of the water after the impact is reduced very rapidly to almost the same order of magnitude as the bit velocity. The water with this greatly reduced velocity cannot drive cracks over long distances, and this also supports the argument for the elimination of the second hypothesis, namely crack drivage by water, as the dominant mechanism of water jet assistance. However, the water can still accelerate and move the rock fragments up for the clearance process. In this process, some fragments might still be caught and pushed ahead by the bit when:

(i) the water velocity before the impact, that is, the jet pressure since they are related, is not sufficiently high. This situation corresponds to the early portion of force reduction-power or

force reduction-pressure curves where there is a rapid increase in the force reductions.

(ii) the frictional forces on the fragments ahead of the bit become so high that the water can no longer remove the fragments. This explains why force reduction-power curves tend to a limiting value. Beyond this limiting value, no further benefits are observed when the jet power is increased.

(iii) the bit velocity is too high. This is probably the reason for the slight decrease in the force reductions in Section 5.1.8 with the high bit speed.

Results of the particle size analysis led to a better understanding of two important benefits of the water jet assist systems. First, it was shown that when water jets were used the formation of dust, which is a major health and safety hazard in the underground environment, was suppressed substantially. Second, it was discovered that only 10 percent of the applied mechanical energy through the bit was used in producing the desired surface and the remaining energy was wasted in increasing the bit temperatures and producing undesirable fines. It was concluded that increasing bit temperatures accelerated bit wear by reducing the strength of the bit material, and the rate of bit wear could be decreased significantly by the use of a coolant water jet.

The technological background for this promising new technique was improved here significantly by optimizing a number of relevant parameters which influence the performance of water jet assist systems. The optimum jet configuration was a single jet positioned 1 mm ahead of

the bit. If this distance was less than 1 mm then the water jet would strike the tungsten carbide insert, thus losing its energy to assist the bit and eroding the insert. If the jet was positioned further ahead of the bit its effectiveness in assisting the bit would be reduced, since the water would not fully penetrate into the bottom of the crushed zone adjacent to the bit. A standoff distance of a hundred times the nozzle diameter, which is generally accepted as a maximum for effectiveness of the water jet cutting, was found to be satisfactory also for the water jet assisted cutting.

Force reductions were found to depend more strongly on the jet pressure than the volume flow rate. The jet power normalized with the bit velocity was found to be the parameter controlling the magnitude of force reductions. The optimum value of this normalized jet power parameter was dependent on the bit velocity. However, this argument needs to be investigated further by conducting a similar experimental program at higher bit speeds.

In general, water jet assisted cutting resulted in the reduction of the mean cutting force by 45 percent for the tungsten carbide pick, and 30 percent for the PDC drill bit. The difference in the force reductions of these two different cutters can be explained in terms of the shallow depth of cut taken by the PDC bit and its relatively small size. Experimental results with PDC bits showed that sintered diamond inserts failed frequently in a brittle manner even for shallow (1 mm), thus highly inefficient cuts. An investigation into specific energies for different PDC bit geometries showed that deeper cuts (3 mm) with these

bits would be highly energy efficient. With a water jet assist system, PDC bits could take deeper cuts, resulting in improved advance rates for drilling since the water jets reduce the bit wear and the bit forces.

By conducting cutting tests with PDC bits a first step was taken here to show that in addition to the mining industry, the oil well drilling industry can also enjoy the benefits of water jet assistance. For a future investigation with drill bits, it is recommended that the conditions in deep boreholes are added to the testing system. These conditions include:

(i) The porous rock used here would be under confinement at the bottom of a deep borehole, and this confinement would make the rock stiffer by keeping the pores and cracks partially closed. Also, under the confinement the rock strength would be higher. It should be noted that these conditions can be simulated well with the indentation specimens described earlier. The steel jacket around these specimens can apply a radial confinement of about 20 MPa (Cook et al., 1984), and this is the same order of magnitude as the radial stress for most deep boreholes.

(ii) High temperatures at the bottom of the borehole would increase the ductility of the rock.

(iii) The water jets would be submerged in the drilling fluid. This would reduce the effectiveness of the water jet assist system.

Finally, the wedge model proposed here should be developed further to include the influence of roughness of the sliding surfaces. This model

should be supported by further cutting experiments using bits with different rake angles. The secondary crushing effect and the confinement effect of the broken material over the cracks opened by the bit should be investigated in a more detailed model.

REFERENCES

Anon, Staff Environmental Assessment and Contaminant Control Branch, MSHA. Environmental Dust Surveys of Longwall Mining Operations, Proceedings Mini Symposium, Longwall Mining: Research and Development: Safety: Health, Society of Mining Engineers of AIME, 83-COAL-01, Atlanta GA, March 1983, pp. 113-133.

Arceneaux, M.A. and Fielder, J.L. Field Experience with PDC Bits in Northeast Texas, Proceedings Drilling Conference, sponsored by Society of Petroleum Engineers/International Association of Drilling Contractors, New Orleans Louisiana, IADC/SPE 11390, Feb. 20-23 1983, pp. 273-278.

Barton, C.C. Variables in Fracture Energy and Toughness Testing of Rock, Proceedings 23rd U.S. Symposium on Rock Mechanics, University of California - Berkeley, Aug., 1982, pp. 449-462.

Bond, F. C. The Third Theory of Comminution, A.I.M.E Transactions, Vol. 193, May 1952, pp. 484-494.

Brook, N. and Summers, D.A. The Penetration of Rock by High-Speed Water Jets, Int. Jr. of Rock Mech. Min. Sci., Vol. 6, 1969, pp. 249-258.

Cook, N.G.W. Wear on Drag Bits in Hard Rock, to be published in the Canadian Mining and Metallurgical Bulletin, " Rock Mechanics" Special Volume, 1984.

Cook, N.G.W. and Harvey, V.R. An Appraisal of Rock Excavation by Mechanical, Hydraulic, Thermal and Electromagnetic Means, Proceedings of the 3rd Congress of the International Society for Rock Mechanics, Denver, Vol. 1, 1974, pp. B 1599-1615.

Cook, N.G.W., Hood, M., and Tsai, F. Observations of Crack Growth in Hard Rock Loaded by an Indenter, International Journal of Rock Mechanics and Mining Sciences, Vol. 21, No. 2, 1984, pp. 97-107.

Cook, N.G.W. and Joughin, N.C. Rock Fragmentation by Mechanical, Chemical and Thermal Means, Proceedings of the 6th International Mining Congress, Madrid, 1970, Paper 1- C.6 .

Courtney, W.G. and Agbede, R. Machine Mounted Water Sprays for Preventing Frictional Ignition, Bureau of Mines, Pittsburgh Research Center In-House Report No. 4375, September 23 1982, 12p.

Cress, L.A. How and When to Run a PDC Bit in the Upper Texas Gulf Coast - An Operator's Viewpoint, Proceedings Drilling Conference, sponsored by Society of Petroleum Engineers/International Association of Drilling Contractors, New Orleans, Louisiana, IADC/SPE 11388, Feb. 20-23 1983, pp. 255-260.

Cummins, A. B. and Given, I. A. (Editors) SME Mining Engineering Handbook, SME, AIME, New York, 1973, pp. 27/32-27/47.

Dubugnon, O. An Experimental Study of Water Assisted Drag Bit Cutting of Rocks, Proceedings of the First U.S. Water Jet Symposium, Golden CO, April 1981, pp. II-4.1 - II-4.11.

Evans, I. and Murrell, S. A. F. Wedge Penetration into Coal, Colliery Guardian, Vol. 39, 1962, pp. 11-16.

Hoagland, R.G., Hahn, G.T. and Rosenfield, A.R. Influence of Microstructure on Fracture Propagation in Rock, Rock Mechanics, 5, 1973, pp. 77-106.

Hobbs, D. W. The Tensile Strength of Rocks, Int. Jr. Rock Mech. Min. Sci., Vol. 1, 1964c, pp. 385-396.

Hood, M. Cutting Strong Rock with a Drag Bit Assisted by High Pressure Water Jets, Journal of the South African Institution of Mining and Metallurgy, Vol. 77, No. 4, November 1976, pp. 79-90.

Hood, M. Phenomena Related to the Failure of Strong Rock Adjacent to an Indenter, Journal of the South African Institution of Mining and Metallurgy, Vol. 78, No. 5, December 1977, pp. 113-123.

Hood, M. A Study of Methods to Improve the Performance of Drag Bits Used to Cut Hard Rock, Ph.D. Thesis, Department of Mining Engineering, University of the Witwatersrand, Republic of South Africa, 1978, 135 p..

Hood, M. and King, M. S. Improved Rock Excavation Techniques, Interim Report No. 1, prepared for the U.S. Department of Energy under L.B.L. Contract DC AC03-768 F00098, B & R No. ED 0201, March 1982, 10 p..

Hood, M. and King, M.S. Improved Rock Excavation Techniques, Interim Report No. 2, prepared for the U.S. Department of Energy under L.B.L. Contract DC AC03-768 F00098, B & R No. ED 0201, Sept. 1982, 81 p..

Jaeger, J.C. and Cook, N.G.W. Fundamentals of Rock Mechanics, 3rd Edition, Chapman and Hall, London, 1979, pp. 405-424.

Krech, W.W., Henderson, F.A. and Hjelmstad, K.E. A Standard Rock Suite for Rapid Excavation Research, U.S. Bureau of Mines Report of Investigations No. 7865, 1974, 29p..

Leach, S.J. and Walker, G.I. The Application of High Speed Liquid Jets to Cutting - Some aspects of rock cutting by high speed water jets, Proceedings of the Royal Society of London, A, Vol. 260, 1966, pp. 295-308.

Nilsson, D. Open Pit or Underground Mining, Underground Mining Methods Handbook, W. A. Hustrulid (Ed.), Society of Mining Engineers of A.I.M.E., 1982, pp. 70-88.

NRC Measurement and Control of Respirable Dust in Mines, Report of the Committee on Measurement and Control of Respirable Dust, National Materials Advisory Board, Commission on Sociotechnical Systems, National Research Council, NMAB-363, National Academy of Sciences, 1980, 405 p..

Offenbacher, L.A., McDermaid, J.D., and Patterson, C.R. PDC Bits Find Application in Oklahoma Drilling, Proceedings Drilling Conference, sponsored by Society of Petroleum Engineers/International Association of Drilling Contractors, New Orleans Louisiana, IADC/SPE 11389, Feb. 20-23 1983, pp. 261-272.

Ortega, A. and Glowka, A.D. Frictional Heating and Convective Cooling of Polycrystalline Diamond Drag Tools During Rock Cutting, Society of Petroleum Engineers Journal, Vol. 24, No. 2, April 1984, pp. 121-128.

Pimental, I.R.A., Urie, J.T. and Douglas, W.J. Evaluation of Longwall Industrial Engineering Data, Final Technical Report to the U.S. Department of Energy, Contract No. U.S.D.O.E. ET-77-C-01-8915 (11), 1981, 136 p..

Powell, J.H. and Simpson, S.P. Theoretical Study of the Mechanical Effects of Water Jets Impinging on a Semi-Infinite Elastic Solid, Int. Jr. of Rock Mech. Min. Sci., Vol. 6, 1969, pp. 353-364.

Rehbinder G. Some Aspects on the Mechanism of Erosion of Rock with a High Speed Water Jet, Proceedings of the 3rd International Symposium on Jet Cutting Technology, Chicago, May 1976, pp. E1- 1-20.

Rehbinder, G. The Drag Force on the Grains in a Permeable Medium Subject to a Water Jet, Zeitschrift fur Angewandte Mathematik und Physik (Journal of Applied Mathematics and Physics), Vol. 28, No. 6, 1977, pp. 1005-1016.

Rehbinder, P.A., Schreiner, L.A., and Zhigach, S.F. Hardness Reducers in Rock Drilling, Academy of Science, U.S.S.R., Moscow, (C.S.I.R.O. Translation, Melbourne (1948)) 1944.

Richmond, J.K., Price, G.C., Sapko, M.J., and Kawenski, E.M. Historical Summary of Coal Mine Explosions in the United States, 1959-81, Bureau of Mines Information Circular IC 8909, 1983, 50 p..

Rittinger, P. von Lehrbuch der Aufbereitungskunde, Berlin, Ernst and Korn, 1867.

Ropchan, D., Wang, F. D., and Wolgamott, J. Application of Water Jet Assisted Drag Bit and Pick Cutter for the Cutting of Coal Measure Rocks, Final Technical Report submitted to the U. S. Department of Energy, Contract Number ET-77-a-01-9082, April 1980, 84 p..

Roxborough, F.F. A Laboratory Investigation into the Application of Picks for Mechanized Tunnel Boring in the Lower Chalk, The Mining Engineer, Vol. 133, No. 156, 1973, pp. 1-13.

Roxborough, F.F. and Pedroncelli, E.J. A Practical Valuation of Some Coal Cutting Theories Using a Continuous Miner, Presented at a Meeting of the North of England Institute of Mining and Mechanical Engineers, Newcastle upon Tyne, U.K., February 4 1982, 22 p..

Schmidt, R.A. Fracture Mechanics of Oil Shale - Unconfined Fracture Toughness, Stress Corrosion Cracking, and Tension Test Results, Proceedings of the 18th U.S. Symposium on Rock Mechanics, 1977, pp. 2A2-1 - 2A2-6.

Tomlin, M.G. Field Trials with a Roadheader Equipped with a 10,000 psi Water Jet Assist System, National Coal Board Mining Research and Development Establishment Project Development Division - Tunnelling Branch, Technical Memorandum No. TU(81)10, July 1981, 39 p..

Tomlin, M. G. Field Trials with 10,000 psi Prototype System, Proceedings of Seminar on Water Jet Assisted Roadheaders for Rock Excavation, Sponsered by the U.S. Department of Energy and the U.K. National Coal Board, Pittsburgh, PA, May 1982, pp. C1-C11.

Wagner H. and Schumann, E.R.H. The Stamp-Load Bearing Strength of Rock - an Experimental and Theoretical Investigation, Rock Mechanics, Vol. 3/4, 1971, pp. 185-207.

Westwood, A.R.C. Control and Application of Environment Sensitive Fracture Processes, Tewksbury Lecture, Journal of Materials Science, Vol. 9, 1974, pp. 1871-1895.

APPENDIX

A.1. Calculation of Jet Parameters

The velocity of the water coming out of a nozzle of diameter d can be calculated by using Bernoulli's equation:

$$u = (2p / \rho_w)^{1/2} \tag{25}$$

where p is the pressure of the water. The cross-sectional area A_n of the nozzle is:

$$A_n = 1/4 \ (\pi d^2) \tag{26}$$

and the volume flow rate is expressed by:

$$Q_v = u \ A_n \tag{27}$$

The jet power is given by:

$$P_j = Q_v \ p \tag{28}$$

The measurements of the actual flow rates at different levels of the jet pressure were conducted for the three nozzle diameters used in this test program. The predicted values of of flow rates from Bernoulli's equation and the actual flow rates are plotted in Figure 66. Flow rate curves in Figure 66 show that the measured values of flow rate are less than the predicted values, and the difference between these increases at high jet pressures. These measured flow rates were used in calculations throughout the test program.

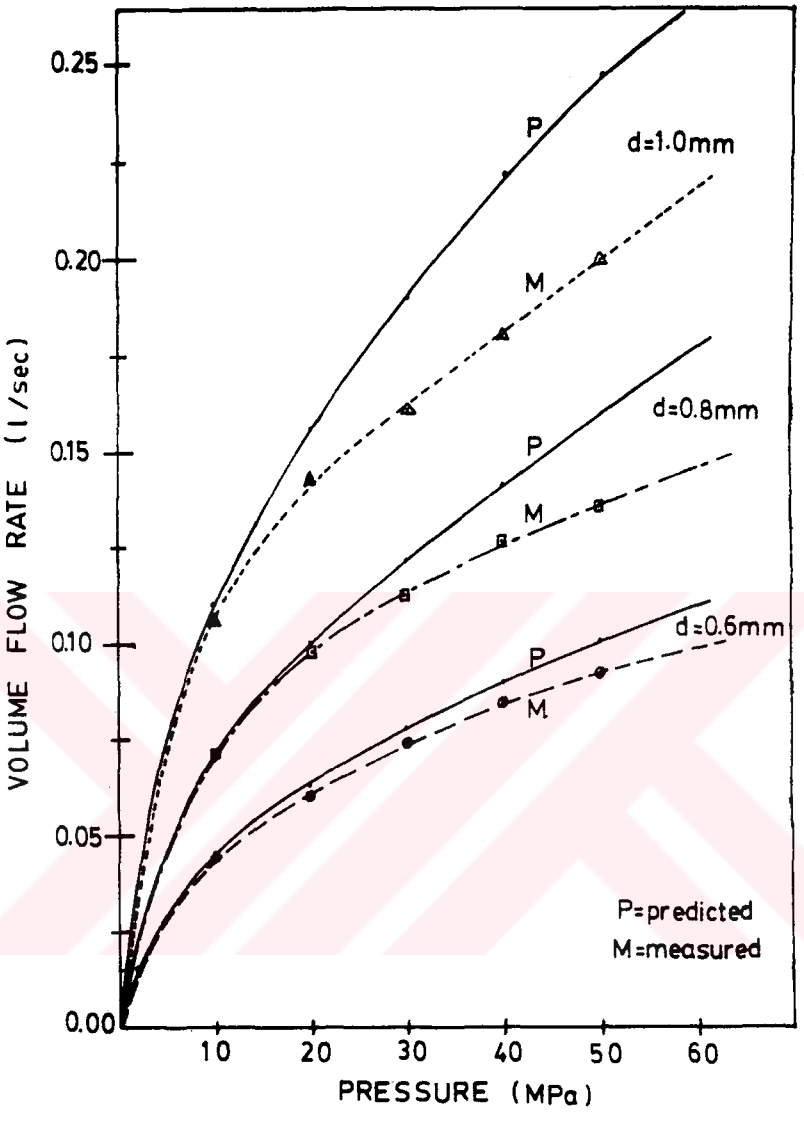

Figure 66. Predicted and measured volume flow rates for three different nozzles.